Remarks

The specification has been amended to remove embedded hyperlinks and invention-unrelated text. Applicants respectfully submit that the amendments to the specification do not introduce new matter.

Claims 13, 14, 16-21, 31, 32, and 43-50 are pending in the instant application. By this amendment, claims 13, 16, 17, 19, 20, 31, 32, and 43-50 have been amended, as discussed in detail below, and claims 1-12, 15, 22-30, and 33-42 have been cancelled without prejudice to applicants' right to pursue the cancelled claims in this or a related application(s). In addition, to more particularly point out and distinctly claim the invention, claim 19 has been further amended to replace the word "receptor" with the word "subunit." Support for this amendment can be found at page 33, paragraph [0096] of the specification as filed.

Applicants request consideration and entry of the amendments and remarks into the record.

I. The Rejections For Lack of Enablement Should Be Withdrawn

Claims 13, 14, 16-21, 31, 32, and 43-50 are rejected under 35 U.S.C. § 112, first paragraph, for allegedly containing subject matter which was not described in the specification in such a way as to enable one skilled in the art to which it pertains, or with which it is most nearly connected, to make and/or use the invention. It is the Examiner's contention that although the specification is enabling for a method of using a tissue protective cytokine receptor complex comprising an EPO receptor (EPO-R) and a βc receptor in screening assays to identify a compound that exhibits a tissue protective activity, the specification does not reasonably provide enablement for a method of using any other tissue protective cytokine receptor complexes in screening assays to identify a compound that exhibits a tissue protective activity. Applicants respectfully submit that, for the reasons discussed below and according to the applicable case law, the instant specification would have enabled one of skill in the art to use and practice the invention corresponding to the scope of the presently pending claims.

The test for enablement is whether one reasonably skilled in the art could make or use the invention, without undue experimentation, from the disclosure in the patent specification coupled with information known in the art at the time the patent application was filed. *U.S. v. Telectronics Inc.*, 857 F.2d 778, 8 USPQ2d 1217 (Fed. Cir. 1988). In fact, well known subject matter is preferably omitted. *See Hybritech Inc. v. Monoclonal Antibodies, Inc.*, 802

F.2d 1367, 1384 (Fed. Cir. 1986) ("a patent need not teach, and preferably omits, what is well known in the art."). Further, one skilled in the art is presumed to use the information available to him in attempting to make or use the claimed invention. *See Northern Telecom, Inc. v. Datapoint Corp.*, 908 F.2d 931, 941 (Fed. Cir. 1990) ("A decision on the issue of enablement requires determination of whether a person skilled in the pertinent art, using the knowledge available to such a person and the disclosure in the patent document, could make and use the invention without undue experimentation."). These enablement rules preclude the need for the patent Applicant to "set forth every minute detail regarding the invention." *Phillips Petroleum Co. v. United States Steel Corp.*, 673 F. Supp. 1278, 1291 (D. Del. 1991); *see also DeGeorge v. Bernier*, 768 F.2d 1318, 1323 (Fed. Cir. 1985).

Undue experimentation is experimentation that would require a level of ingenuity *beyond* what is expected from one of ordinary skill in the field. *Fields v. Conover,* 170 USPQ 276, 279 (CCPA 1971). As referenced by the Examiner, the factors that can be considered in determining whether an amount of experimentation is undue have been listed in *In re Wands,* 8 USPQ2d 1400, 1404 (Fed. Cir. 1988). Among these factors are: the amount of effort involved, the guidance provided by the specification, the presence of working examples, the amount of pertinent literature and the level of skill in the art. The test for undue experimentation is not merely quantitative, since a considerable amount of experimentation is permissible, so long as it is merely routine. *Id.*

Further, while the predictability of the *art* can be considered in determining whether an amount of experimentation is undue, mere unpredictability of the *result* of an experiment is *not* a consideration. Indeed, the Court of Custom and Patent Appeals in *In re Angstadt,* has specifically cautioned that the unpredictability of the result of an experiment is *not* a basis to conclude that the amount of experimentation is undue. In particular, in an unpredictable art it is not necessary for an inventor to disclose a test with every *species* covered by a claim, as it would force an inventor seeking adequate patent protection to carry out a prohibitive number of experiments – and discourage inventors from filing applications in an unpredictable area. *In re Angstadt,* 190 USPQ 214 (CCPA 1976).

The instant specification describes tissue protective cytokine receptor complexes comprising the EPO-R together with the βc receptor, the γc receptor, and the GP130 signaling subunit. The specification further goes on to describe complexes comprising the EPO-R together with segments and portions of other Type-1 cytokine receptors including, but

not limited to, GM-CSF, IL-3, and IL-5. Finally, receptor complexes comprising the EPO-R and orphan receptors including, but not limited to, ROR1, NR6, and HM74 are described (*see, e.g.*, page 15, paragraph [0052] of the specification as filed).

The Examiner's attention is next directed to Section 5.1 at page 16 of the specification as filed. Section 5.1, entitled "The Tissue Protective Cytokine Receptor Complex" describes in detail multiple forms that the receptors of the invention may take that were already known in the art (*see, e.g.*, paragraphs [0057] and [0060] for the forms of the EPO-R and βc receptors, respectively). This section further describes various multimeric receptor structures of the invention (*see, e.g.*, paragraph [0062]), provides for the preferred formulation of the tissue protective cytokine receptor complex of the invention (*see, e.g.*, paragraph [0063] and Figure 6), and describes how the receptor polypeptides of the invention may be produced (*see, e.g.*, paragraph [0064]). The instant specification also describes various cell types in which the receptors and receptor complexes of the invention may be expressed (*see, e.g.*, Section 5.2.2.1 at page 33) and provides a working example of how one of skill in the art could determine whether the receptors of the invention are associated with each other within cells (*see, e.g.*, Example 4 at page 105).

In addition to the ample guidance and support provided in the specification, applicants point to relevant art which existed at the time of the invention that, together with the disclosure of the instant specification, would enable one of skill in the art to make and use the claimed invention without undue experimentation. In addition to the work of Jubinsky *et al.* (Blood, 90:1867-1873, 1997), which was referenced by the Examiner, others have characterized multimeric receptor complexes involved in cytokine signaling. It has been shown that the βc receptor is known to work as a multimeric complex (2 βc) with other receptors that are in the same cytokine family as EPO, such as GM-CSF. The process of receptor assembly for this family also occurs in a highly conserved manner and as such it is highly likely that this too is the case with βc and EPO-R (*see, e.g.*, Rossjohn, *et al.*, Blood, 95:2491-2498, 2000 (Exhibit C) and McClure, *et al.*, Blood, 101:1308-1315, 2000 (Exhibit A)).

In view of the foregoing, applicants submit that the specification, coupled with the state of the art as of the effective filing date of the instant application, fully enables one of skill in the art to make, use, and practice the invention as claimed without undue experimentation. Applicants respectfully request that the rejection under 35 U.S.C. § 112, first paragraph, for lack of enablement, be withdrawn.

II. The Rejections For Indefiniteness Should be Withdrawn

Claims 13, 14, 16-20, 31, 32, and 43-50 are rejected under 35 U.S.C. § 112, second paragraph, for failing to particularly point out and distinctly claim the subject matter which applicants regard as the invention. In particular, the Examiner contends that claims 13, 14, 16-20, and 43-50 are indefinite for their recitation of a method comprising "contacting" and "identifying," but failing to recite how a test compound is assayed for tissue protective activity, making it unclear what tissue protective activity is determined, and claim 32 has been rejected for being dependent on rejected claim 13. Further, the Examiner has rejected claim 31 because it is allegedly unclear how "detecting the presence of nucleolin in the cell" correlates with assaying for a tissue protective activity. Finally, claim 48 has been rejected by the Examiner for recitation of the limitation "wherein the tissue protective cytokine receptor complex *ligand* is an EPO," without proper antecedent basis for the limitation in either of claims 13 or 16 from which this claim depends.

In response, claim 13 has been amended to add the phrase "wherein a test compound that increases the level of reporter gene expression relative to the level of reporter gene expression in the absence of the test compound is identified as a compound that modulates a tissue protective activity." The specification as filed clearly describes the identification of compounds having tissue protective activity by use of assays that measure reporter gene activity in a host cell (*see, e.g.*, section 5.2.2.3 at page 42). As such, applicants assert that the amendment overcomes the Examiner's rejection of claim 13, and claims dependent thereon, *i.e.*, claims 14, 16-20, 32, and 43-50, on the grounds of indefiniteness.

In response to the Examiner's rejection of claim 31 as being allegedly unclear as to how detecting the presence of nucleolin in the cell correlates with assaying for a tissue protective activity, claim 31 has been amended to include the phrase "wherein an upregulation of nucleolin in the cell indicates a tissue protective activity." This amendment is supported by the specification as filed. For example, page 16, paragraph [0053], discloses that "activation of a tissue protective cytokine receptor complex may lead to the upregulation of the production of protective proteins, including, but not limited to, nucleolin and globins such as neuroglobins and cytoglobins (histoglobin). Accordingly, the screening methods for identifying compounds with tissue protective activity may utilize detection of such upregulated proteins." The Examiner's attention is also directed to Example 10 of the instant

specification at page 110, entitled "Detecting the Presence of Nucleolin," in which ample support and direction are provided with respect to how a tissue protective activity is assayed by detecting the presence of nucleolin in a cell. Thus, claim 31, as amended, makes clear how the presence of nucleolin correlates with tissue protective activity. As such, Applicants assert that the rejection to claim 31 has been overcome and should be withdrawn.

Claim 32 has been amended to include the phrase "wherein an upregulation of neuroglobin or cytoglobin in the cell indicates a tissue protective activity." Applicants assert that in light of the arguments presented above, this amendment makes it apparent how the presence of neuroglobin or cytoglobin is an indicator of tissue protective activity.

Finally, Applicants have amended claims 48 and 50 to correct dependencies. The dependency of claims 48 and 50 have been amended, such that these claims now depend on claim 44. There is sufficient antecedent basis in claim 44 for the limitations provided in claims 48 and 50, thus obviating the Examiner's rejection.

For the reasons detailed above, applicants submit that claims 13, 14, 16-20, 31, 32, and 43-50, as amended, particularly point out and distinctly claim the subject matter which applicants regard as their invention. Applicants respectfully request that the rejection under 35 U.S.C. § 112, second paragraph, for indefiniteness, be withdrawn.

III. The Rejections For Obviousness Should be Withdrawn

Claims 13, 14, 17, 19, 20, 48, and 49 are rejected under 35 U.S.C. § 103(a) as being unpatentable over Jubinsky, *et al.* (Blood 90:1867-1873, 1997, "Jubinsky") in view of Mercury™ Pathway Profiling System User Manual (Clontech, March 2, 2001, "Mercury"). The Examiner alleges that: (i) Jubinsky teaches a functional complex comprising the EPO receptor (EPO-R) and a βc receptor in murine Ba/F3 cells that were transfected with either the murine EPO-R or EPO-R/βc, a functional role for the βc receptor in the EPO-dependent proliferation of Ba/F3 cells expressing the EPO-R, and a method for identifying the effect of sense, antisense, and nonsense oligodeoxynucleotides to βc on EPO-dependent proliferation and β-globin expression in Ba/F3 cells; and (ii) Mercury teaches various reporter genes and vectors containing a promoter and response element which control the transcription of the reporter genes and an assay for screening a compound for its effect based upon the reporter gene activity. The Examiner argues that it would have been obvious to one of ordinary skill in the art at the time of the invention to modify the method of Jubinsky to include the reporter

system of Mercury with a reasonable expectation of success. The Examiner further posits that one would have been motivated to do so because the system provided by Mercury is ideal for use with membrane receptors.

Furthermore, the Examiner has rejected claims 13, 16-18, 21, 43-48, and 50 under 35 U.S.C. § 103(a) as being unpatentable over Jubinsky in view of Trueheart *et al.* (U.S. Patent No: 6,159,705, December 12, 2000, "Trueheart"). The Examiner concluded that Trueheart teaches rapid, reliable, and effective assays for screening and identifying pharmaceutically effective compounds that specifically interact with and modulate the activity of a heterologous receptor and that the cells used in the assays provided by Trueheart may be of prokaryotic or eukaryotic origin and may include yeast cells. The Examiner asserts that it would have been obvious to one having skill in the art to combine the method of Jubinsky to functionally express the EPO-R and βc receptor in a prokaryotic cell, such as a yeast cell, or a human cell in order to screen various compounds using a reporter gene taught by Trueheart, in order to identify a compound that modulates a tissue protective productive activity of the EPO-R/βc receptor complex with a reasonable expectation of success. The Examiner argues that one would have been motivated to do so because the assay system of Trueheart provides a rapid, reliable, and effective assay for screening and identifying effectors of a receptor protein or complex thereof.

For the reasons set forth below, applicants disagree with the Examiner's contention that the instant invention is unpatentable over Jubinsky in view of Mercury or in view of Trueheart for reasons of obviousness.

A. <u>The Legal Standard</u>

A finding of obviousness requires that "the differences between the subject matter sought to be patented and the prior art are such that the subject matter as a whole would have been obvious at the time the invention was made to a person having ordinary skill in the art to which said subject matter pertains." 35 U.S.C. §103(a).

In its recent decision addressing the issue of obviousness, *KSR International Co. v. Teleflex Inc.*, 127 S.Ct. 1727, 82 USPQ2d 1385 (2007), the Supreme Court stated that the following factors set forth in *Graham v. John Deere Co.*, 383 U.S. 1, 148 USPQ 459 (1966) still control an obviousness inquiry: (1) the scope and content of the prior art; (2) the differences between the prior art and the claimed invention; (3) the level of ordinary skill in

the art; and (4) objective evidence of nonobviousness. *KSR*, 127 S.Ct. at 1734, 82 USPQ2d at 1388 quoting *Graham*, 383 U.S. at 17-18, 14 USPQ at 467.

The *Graham* Court stated:

> Under § 103, the scope and content of the prior art are to be determined; differences between the prior art and the claims at issue are to be ascertained; and the level of ordinary skill in the pertinent art resolved. Against this background, the obviousness or nonobviousness of the subject matter is determined. Such secondary considerations as commercial success, long felt but unsolved needs, failure of others, etc., might be utilized to give light to the circumstances surrounding the origin of the subject matter to be patented.

Thus, the standard set forth in *Graham* is a broad inquiry which invites looking at any secondary considerations that would prove instructive in the obviousness analysis. *KSR Intern. Co. v. Teleflex, Inc.*, 127 S.Ct. 1727, 1736 (2007). When an invention combines two known devices according to their established functions, it can be important to identify a reason that would have prompted a person of ordinary skill in the relevant field to combine the elements in the way the claimed invention does. *Id.* at 1737. If a person of ordinary skill can implement a predictable variation, § 103 likely bars its patentability. *Id.* at 1737. A court must ask whether the improvement is more than the predictable use of prior art elements according to their established functions. *Id.* at 1737. Further, the relevant inquiry is whether the prior art suggests the invention and whether the prior art provides one of ordinary skill in the art with a reasonable expectation of success. *In re O'Farrell*, 853 F.2d 894 (Fed. Cir. 1988).

In making a determination of obviousness, one must consider the prior art from the perspective of a person having ordinary skill in the art at the time the invention was made. "Measuring a claimed invention against the standard established by section 103 requires the oft-difficult but critical step of casting the mind back to the time of invention, to consider the thinking of one of ordinary skill in the art, guided only by the prior art references and the then-accepted wisdom in the field." *In re Dembiczak*, 175 F.3d 994, 999 (Fed. Cir. 1999), citing to *W.L. Gore & Assoc., Inc. v. Garlock, Inc.*, 721 F.2d 1540, 1553 (Fed. Cir. 1983). The *KSR* Court, citing *Graham,* upheld the principle of *avoiding hindsight bias* and cautioned courts to *guard against reading into the prior art the teachings of the invention in issue.* 127 S.Ct. at 1742, 82 USPQ at 1397:

> A factfinder should be aware, of course, of the distortion caused by hindsight bias and must be cautious of arguments reliant upon *ex post* reasoning. See *Graham*, 383 U.S., at 36, 86 S.Ct. 684 (warning against a "temptation to read into the prior art the teachings of the invention in issue" and instructing

courts to "'guard against slipping into the use of hindsight'" (quoting *Monroe Auto Equipment Co. v. Heckethorn Mfg. & Supply Co.*, 332 F.2d 406, 412 (C.A.6 1964))).

Finally, evidence of unexpected or unobvious results is objective evidence of nonobviousness, and may be used to rebut a *prima facie* case of obviousness. *In re Wagner*, 371 F.2d 877 (C.C.P.A. 1967); M.P.E.P. § 716.02.

B. Jubinsky, Either Alone Or Combined With Either Mercury or Trueheart, Does Not Teach Or Suggest the Claimed Invention

Applicants submit that, standing in the shoes of the ordinary skilled artisan as of the effective filing date of the application, there was no suggestion of the claimed invention in the art. The combination of Jubinsky with either Mercury or Trueheart, cited by the Examiner, are discussed below to demonstrate that the claimed methods for identifying compounds with tissue-protective activity were not obvious over the prior art.

First, applicants submit that the Examiner has mischaracterized the findings reported by Jubinsky as they relate to the claimed invention. The claimed invention relates to cell based assays for screening compounds for *tissue protective activity* using cells that express the heteromultimer tissue protective receptor complex. In this case, a tissue protective activity encompasses such activities that would serve to inhibit or delay either damage or death of a certain cell, tissue, organ (*see, e.g.*, page 13, paragraph [0038] of the specification as filed). The invention is based, in part, on the surprising discovery that a limited class of tissue protective cytokines modulate tissue protective activity through a receptor pathway that does *not* involve the classical EPO receptor dimer (*see, e.g.*, page 3, paragraph [0006] of the specification as filed). This alternative receptor is in fact a heteromultimer receptor complex comprising EPO-R and the βc receptor which is found in excitable tissues such as the brain, the spinal cord, and the heart (*see, e.g.*, page 16, paragraph [0052] of the specification as filed). Applicants discovered that EPO binds to this receptor complex and mediates its tissue protective activity through this alternative receptor pathway (*see, e.g.*, page 3, paragraph [0007] of the specification as filed). Next, Applicants invented the claimed methods for using this heteromultimer receptor complex to screen potential compounds for tissue protective activity (*see, e.g.*, Section 5.2, beginning at page 21 of the specification as filed).

In contrast, Jubinsky's focus lies primarily in the relationship between the traditional signalling function of EPO, *i.e.*, its ability to stimulate cell proliferation, and the EPO-R/βc

receptor complex. Jubinsky demonstrates that the βc receptor and the EPO-R form a complex through which EPO-dependent cell-proliferation of Ba/F3 cells is mediated (pages 1869-70). Jubinsky further establishes that antisense oligodeoxynucleotides to β mRNA capably reduce EPO-dependent proliferation of Ba/F3 cells expressing the EPO-R, further establishing a role for the EPO-R/βc receptor complex in cell proliferation in response to EPO (page 1869).

Thus, Jubinsky only examines the role of the EPO-R/βc receptor complex in cellular proliferation and never contemplates or suggests a tissue protective role for this receptor complex. Nowhere does Jubinsky suggest a tissue protective activity mediated by the EPO-R/βc receptor complex. Consequently, Jubinsky alone cannot render obvious the claimed assays for using the heteromultimer receptor complex to screen potential compounds for tissue protective activity.

The Examiner alleges that the combination of Jubinsky with Mercury renders obvious claims 13, 14, 17, 19, 20, 48, and 49, and that the combination of Jubinsky with Trueheart renders obvious claims 13, 16-18, 21, 43-48, and 50. However, neither Mercury nor Trueheart compensate for the deficiencies of Jubinsky.

Mercury teaches reporter gene systems by which various signal transduction pathways can be elucidated in eukaryotic cells. Trueheart teaches assays for screening and identifying pharmaceutically effective compounds that specifically interact with and modulate the activity of a given heterologous receptor in a cell of prokaryotic or eukaryotic origin. However, one of ordinary skill in the art at the time of the invention would not have contemplated applying the teachings of either Mercury or Trueheart to the findings of Jubinsky to identify compounds that modulate tissue protective activity because Jubinsky only examines the role of the EPO-R/βc receptor complex in cellular proliferation and never contemplates or suggests a tissue protective role for this receptor complex.

Moreover, the results disclosed in the instant application concerning the unexpected pathway for signalling of tissue protective cytokine activity through the EPO-R/βc receptor complex was completely unexpected based on the teachings of Jubinsky and others at the time of the presently claimed invention. In fact, Jubinsky, by reporting that transgenic knock-out mice lacking the EPO-R/βc receptor retained normal EPO signalling activity, actually *taught away* from the claimed invention. For example, Jubinsky, at page 1872, points out that "animals deficient in either βc or βIL-3 have not been reported to have impaired erythropoiesis," citing to Nishinakamura, *et al.*, Immunity 2:211, 1995

("Nishinakamura"; Exhibit B) and Stanley, *et al.*, Proc. Natl. Acad. Sci. 91:5592, 1994 ("Stanley"; Exhibit D). These papers referenced by Jubinsky represent studies performed on mice with one intact β chain remaining (either the βc or βIL-3). Jubinsky contemplates the possibility that EPO interacts with the non-disrupted chain, thus providing a potential reason as to why both Nishinakamura and Stanley saw no change in the test animals' responsiveness to EPO despite the lack of either βc or βIL-3 receptor genes. However, Scott, *et. al.*, (cited as reference C39 in the Information Disclosure Statement filed on March 9, 2005; "Scott"), works to rebut Jubinsky's hypothesis that the non-disrupted β chain in the animals described by Nishinakamura and Stanley might be compensating for the absence of the deleted β chain. Scott teaches mice lacking *both* the βc and βIL-3 receptor genes and demonstrates that bone marrow progenitor cells taken from said βc/βIL-3 null mice show no observable difference in their responsiveness to EPO relative to wild-type mice (*see* Scott at page 1590, Fig. 2B).

Against this background, the finding that the EPO/βc receptor complex mediated tissue protective activity of certain forms of EPO was entirely unexpected. In particular, experiments presented in the instant application demonstrate that cardiomyocytes isolated from βc (-/-) knock-out mice lack tissue protective activity (see Example 5 at page 106 of the specification as filed and Figure 7). The results of these βc (-/-) knock-out mice demonstrate that there is no tissue protective activity of EPO in cardiomyocytes isolated from βc chain knockout mice, as evidenced by the fact that the percent of apoptosis in βc (-/-) cardiomyocyte cells in the presence of EPO was equivalent to that in the absence of EPO. However, cardiomyocytes from wild-type mice having intact βc chains did demonstrate a tissue protective effect of EPO, as evidenced by a significantly lessened degree of apoptosis in these cells. These results were completely unexpected given the teachings of Nishinakamura, Stanley, and Scott which demonstrated that such knock-out mice exhibit completely the normal EPO activity. Based on this surprising discovery, the inventors designed the claimed assays to identify compounds that modulate tissue protective activity.

As such, applicants assert that, at the time of filing of the instant application, the claimed invention was not only non-obvious, but in fact entirely unexpected, in light of what was known in the field at the time, as evidenced by the published results of Jubinsky, Nishinakamura, Stanley, and Scott.

In view of the arguments above, applicants assert that it would not have been obvious to one of ordinary skill in the art to combine the teachings of Jubinsky with either Mercury or Trueheart to identify a compound that modulates a tissue protective activity of the EPO-R/βc

complex. Therefore, Applicants respectfully request that the rejection under 35 U.S.C. § 103(a), for obviousness, be withdrawn.

Conclusion

Applicants respectfully request entry and consideration of the foregoing amendments and remarks. Withdrawal of all the rejections and an allowance are earnestly sought.

Respectfully submitted,

Date: November 30, 2007

Laura A. Coruzzi 30,742
Laura A. Coruzzi (Reg. No.)

JONES DAY
222 East 41st Street
New York, New York 10017
(212) 326-3939

Enclosures

by Aileen F. Falvey 46,097

Molecular assembly of the ternary granulocyte-macrophage colony-stimulating factor receptor complex

Barbara J. McClure, Timothy R. Hercus, Bronwyn A. Cambareri, Joanna M. Woodcock, Christopher J. Bagley, Geoff J. Howlett, and Angel F. Lopez

Granulocyte-macrophage colony-stimulating factor (GM-CSF) is a hematopoletic cytokine that stimulates the production and functional activity of granulocytes and macrophages, properties that have encouraged its clinical use in bone marrow transplantation and in certain infectious diseases. Despite the importance of GM-CSF in regulating myeloid cell numbers and function, little is known about the exact composition and mechanism of assembly of the GM-CSF receptor complex. We have now produced soluble forms of the GM-CSF receptor α chain (sGMRα) and β chain (sβc) and utilized GM-CSF, the GM-CSF antagonist E21R (Glu21Arg), and the βc-blocking monoclonal antibody BION-1 to define the molecular assembly of the GM-CSF receptor complex. We found that GM-CSF and E21R were able to form low-affinity, binary complexes with sGMRα, each having a stoichiometry of 1:1. Importantly, GM-CSF but not E21R formed a ternary complex with sGMRα and sβc, and this complex could be disrupted by E21R. Significantly, size-exclusion chromatography, analytical ultracentrifugation, and radioactive tracer experiments indicated that the ternary complex is composed of one sβc dimer with a single molecule each of sGMRα and of GM-CSF. In addition, a hitherto unrecognized direct interaction between βc and GM-CSF was detected that was absent with E21R and was abolished by BION-1. These results demonstrate a novel mechanism of cytokine receptor assembly likely to apply also to interleukin-3 (IL-3) and IL-5 and have implications for our molecular understanding and potential manipulation of GM-CSF activation of its receptor. (Blood. 2003;101: 1308-1315)

Introduction

Granulocyte-macrophage colony-stimulating factor (GM-CSF) is a cytokine produced by many cells in the body that regulates the production, effector cell function, and survival of myeloid cells.[1-4] Macrophages and granulocytes rise in numbers and exhibit a prolonged life span and enhanced effector function in response to GM-CSF,[5,6] properties that have encouraged its use in bone marrow transplantation[7] and infectious diseases such as those associated with AIDS.[8] In addition, GM-CSF controls dendritic cell production, differentiation, and function and potentiates responses of $CD4^+$ T cells in vivo.[9,10] This dual action of GM-CSF has encouraged its utilization in different vaccination strategies.[11] On the other hand, these same properties have implicated GM-CSF in myeloid leukemia and several inflammatory conditions such as asthma[12] and rheumatoid arthritis.[13]

The actions of GM-CSF are mediated by specific receptors composed of 2 different subunits, a receptor α chain (GMRα),[14] which provides specificity and the major binding contact, and a β chain (βc),[15] which is common with the interleukin-3 (IL-3) and IL-5 receptors, promotes affinity conversion, and acts as the major signal transducer. For this complex to be assembled and to signal, there exist structural and dimerization requirements, some of which have been defined. Extensive structure-function analysis has identified several residues involved in GM-CSF, GMRα, and βc protein interaction and biologic activity. For example, the binding of GM-CSF to GMRα involves an electrostatic interaction between Asp112 in the fourth α helix of GM-CSF and Arg280 in the F-G loop of GMRα.[16,17] The biologic activities and high-affinity binding of GM-CSF are exquisitely dependent on Glu21 in the first α helix of GM-CSF, although direct contact with βc has not been demonstrated. Substitution of this amino acid with arginine generates a GM-CSF analog, E21R (Glu21Arg), which exhibits only low-affinity binding and is unable to stimulate cellular proliferation and mature cell functions.[18] Importantly, E21R is able to antagonize GM-CSF binding and function[19]; however, the molecular basis of this antagonism is not fully understood. In βc, residues in the B-C loop (Tyr365, His367, Ile368) and F-G loop (Tyr421) of domain 4 are involved in GM-CSF high-affinity binding and function.[20-23] The monoclonal antibody (mAb) BION-1, which binds an area in βc encompassing these loops, blocks GM-CSF binding and biologic activities.[24]

Dimerization of the α and βc subunits of this family of cytokine receptors is recognized as a crucial step for their activation; however, the exact composition of the assembled complex remains unclear. A number of studies suggest that simple heterodimerization is sufficient to activate the GM-CSF receptor,[25] whereas both cross-linking and dominant-negative studies using surface-expressed receptors suggest that the formation of higher-order GM-CSF receptor complexes is required for receptor activation.[26,27] Dimerization of βc in

From the Cytokine Receptor Laboratory and Protein Laboratory, Division of Human Immunology, Institute of Medical and Veterinary Science (IMVS), Adelaide, South Australia; and Department of Biochemistry and Molecular Biology, University of Melbourne, Parkville, Australia.

Submitted June 27, 2002; accepted September 10, 2002. Prepublished online as *Blood* First Edition Paper, October 10, 2002; DOI 10.1182/blood-2002-06-1903.

Supported by grants from the National Health and Medical Research Council of Australia.

Reprints: Angel Lopez, Cytokine Receptor Laboratory, Division of Human Immunology, IMVS, Frome Road, Adelaide, South Australia, 5000, Australia; e-mail: angel.lopez@imvs.sa.gov.au.

The publication costs of this article were defrayed in part by page charge payment. Therefore, and solely to indicate this fact, this article is hereby marked "advertisement" in accordance with 18 U.S.C. section 1734.

particular has also been shown to be an important and necessary step for receptor activation,[28,29] probably reflecting the need to bring into close proximity the cytoplasmic domains of 2 βc molecules associated with Janus kinase-2 (JAK-2), resulting in JAK transphosphorylation and receptor phosphorylation. Interestingly, βc has been shown to crystallize as a dimer[30] and to exist as a preformed homodimer on the cell surface.[26,28] Despite these findings, little is known about the full assembly of this family of receptors, the intermediate steps in their formation, and how receptor assembly may be selectively modulated.

In this paper we show for the first time the full assembly of the human GM-CSF receptor in solution. This shows a novel mode of cytokine receptor assembly in which 1 molecule of GM-CSF associates with 1 molecule of GMRα and 2 molecules of βc. In addition, these studies reveal an essential, direct interaction between GM-CSF and βc and provide a molecular understanding of GM-CSF antagonism by E21R or BION-1. This novel mode of receptor assembly may also apply to the IL-5 and IL-3 receptors.

Materials and methods

Human GM-CSF and GM-CSF analogs

Soluble wild-type human GM-CSF was produced in *Escherichia coli* and recovered from the periplasmic space by osmotic shock as described previously.[19] Crude periplasmic extracts were adjusted to 25 mM N-ethylmorpholine HCl (NEM), pH 7.0, loaded onto Q Sepharose Fast Flow (Amersham Biosciences, Sydney, Australia) equilibrated in 25 mM NEM, pH 7.0, and a linear gradient of 0 to 600 mM NaCl in 25 mM NEM, pH 7.0, used to elute the bound proteins. GM-CSF purified by anion exchange was further purified by reversed phase high-performance liquid chromatography (HPLC), lyophilized, dissolved in phosphate-buffered saline (PBS) as previously described,[19] and sterile-filtered (0.45 μm). The E21R analog of GM-CSF (BresaGen, Adelaide, South Australia) contains a glutamate to arginine substitution at residue 21 and a modified 12–amino acid leader peptide, MFATSSSTGNDG, to facilitate expression in *E coli*.[31]

Radiolabeling of human GM-CSF

To enable phosphorylation of GM-CSF under mild conditions, we made the GM-CSF analog, SGMKIN, in which the amino acids from alanine at position 3 to proline at position 6 were replaced by the peptide sequence RRASV, which is recognized by the catalytic subunit of cyclic adenosine monophosphate (cAMP)–dependent protein kinase from heart muscle.[32] Complementary oligonucleotides were used to create a *Hin*dIII/*Nco*I fragment encoding the N-terminal 12 amino acids of SGMKIN. This fragment was ligated with an *Nco*I/*Bam*HI fragment encoding the C-terminal 116 amino acids of human GM-CSF (hGM-CSF) into *Hin*dIII/*Bam*HI–digested pIN-III-OmpH3 expression vector[19] to create the plasmid, pSGMKIN. Soluble SGMKIN was expressed in *E coli* and purified as described for wild-type GM-CSF. The final product was at more than 95% purity by sodium dodecyl sulfate–polyacrylamide gel electrophoresis (SDS-PAGE), and the SGMKIN analog displayed biologic activity indistinguishable from the wild-type GM-CSF (data not shown). Labeling of SGMKIN with ^{32}P used a protocol adapted from Kaelin et al.[32] Fifty micrograms of purified SGMKIN was incubated in a 200-μL reaction mix containing 20 mM Tris (tris(hydroxymethyl)aminomethane) HCl, pH 7.5; 100 mM NaCl; 12 mM $MgCl_2$; 10 mM β-mercaptoethanol; 1 μCi/μL (0.037 MBq/μL) [γ-^{32}P]adenosine triphosphate ([γ-^{32}P]ATP) (3000 Ci/mmol [111 000 GBq/mmol]; Geneworks, Adelaide, South Australia), and 1 U/μL of the protein kinase catalytic subunit (Sigma, Castle Hill, Australia). The reaction proceeded at 4°C for 30 minutes, was terminated by the addition of 200 μL of 100 mM EDTA (ethylenediaminetetraacetic acid), adjusted to 0.1% (vol/vol) trifluoroacetic acid (TFA; Auspep, Parkville, Australia), 1% (vol/vol) acetic acid, and loaded onto a Sep-Pak C18 reversed phase cartridge (Waters, Rydalmere, Australia) equilibrated in 0.01% TFA. The cartridge was washed with 0.01% TFA and bound SGMKIN eluted using 10 mL of 50% (vol/vol) acetonitrile in the presence of 0.01% TFA. Ten equal fractions were collected, and those containing the peak of eluted radioactivity were pooled and concentrated using a Speed-vac (Savant Instruments, Farmingdale, NY) to a final volume of approximately 100 μL.

Production of recombinant soluble GM-CSF receptor subunits

DNA fragments encoding the soluble extracellular domains of GMRα (sGMRα) or βc (sβc) were generated by PCR using the primers 5′-CTGACCGGATCCATGCTTCTCCTGGTGACAAGCC-3′ and 5′-GTACACGGATCCGAATTCTTACCCGTCGTCAGAACCAAATTC-3′ for sGMRα and 5′-CTGACCGGATCCATGGTGCTGGCCCAGGGGCTGC-3′ and 5′-CAGCACGGATCCGAATTCTTACGACTCGGTGTCCCAGGAGCG-3′ for sβc, with *Eco*RI and *Bam*HI restriction sites underlined. Stop codons were inserted immediately prior to the transmembrane domain for each receptor molecule, following Gly at position 320 for GMRα and Ser at position 438 for βc. The PCR products were digested with *Bam*HI and *Eco*RI and cloned into the baculovirus transfer vector BacPAK9 (Clontech, Palo Alto, CA) and the sequence of the cloned inserts were verified by cycle sequencing with BigDye chemistry (Applied Biosystems, Foster City, CA). The cDNA encoding sGMRα and sβc was introduced into the genome of *Bsu*36I-digested BacPAK6 viral DNA (Clontech) by homologous recombination following the manufacturer's instructions. Expression of recombinant protein is under the control of the strong polyhedrin promoter. Large-scale expression of sGMRα or sβc was performed by infection of Sf21 cells, grown in serum-free Ex-Cell 420 medium (JRH Biosciences, Brooklyn, Australia), with recombinant baculovirus at a multiplicity of infection of 0.3. Supernatant containing soluble receptor was harvested following incubation at 27°C for 5 to 7 days.

Purification of soluble GMRα and sβc

Conditioned media containing sGMRα (20 L) or sβc (9 L) were concentrated to less than 1 L using tangential flow filtration cartridges (10 000 molecular weight cutoff, 0.23 m^2) (Millipore, Northryde, Australia) operated at 80 kPa and 4°C. Insoluble material in the concentrate was pelleted at 3000*g* for 30 minutes and the resulting supernatant filtered (3 μm) prior to affinity chromatography. Affinity matrices were prepared by coupling E21R or the anti-βc mAb, BION-1,[24] to cyanogen bromide (CNBr)–activated Sepharose 4B (Amersham Biosciences) following the manufacturer's instructions. Recombinant soluble receptor was bound to the affinity matrix, washed extensively in PBS containing 0.01% (vol/vol) polyoxyethylene 20 sorbitan monolaurate (Tween 20), and bound proteins eluted with 100 mM NaCl, 100 mM sodium acetate (pH 4.0). The eluate fractions were immediately neutralized using 2 M Tris and analyzed for the presence of soluble receptor by SDS-PAGE. Fractions containing purified soluble receptor were pooled and concentrated using a stirred-cell device with a 10 000 molecular weight cutoff, low protein-binding membrane (YM10; Millipore) operated at 300 kPa and 4°C. Concentrated soluble receptor was dialyzed extensively into PBS, sterile-filtered (0.2 μm), and stored at 4°C.

SDS-PAGE

Samples were analyzed on 10% or 12.5% polyacrylamide gels containing 38:1 acrylamide/bisacrylamide under reducing or nonreducing conditions as specified. Bands were visualized by staining with either Coomassie brilliant blue R-250 or silver.[33]

Mass spectrometry

Electrospray ionization mass spectrometry was performed using a PE/Sciex API100 mass spectrometer (Perkin-Elmer Sciex Instruments, Ontario, Canada). Protein samples were desalted in-line using a 1 × 10 mm reversed phase column eluted with 60% (vol/vol) acetonitrile in the presence of 0.04% (vol/vol) TFA and the primary mass spectrum transformed to give a true-mass profile using instrument software.

Protein analyses by size-exclusion chromatography

Size-exclusion chromatography was initially used to quantify purified soluble receptors and their ligands. Samples were chromatographed on a

SMART system with a Superdex 200PC 3.2/30 (3.2 mm × 300 mm) column (Amersham Biosciences) operated at 40 μL/min at 25°C using 150 mM NaCl, 50 mM sodium phosphate, pH 7.0, as running buffer. The area under the protein peak was integrated using the extinction coefficient (absorbance units × mL^{-1} × mg^{-1}) calculated for each protein: GM-CSF, 0.95; E21R, 0.88; sGMRα, 1.17; sβc, 1.95.

To analyze protein-protein interactions, individual proteins and protein complexes were prepared in a final volume of 50 μL, adjusted with PBS as required, and incubated at 25°C for at least 1 hour. Samples were analyzed by size-exclusion chromatography using the SMART system as described above with data presented from representative experiments (n = 5). The dependence of elution time on the $\log_{10}$ (MW) of protein standards was used to calibrate the column and to generate a trend line for each set of standards. External standards included myoglobin, MW 17 kDa; ovalbumin, MW 44 kDa; γ-globulin, MW 158 kDa; and thyroglobulin, MW 670 kDa (Biorad Laboratories, Hercules, CA). Internal standards were GM-CSF, MW 14.5 kDa; E21R, MW 15.7 kDa; sGMRα, MW 43 kDa; and sβc, MW 101 kDa as determined by mass spectrometry and SDS-PAGE. Soluble βc was found to be a dimer by size-exclusion chromatography consistent with previous reports.[30] Calibration curves constructed from the external and internal standards were essentially parallel (see Figure 2A). The calibration curve for the internal standards was extrapolated to higher mass (670 kDa) because this was found to be the limit of the linear range for the external standards.

Analytical ultracentrifugation

The molecular weights of GM-CSF, E21R, sGMRα, sβc, and the binary and ternary complexes were determined by sedimentation equilibrium. Individual proteins and protein complexes were isolated by size-exclusion chromatography using a fast protein liquid chromatography (FPLC) system with a Superdex 200 10/30 (10 mm × 300 mm) column (Amersham Biosciences) operated at 0.5 mL/min at 25°C using 150 mM NaCl, 50 mM sodium phosphate, pH 7.0, as running buffer. Pooled fractions were concentrated using Centricon 10 microconcentrators (Amicon, Beverly, MA). Sedimentation equilibrium experiments were performed using a Beckman XL-A analytical ultracentrifuge equipped with a Ti60 rotor (Beckman, Palo Alto, CA) and filled epon centerpieces (12-mm path length). Sedimentation equilibrium profiles were obtained at 20°C using the rotor speeds indicated. Equilibrium distributions were fitted by nonlinear regression analysis to obtain best-fit values for the M (1-νρ), where M is the molecular weight and ν the partial specific volume of the sedimenting species and ρ the solution density. The compositional molecular weights of the proteins and the partial specific volumes of GM-CSF and E21R were calculated from their amino acid sequences. Partial specific volumes for the glycosylated forms of sGMRα and sβc were calculated assuming these proteins were monomer and dimmer, respectively. A value of 0.622 mL/g was assumed for the partial specific volume of carbohydrate. The experimental value of M (1-νρ) and the molecular weight (M_ρ) and partial specific volume of the protein component were then used to solve for the weight fraction of bound carbohydrate and hence the partial specific volume of the carbohydrate-bound protein. Values for the partial specific volumes of the GM-CSF/sGMRα and E21R/sGMRα complexes were calculated assuming a 1:1 complex and no volume change on association. A value of 0.72 mL/g was assumed for the GM-CSF/sGMRα/sβc complex.

Cross-linking experiments

Stable cross-linking of sβc or soluble complexes of ligand with sβc was performed by incubation of 2.6 μg sβc with either 2.4 μg GM-CSF or E21R for 1 hour at 25°C followed by addition of BS^3 cross-linker (Pierce, Rockford, IL) at a final concentration of 0.1 mg/mL for 10 minutes. The reaction was then stopped by addition of ethanolamine HCl, pH 8.0, to a final concentration of 100 mM. Cross-linked proteins were subjected to reducing SDS-PAGE and compared with non–cross-linked material. Antibody Fab fragments of BION-1 (anti-βc fourth domain blocking mAb) and 2H1 (anti-βc fourth domain control mAb) used in cross-linking experiments were generated by digestion with ficin using the Immunopure IgG_1 Fab Preparation Kit (Pierce) following the manufacturer's instructions. Fab fragment (18 μg) was preincubated with 2.6 μg sβc for 30 minutes at 25°C prior to the addition of 2.4 μg GM-CSF in a final volume of 20 μL for a further hour. Cross-linking was then performed as above followed by SDS-PAGE analysis.

Results

Production, purification, and analysis of GM-CSF soluble receptor components

Complementary DNA fragments encoding the extracellular domains of GMRα and βc (sGMRα and sβc) were generated by PCR and cloned into a baculovirus transfer vector. Following introduction into a baculovirus expression system by homologous recombination, the soluble receptor components were generated by infection of Sf21 cells. Purification of the soluble receptors was achieved by affinity chromatography using immobilized ligand for sGMRα and immobilized mAb BION-1[24] for sβc. Purified soluble receptors were recovered at more than 95% purity as assessed by silver-stained SDS-PAGE under reducing conditions (Figure 1A) with an apparent molecular weight (MW) of approximately 43 kDa for sGMRα and 55 kDa for sβc. Importantly, these MWs determined for sGMRα and for sβc did not alter when analyzed under nonreducing conditions (Figure 1B), indicating the absence of disulfide-linked dimers. A small amount of disulfide-aggregated sβc was visible by nonreducing SDS-PAGE (Figure 1B) and as an early, minor peak during size-exclusion chromatography (Figure 2C). The absence of detectable disulfide-linked dimers in sβc was confirmed by ion-spray mass spectrometry, which demonstrated that the protein preparation had a major species of 50.623 kDa with several minor species representing glycosylation variants.

The physical properties of sGMRα and sβc were further characterized by size-exclusion chromatography. We initially determined the retention times of sGMRα (Figure 2B), sβc (Figure 2C), GM-CSF (Figure 2D), and E21R (Figure 2G). The individual proteins eluted at 39.17 minutes for sGMRα, 34.75 minutes for sβc, 44.56 minutes for GM-CSF, and 44.11 minutes for E21R. External MW standards for calibration of the size-exclusion chromatography (Figure 2A) indicated that sGMRα, GM-CSF, and E21R were monomeric but that sβc was dimeric. The dimeric nature of sβc was confirmed by cross-linking experiments with purified sβc, which produced a covalent dimer with a MW of 100 kDa as determined by SDS-PAGE (see Figure 8B). The observation that sβc exists as a dimer is consistent with a recent report describing the structure of the extracellular domain of βc expressed in insect cells.[30,34] We observed that both the ligands and the receptor components eluted from size-exclusion chromatography

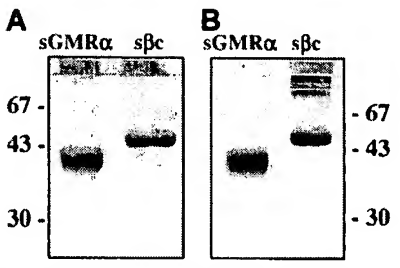

Figure 1. SDS-PAGE analysis of purified sGMRα and sβc. Soluble GMRα and sβc were produced by Sf21 cells infected with recombinant baculovirus encoding appropriate cDNA and affinity purified from the supernatant as described in "Materials and methods." Soluble GMRα (1 μg) and sβc (0.5 μg) were fractionated by 10% SDS-PAGE under reducing (A) and nonreducing (B) conditions and silver stained. The positions of molecular weight markers are shown in kilodaltons.

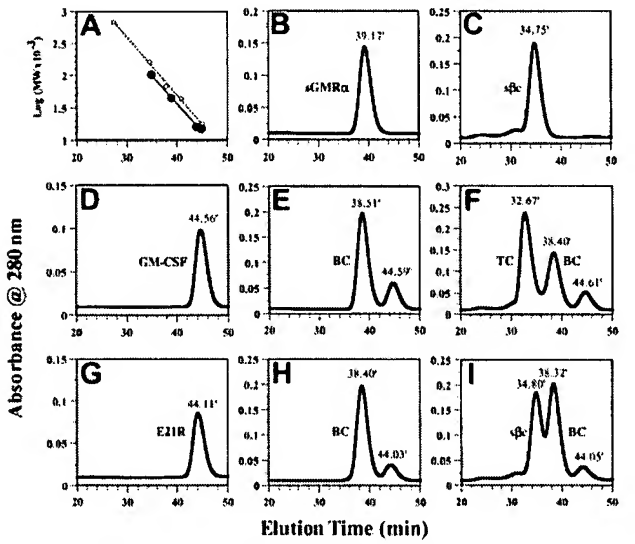

Figure 2. GM-CSF but not the GM-CSF analog E21R induces the assembly of the ternary GM-CSF receptor complex in solution. The presence and molecular weight of individual proteins and protein complexes were determined using size-exclusion chromatography as described in "Materials and methods." (A) Linear regression of $\log_{10}$ (MW × 10^{-3}) versus elution times using external (○) and internal (●) standards for calibration of the column. (B-I) Individual proteins sGMRα (B), sβc (C), GM-CSF (D), and E21R (G) were applied separately. Mixtures of sGMRα (6 μM) and GM-CSF (12 μM) (E); sβc (3 μM), sGMRα (6 μM), and GM-CSF (12 μM) (F); sGMRα (6 μM) and E21R (12 μM) (H); sβc (3 μM), sGMRα (6 μM), and E21R (12 μM) (I) were incubated for 1 hour before being applied to the column. The number above each peak represents elution time. Peaks containing binary (BC) or ternary (TC) complexes are indicated.

earlier than expected from the elution times of the external MW standards (Figure 2A). We chose to use the proteins of interest as internal MW standards and constructed a calibration curve for the internal MW standards that is parallel to that constructed from the external MW standards (Figure 2A). This is expected to provide a superior estimate of the masses of the receptor complexes.

Soluble GMRα interactions with GM-CSF and E21R

Purified sGMRα (6 μM) was incubated with GM-CSF (12 μM) and fractionated on a Superdex 200 column, producing a modest shift (from 39.17 minutes to 38.51 minutes) in the elution time of sGMRα (Figure 2E). The shifted peak, with an apparent MW of 48 kDa, contained both GM-CSF and sGMRα as determined by SDS-PAGE analysis of fractions (data not shown). The MW of the GM-CSF/sGMRα binary complex is consistent with a stoichiometry of 1:1 as has previously been described.[35] The complete peak shifts observed when sGMRα binds GM-CSF suggest that all of this soluble receptor is competent to bind ligand. Saturation binding experiments revealed that GM-CSF bound to sGMRα with a dissociation constant (K_d) of 1.5 to 9 nM, similar to that seen with cell surface–expressed GMRα (data not shown).

Purified sGMRα (6 μM) was incubated with E21R (12 μM) and fractionated on a Superdex 200 column, producing a modest shift (from 39.17 minutes to 38.40 minutes) in the elution time of sGMRα (Figure 2H). The shifted peak, with an apparent MW of 49 kDa, contained both E21R and sGMRα as determined by SDS-PAGE analysis of fractions (data not shown). The MW of the E21R:sGMRα binary complex is consistent with a stoichiometry of 1:1.

The sβc induces the formation of a GM-CSF ternary complex

Purified sβc (3 μM) was incubated with sGMRα (6 μM) plus GM-CSF (12 μM) and fractionated on a Superdex 200 column,

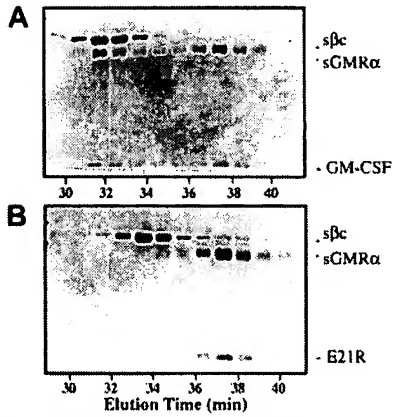

Figure 3. SDS-PAGE analysis of the ternary GM-CSF receptor complex. Mixtures of sβc, sGMRα, and either GM-CSF (A) or E21R (B) were analyzed by size-exclusion chromatography as described for Figure 2F and I. Fractions were collected at 1-minute intervals, fractionated by 12.5% SDS-PAGE under reducing conditions, and silver stained.[33] The positions of individual components are indicated.

producing a complete shift in the elution time of sβc (from 34.75 minutes to 32.67 minutes) as well as peaks corresponding to the binary complex at 38.40 minutes and free ligand at 44.61 minutes (Figure 2F). The peak eluting at 32.67 minutes had an apparent MW of 155 kDa and contained GM-CSF, sGMRα, and sβc as determined by SDS-PAGE analysis of fractions (Figure 3A). The MW of this ternary GM-CSF receptor complex is consistent with a stoichiometry of 1 GM-CSF:1 sGMRα:2 sβc.

In contrast, no ternary complex was observed when purified sβc (3 μM) was incubated with sGMRα (6 μM) plus E21R (12 μM) and fractionated on a Superdex 200 column (Figure 2I). Whereas the binary complex eluting at 38.32 minutes contained E21R and sGMRα, the peak at 34.80 minutes contained sβc but no sGMRα or E21R as determined by SDS-PAGE analysis of fractions (Figure 3B).

E21R disrupts the formation of the ternary GM-CSF receptor complex

To investigate whether the formation of a binary complex was an intermediate step in the formation of the ternary GM-CSF receptor complex, we tested the effect of E21R in this process. Purified sβc (3 μM) was incubated with sGMRα (6 μM) and GM-CSF (12 μM) for 1 hour. A 100-fold molar excess of E21R was then added, and after a further 1-hour incubation the mixture was fractionated on a Superdex 200 column. In the absence of E21R the ternary GM-CSF receptor complex eluted at 33.12 minutes (Figure 4). Significantly, in the presence of a 100-fold molar excess of E21R (Figure 4) there was a reduction in the amount of ternary GM-CSF receptor complex and an increase in its elution time (34.10 minutes), more comparable with the elution time of free sβc (34.75 minutes). The

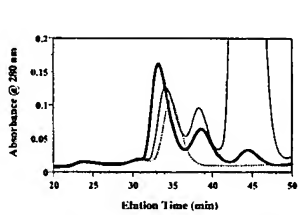

Figure 4. E21R prevents formation of the ternary GM-CSF receptor complex. Following formation of the GM-CSF/sGMRα/sβc ternary complex using a 1:2:4 molar ratio, a 100-fold molar excess of E21R over GM-CSF was added for a further hour at 25°C before size-exclusion chromatography. The chromatogram shows the A_{280} profile of a GM-CSF/sGMRα/sβc mixture in the absence (thick line) or presence of E21R (thin line) or in sβc alone (dashed line).

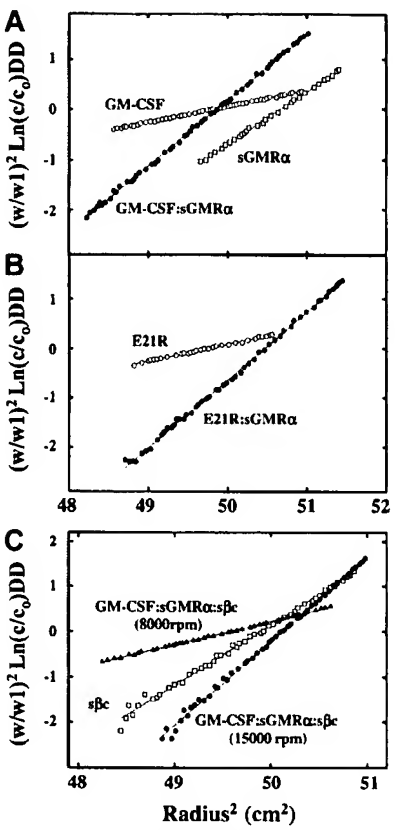

Figure 5. Analyses of the ternary GM-CSF receptor complex by sedimentation equilibrium. The individual proteins or protein complexes in 150 mM NaCl/50 mM sodium phosphate, pH 7.0, were centrifuged at 20°C at angular velocity, W rpm, for 16 hours. The equilibrium profiles are presented as $(W/W1)^2$ $Ln(c/c_0)$ versus the square of the radial distance, where c/c_0 is the optical density at 280 nm divided by the initial optical density and W1 is 20 000 rpm. For a single species, this plot is linear with a slope proportional to the molecular weight of the sedimenting species. The initial concentrations were in the range 0.40 to 0.47 mg/mL, and samples were centrifuged at 20 000 rpm except for E21R, where the initial concentration was 0.2 mg/mL and the angular velocity 15 000 rpm. Panel A samples: GM-CSF (○), sGMRα (□), GM-CSF/sGMRα complex (●). Panel B samples: E21R (○), E21R/sGMRα complex (●). Panel C samples: purified sβc (□) was centrifuged at 15 000 rpm with an initial concentration of 0.45 mg/mL, whereas the GM-CSF/sGMRα/sβc ternary complex at an initial concentration of 0.47 mg/mL was centrifuged at either 8000 rpm (▲) or 15 000 rpm (●) for 16 hours at 20°C.

reduction in the amount of ternary complex along with an increased amount of binary complex (38.40 minutes) and free ligand (44.00 minutes) is consistent with sGMRα preferentially forming a binary complex with E21R, which is unable to recruit sβc into a ternary complex.

Stoichiometry of the ternary GM-CSF receptor complex

To confirm the 1 GM-CSF:1 sGMRα:2 sβc stoichiometry of the ternary GM-CSF receptor complex obtained by size-exclusion chromatography, we utilized 2 other complementary and independent methods. In one of these the molecular weights of the individual proteins and of the binary and ternary complexes were determined by sedimentation equilibrium. The results showed (Figure 5; Table 1) values similar to those obtained by gel filtration. The estimates of the molecular weight of the binary complexes GM-CSF/sGMRα, 52.7 kDa (Figure 5A; Table 1), and E21R/sGMRα, 54.8 kDa, (Figure 5B; Table 1), are consistent with a 1:1 stoichiometry. The molecular weight of the ternary GM-CSF/sGMRα/sβc complex was determined to be 135 kDa (Figure 5C and Table 1). This value is consistent with a model where one sβc dimer (97.4 kDa) associates with one GM-CSF/sGMRα binary complex (52.7 kDa) (Table 1) with a theoretical molecular weight of 150.1 kDa.

In a separate approach, we used radiolabeled GM-CSF as a tracer molecule. Purified sβc (0 to 7 μM) was titrated against a mixture of sGMRα (3.2 μM) and cold GM-CSF (7.3 μM) spiked with the GM-CSF analog ^{32}P-SGMKIN and subjected to size-exclusion chromatography as above. Addition of sβc to the GM-CSF/sGMRα mixture led to the dose-dependent formation of the ternary complex and depletion of the binary complex (Figure 6A). Once the concentration of sβc saturated the available binary complex, a shoulder appeared on the trailing edge of the ternary complex peak, presumably reflecting the presence of free sβc. Formation of the ternary complex was associated with a dose-dependent accumulation of radioactivity at the appropriate elution time of the ternary complex and was accompanied by a reduction of radioactivity at the elution time of the binary complex (Figure 6B). Titration of sβc did not lead to a reduction of radioactivity at the elution time of free ligand, although a modest shift at the leading edge of the free ligand peak was observed. We then determined the distribution of ^{32}P-SGMKIN into the ternary complex and expressed it as a percentage of total label in the ternary and binary complexes versus proportion of sβc present (Figure 6C). When compared with the theoretical distribution predicted for a ternary complex with a GM-CSF/sGMRα/sβc ratio of 1:1:2 or 2:2:2, the observed distribution was consistent with a 1:1:2 stoichiometry. The observed distribution only departed from the modeled linear distribution as the concentration of binary complex became limiting.

The use of radiolabeled GM-CSF also allowed us to investigate whether the presence of sβc in the ternary complex led to affinity conversion. GM-CSF spiked with the GM-CSF analog ^{32}P-SGMKIN was titrated against an equimolar mixture of sGMRα and sβc, allowed to equilibrate, and fractionated by size-exclusion chromatography. For each GM-CSF concentration point, radioactivity bound in the binary and ternary complexes was determined and the proportion in each complex was expressed as a percentage of total bound counts. We found (Figure 6D) a 4-fold preferential distribution of ^{32}P-SGMKIN into ternary complexes at subsaturating concentrations of ligand, indicating that the

Table 1. Sedimentation equilibrium analysis of the molecular weights of GM-CSF, E21R, sGMRα, sβc, and their complexes

Species	M (1-νρ)	ν	MW	Predicted MW	Predicted stoichiometry
GM-CSF	3 590	0.734	13 700	—	—
E21R	4 050	0.734	14 300	—	—
sGMRα	11 800	0.706	40 700	—	—
sβc	26 600	0.723	97 400	—	—
sGMRα plus GM-CSF	14 600	0.718	52 700	54 400	1:1
sGMRα plus E21R	15 400	0.714	54 800	55 000	1:1
sβc plus sGMRα plus GM-CSF	37 300	0.72	135 300	151 800	2:1:1

The buffer used was 150 mM NaCl/50 mM sodium phosphate, pH 7.0, and the temperature was 20°C. The complexes formed between GM-CSF and E21R with sGMRα and between GM-CSF, sGMRα, and sβc were isolated by gel filtration. The initial concentration used for all samples was between 0.40 and 0.47 mg/mL except for E21R, where the starting concentration was 0.2 mg/mL. The reduced molecular weights of the samples, M (1-νρ), were determined by direct fitting of the sedimentation data presented in Figure 5. These values were used to calculate the molecular weight (MW) of the sedimenting species using the partial specific volumes (ν) indicated.

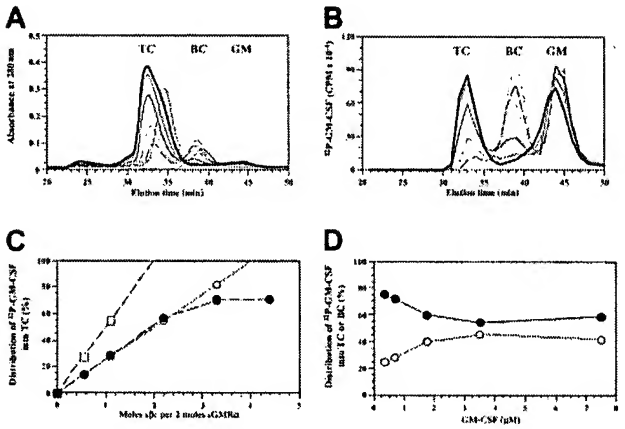

Figure 6. Radiolabeled GM-CSF differentially partitions to the ternary GM-CSF receptor complex. (A-C) A titration of purified sβc (0 to 7.03 μM) against a mixture of 3.2 μM sGMRα and 7.3 μM GM-CSF spiked with ^{32}P-labeled SGMKIN. Reaction mixes were set up with 0 (dashed gray), 0.88 μM (dashed black), 1.76 μM (thin gray), 3.52 μM (thin black), 5.27 μM (thick gray), or 7.03 μM (thick black) sβc and incubated at 25°C for 1 hour before size-exclusion chromatography. Fractions were collected at 1-minute intervals. A control reaction was also prepared with 5.27 μM sβc and 3.2 μM sGMRα but no GM-CSF (dashed black). (A) Chromatogram of A_{280} profiles for each sample with the location of the ternary complex (TC), binary complex (BC), and free ligand (GM) indicated. (B) Distribution of radioactivity among the ternary complex, binary complex, and free ligand for the reactions described in panel A. (C) Radioactive GM-CSF distributed into the ternary complex, expressed as a percentage of the total radioactive GM-CSF in ternary and binary complexes; comparing experimentally observed values for the reactions described in panel A (●) with a theoretical distribution based on 1GM:1α:2β (○) and 2GM:2α:2β (□) models. (D) Titration of GM-CSF (0 to 7 μM) spiked with ^{32}P-labeled SGMKIN against a mixture of 3.5 μM sGMRα and 3.5 μM sβc. Reaction mixes were allowed to reach equilibrium at 25°C for at least 2 hours before being fractionated by size-exclusion chromatography. The distribution of radioactivity among ternary (●) and binary (○) complexes was determined and the radioactivity in each complex was expressed as a percentage of total bound counts where counts in TC plus counts in BC is 100%.

presence of sβc in the ternary complex induces a measurable degree of affinity conversion.

GM-CSF binds sβc in the absence of sGMRα

Initial chromatography experiments at approximately equimolar concentrations indicated that GM-CSF was unable to form a complex with sβc in the absence of sGMRα. However, close inspection of the elution profile of radiolabeled GM-CSF in the presence of free sβc (Figure 6B) revealed a modest decrease in the elution time of GM-CSF suggestive of a weak interaction between sβc and GM-CSF. To investigate this further and to determine the specificity of this interaction, we titrated sβc against GM-CSF or the E21R analog (Figure 7). Titration of sβc against GM-CSF had a dose-dependent effect on GM-CSF peak height with a concomitant spreading of the GM-CSF profile to earlier elution times (Figure 7A). Titration of sβc against E21R had no effect on E21R elution time or profile (Figure 7B). These results show that GM-CSF directly interacts with sβc through the functionally important Glu21

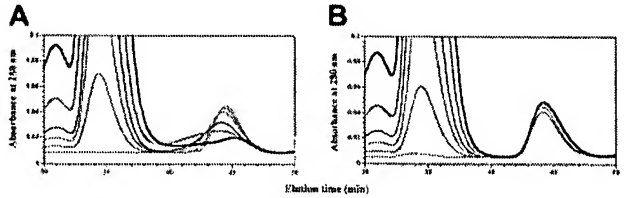

Figure 7. GM-CSF binds directly to βc. Purified sβc was titrated (0 to 20 μM) against 5 μM GM-CSF (A) or 5 μM E21R (B). Reaction mixes were set up with 0 (dashed black), 1 μM (thin black), 2.5 μM (medium gray), 5 μM (medium black), 10 μM (thick gray), or 20 μM (thick black) sβc, incubated at 25°C for 2 hours, and fractionated by size-exclusion chromatography.

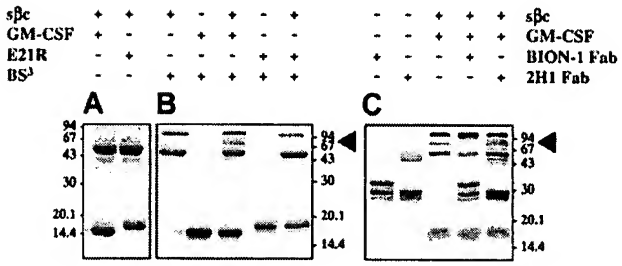

Figure 8. Discrete regions in GM-CSF and βc mediate their direct interaction. Purified sβc was incubated at 25°C for 1 hour alone or in the presence of either GM-CSF or E21R. Samples were left untreated (A) or were treated for 10 minutes with BS^3 cross-linker (B). To determine if GM-CSF was interacting with the cytokine-binding site in the fourth domain of βc, purified sβc was preincubated with a Fab fragment of the neutralizing anti-βc mAb, BION-1, or the nonneutralizing control anti-βc mAb, 2H1. GM-CSF was then allowed to bind and the mixture and individual mAb treated with BS^3 cross-linker (C). Samples were analyzed on 12.5% (A) or 10% (B-C) SDS-PAGE gels and stained with Coomassie. The positions of molecular weight markers are shown in kilodaltons, and the position of sβc cross-linked to GM-CSF is indicated by ◀.

residue and that substitution of this residue makes a qualitative difference to the GMRα-independent recognition of βc by GM-CSF.

A second approach confirmed the direct interaction of GM-CSF with βc and extended these findings to the identification of the reciprocal region in βc. We incubated purified sβc with a 3-fold molar excess of GM-CSF or E21R, treated with the BS^3 cross-linker and analyzed the mixture by SDS-PAGE under reducing conditions (Figure 8). No covalent interactions between sβc and GM-CSF or E21R were observed in the absence of cross-linker (Figure 8A). GM-CSF and E21R were not dimerized by cross-linker under the conditions used, whereas the sβc dimer was partially cross-linked, yielding a band of MW 100 kDa (Figure 8B). Significantly, when GM-CSF was incubated with sβc and cross-linked, a unique band of MW 70 kDa was observed (Figure 8B). Western blotting with anti-βc or anti–GM-CSF antibodies showed that this band contains both sβc and GM-CSF (data not shown). E21R could not be cross-linked directly to sβc as seen by the absence of the 70 kDa band (Figure 8B), thus confirming that Glu21 of GM-CSF is necessary for direct contact with βc. Neither the structurally related cytokine human growth hormone nor sGMRα was able to be cross-linked to sβc under these conditions (data not shown).

To determine if the interaction between sβc and GM-CSF was occurring through a functionally relevant region of βc, we used BION-1, a mAb that blocks GM-CSF, IL-3, and IL-5 binding and signaling through βc.[24] BION-1 recognizes a discrete region in the fourth domain of βc associated with high-affinity GM-CSF binding and function.[20,22,36] Preincubation of sβc with BION-1 Fab fragment prevented GM-CSF from being cross-linked to sβc, as seen by the absence of the 70-kDa band (Figure 8C). The Fab fragment of a mAb that binds to the fourth domain of βc but does not block cytokine binding was unable to perturb the cross-linking of sβc to GM-CSF (Figure 8C).

Discussion

We report here the first demonstration of a fully assembled GM-CSF/GM-CSF receptor ternary complex in solution and describe the molecular interactions required for its formation. It is shown that the ternary complex exhibits a novel mode of cytokine receptor assembly that comprises 1 molecule of GM-CSF and 1 molecule of GM-CSF receptor α chain interacting monovalently with a noncovalently linked dimer of βc. In addition, a direct interaction between GM-CSF and βc in the absence of the receptor

α chain could be demonstrated. The recruitment of βc as a preformed dimer may facilitate receptor activation and may also represent a mechanism utilized by the related IL-3 and IL-5 receptors. The GM-CSF ternary complex was demonstrated by gel filtration and sedimentation equilibrium analyses to have a molecular weight of between 135 kDa and 156 kDa, consistent with a GM-CSF/sGMRα/sβc stoichiometry of 1:1:2. In addition, the relative distribution of radiolabeled GM-CSF fitted a ternary complex with a 1:1:2 stoichiometry. The preferential distribution of radiolabeled GM-CSF into the ternary complex is indicative of sβc-mediated, affinity conversion. No disulfide linkages between receptor subunits were observed; there were no differences seen when the ternary complex was analyzed by SDS-PAGE under either reducing or nonreducing conditions or when the free cysteine groups in sβc were blocked with iodoacetamide (data not shown). These results are consistent with previous reports suggesting that GM-CSF receptor heterodimerization is required to activate the GM-CSF receptor,[25] the dimeric nature of βc observed both on the cell surface and in solution,[26,28,30] the affinity conversion afforded by βc,[15,20] and the requirement of at least a βc dimer for function and activation of downstream signaling molecules.[28,29] The intermediate binding affinity for GM-CSF in the ternary complex is consistent with a report describing the low-affinity binding of murine GM-CSF to detergent-solubilized GM-CSF receptors extracted from a murine cell line.[37] In addition, these results do not rule out the formation of higher-order complexes on the cell surface,[27,38] which may lead to further affinity conversion and disulfide linkage required for receptor stabilization, activation, or internalization purposes. The assembly of the human GM-CSF receptor shown here is different from that seen for the IL-6[39] and LIF[40] receptors, which exhibit a stoichiometry of 2:2:2 and 1:1:1, respectively. Interestingly, the dynamics of the GM-CSF receptor assembly are analogous to the IL-6 receptor in that following the binding of ligand to the major binding subunit (α chain) there is recruitment of the signaling subunit (βc or gp130). However, although dimerization of gp130 requires a second IL-6/IL-6Rα chain binary complex, this is not the case with βc, which is recruited to a single GM-CSF/sGMRα binary complex as a preformed dimer. Despite the dimeric nature of sβc and even in the presence of a 2-fold molar excess of the GM-CSF/sGMRα binary complex, we saw no evidence for the formation of a ternary complex with a stoichiometry of 2:2:2. The functional monovalency of sβc may be due to conformational changes within the sβc dimer, induced by the binding of one GM-CSF/sGMRα binary complex that prevents the binding of a second binary complex.

The recruitment of sβc to the GM-CSF/sGMRα binary complex occurs through functionally relevant sites in GM-CSF and βc itself. This is demonstrated by the inability of the GM-CSF analog E21R to form the ternary complex and by the inhibition of sβc cross-linking to GM-CSF by the anti-βc mAb BION-1, which blocks the high-affinity binding of GM-CSF.[24] Given that there is an homologous glutamic acid in IL-3 (position 22) and in IL-5 (position 13) and the fact that BION-1 also blocks high-affinity binding of IL-3 and IL-5, it is possible that this mode of receptor assembly will also apply to the IL-3 and IL-5 receptors. The recruitment of dimerized βc and associated JAK-2 molecules may facilitate receptor phosphorylation and activation in this subfamily of receptors. Using a soluble receptor system we could detect for the first time a direct interaction between GM-CSF and βc in the absence of the GM-CSF receptor α subunit. We observed this by gel filtration (Figure 7) and cross-linking studies (Figure 8). The interaction was sensitive to the E21R substitution and the mAb BION-1, indicating that the direct interaction observed between GM-CSF and sβc is chemically and spatially equivalent to the interaction that occurs with the cell membrane–anchored receptor. Considering that all βc-interacting cytokines do so through a chemically and structurally conserved mechanism,[36] it is likely that a direct interaction between βc and IL-3 or IL-5 will also exist. The relative affinity of the direct βc interaction for each cytokine may help to explain differences in βc-mediated affinity conversion in the high-affinity binding of IL-3, GM-CSF, or IL-5. Despite the direct interaction of βc with GM-CSF seen in the soluble system, this may not be sufficient to activate the receptor in vivo given the very high concentrations of both receptor and ligand needed to detect this weak interaction (in the micromolar range) and the fact that GMRα intracellular domain has been previously shown to be crucial for GM-CSF signaling.[41]

In the IL-4 system, a high-affinity (K_d = 0.15 nM) interaction between IL-4 and the IL-4 receptor α chain[42] utilizes a chemically and structurally homologous mechanism, suggesting that the type of direct interaction we observed between GM-CSF and βc may be conserved among other cytokines. The direct interaction we detected between GM-CSF and sβc also suggests that conformational changes in the GM-CSF/sGMRα binary complex may not be necessary for the recruitment of βc. However, the monovalent binding of the GM-CSF/sGMRα binary complex to sβc suggests the possibility of an induced conformational change within the extracellular domain of sβc. Conformational changes in the cytoplasmic region of βc may be induced by the assembly of the ternary complex to promote βc/JAK-2 proximity and receptor activation as shown for the erythropoietin receptor.[43] The assembly of the human GM-CSF receptor system in solution described herein also provides a useful tool for investigating its dynamics and structural requirements. The initial event in activation of the GM-CSF receptor is the binding of ligand to the GMRα with low affinity prior to recruitment of βc. The soluble system used here revealed a 1:1 stoichiometry of binding between the sGMRα chain and GM-CSF with a K_d equivalent to that seen with the full-length GMRα on the cell surface. We were able to show that E21R, a GM-CSF analog defective in high-affinity binding and a specific GM-CSF antagonist currently in phase 2 clinical trials, also binds sGMRα with a 1:1 stoichiometry. Importantly, E21R is incapable of forming a ternary receptor complex and when present in excess is able to prevent the formation of the ternary GM-CSF receptor complex, thus explaining its antagonistic activity. This set of experiments also demonstrates that the assembly of the GM-CSF receptor is a sequential process that involves first the formation of a binary complex. In structural terms it will be interesting to use single point mutants of βc to examine the residues that participate in direct contact with GM-CSF or the GM-CSF receptor α chain. This may be also a useful system for the identification of small molecules that prevent the formation of the ternary complex. Finally, the assembly of the human GM-CSF ternary complex in solution should aid in its crystallization and ultimately in the solving of its structure.

References

1. Lopez AF, Williamson DJ, Gamble JR, et al. Recombinant human granulocyte-macrophage colony-stimulating factor stimulates in vitro mature human neutrophil and eosinophil function, surface receptor expression, and survival. J Clin Invest. 1986;78:1220-1228.
2. Metcalf D, Begley CG, Williamson DJ, et al. Hemopoietic responses in mice injected with purified recombinant murine GM-CSF. Exp Hematol. 1987;15:1-9.
3. Gasson JC. Molecular physiology of granulocyte-macrophage colony-stimulating factor. Blood. 1991;77:1131-1145.
4. Metcalf D. Hematopoietic regulators: redundancy or subtlety? Blood. 1993;82:3515-3523.
5. Rabinowe SN, Neuberg D, Bierman PJ, et al. Long-term follow-up of a phase III study of recombinant human granulocyte-macrophage colony-stimulating factor after autologous bone marrow

transplantation for lymphoid malignancies. Blood. 1993;81:1903-1908.

6. Bilgin K, Yaramis A, Haspolat K, Tas MA, Gunbey S, Derman O. A randomized trial of granulocyte-macrophage colony-stimulating factor in neonates with sepsis and neutropenia. Pediatrics. 2001;107:36-41.
7. Bradstock KF. The use of hematopoietic growth factors in the treatment of acute leukemia. Curr Pharm Des. 2002;8:343-355.
8. Vazquez JA, Hidalgo JA, De Bono S. Use of sargramostim (rh-GM-CSF) as adjunctive treatment of fluconazole-refractory oropharyngeal candidiasis in patients with AIDS: a pilot study. HIV Clin Trials. 2000;1:23-29.
9. Mellman I, Steinman RM. Dendritic cells: specialized and regulated antigen processing machines. Cell. 2001;106:255-258.
10. Barouch DH, Santra S, Tenner-Racz K, et al. Potent CD4+ T cell responses elicited by a bicistronic HIV-1 DNA vaccine expressing gp120 and GM-CSF. J Immunol. 2002;168:562-568.
11. Sun X, Hodge LM, Jones HP, Tabor L, Simecka JW. Co-expression of granulocyte-macrophage colony-stimulating factor with antigen enhances humoral and tumor immunity after DNA vaccination. Vaccine. 2002;20:1466-1474.
12. Shaver JR, Zangrilli JG, Cho S-K, et al. Kinetics of the development and recovery of the lung from IgE-mediated inflammation: dissociation of pulmonary eosinophilia, lung injury, and eosinophil-active cytokines. Am J Crit Care Med. 1997;155: 442-448.
13. Cook AD, Braine EL, Campbell IK, Rich MJ, Hamilton JA. Blockade of collagen-induced arthritis post-onset by antibody to granulocyte-macrophage colony-stimulating factor (GM-CSF): requirement for GM-CSF in the effector phase of disease. Arthritis Res. 2001;3:293-298.
14. Gearing DP, King JA, Gough NM, Nicola NA. Expression cloning of a receptor for human granulocyte-macrophage colony-stimulating factor. EMBO J. 1989;8:3667-3676.
15. Hayashida K, Kitamura T, Gorman DM, Arai K, Yokota T, Miyajima A. Molecular cloning of a second subunit of the receptor for human granulocyte-macrophage colony-stimulating factor (GM-CSF): reconstitution of a high-affinity GM-CSF receptor. Proc Natl Acad Sci U S A. 1990;87: 9655-9659.
16. Hercus TR, Cambareri B, Dottore M, et al. Identification of residues in the first and fourth helices of human granulocyte-macrophage colony-stimulating factor involved in binding to the α- and β-chains of the receptor. Blood. 1994;83:3500-3508.
17. Rajotte D, Cadieux C, Haman A, et al. Crucial role of the residue R280 at the F'-G' loop of the human granulocyte/macrophage colony-stimulating factor receptor α chain for ligand recognition. J Exp Med. 1997;185:1939-1950.
18. Lopez AF, Shannon MF, Hercus T, et al. Residue 21 of human granulocyte-macrophage colony-stimulating factor is critical for biological activity and for high but not low affinity binding. EMBO J. 1992;11:909-916.
19. Hercus TR, Bagley CJ, Cambareri B, et al. Specific human granulocyte-macrophage colony-stimulating factor antagonists. Proc Natl Acad Sci U S A. 1994;91:5838-5842.
20. Woodcock JM, Zacharakis B, Plaetinck G, et al. Three residues in the common β chain of the human GM-CSF, IL-3 and IL-5 receptors are essential for GM-CSF and IL-5 but not IL-3 high affinity binding and interact with Glu21 of GM-CSF. EMBO J. 1994;13:5176-5185.
21. Lock P, Metcalf D, Nicola NA. Histidine-367 of the human common β chain of the receptor is critical for high-affinity binding of human granulocyte-macrophage colony-stimulating factor. Proc Natl Acad Sci U S A. 1994;91:252-256.
22. Woodcock JM, Bagley CJ, Zacharakis B, Lopez AF. A single tyrosine residue in the membrane-proximal domain of the GM-CSF, IL-3 and IL-5 receptor common β chain is necessary and sufficient for high affinity binding and signalling by all three ligands. J Biol Chem. 1996;271:25999-26006.
23. Haman A, Cadieux C, Wilkes B, et al. Molecular determinants of the granulocyte-macrophage colony-stimulating factor receptor complex assembly. J Biol Chem. 1999;274:34155-34163.
24. Sun Q, Jones K, McClure B, et al. Simultaneous antagonism of interleukin-5, granulocyte-macrophage colony-stimulating factor, and interleukin-3 stimulation of human eosinophils by targetting the common cytokine binding site of their receptors. Blood. 1999;94:1943-1951.
25. Eder M, Ernst TJ, Ganser A, et al. A low affinity chimeric human α/β-granulocyte-macrophage colony-stimulating factor receptor induces ligand-dependent proliferation in a murine cell line. J Biol Chem. 1994;269:30173-30180.
26. Stomski FC, Sun Q, Bagley CJ, et al. Human interleukin-3 (IL-3) induces disulphide-linked receptor α and β chain heterodimerization which is required for receptor activation but not high affinity binding. Mol Cell Biol. 1996;16:3035-3046.
27. Lia F, Rajotte D, Clark SC, Hoang T. A dominant negative granulocyte-macrophage colony-stimulating factor receptor α chain reveals the multimeric structure of the receptor complex. J Biol Chem. 1996;271:28287-28293.
28. Muto A, Watanabe S, Miyajima A, Yokota T, Arai K-I. The β subunit of human granulocyte-macrophage colony-stimulating factor receptor forms a homodimer and is activated via association with the α subunit. J Exp Med. 1996;183:1911-1916.
29. McClure BJ, Woodcock JM, Harrison-Findik D, Lopez AF, D'Andrea RJ. GM-CSF binding to its receptor induces oligomerisation of the common β-subunit. Cytokine. 2001;14:240-243.
30. Carr PD, Gustin SE, Church AP, et al. Structure of the complete extracellular domain of the common β subunit of the human GM-CSF, IL-3, and IL-5 receptors reveals a novel dimer configuration. Cell. 2001;104:291-300.
31. Iversen PO, Lewis ID, Turczynowicz S, et al. Inhibition of granulocyte-macrophage colony-stimulating factor prevents dissemination and induces remission of juvenile myelomonoytic leukemia in engrafted immunodeficient mice. Blood. 1997;90: 4910-4917.
32. Kaelin WG Jr, Krek W, Sellers WR, et al. Expression cloning of a cDNA encoding a retinoblastoma-binding protein with E2F-like properties. Cell. 1992;70:351-364.
33. Morrissey JH. Silver stain for proteins in polyacrylamide gels: a modified procedure with enhanced uniform sensitivity. Anal Biochem. 1981; 117:307-310.
34. Gustin S, Church A, Ford S, et al. Expression, crystallization and derivatization of the complete extracellular domain of the β_c subunit of the human IL-5, IL-3 and GM-CSF receptors. Eur J Biochem. 2001;268:2905-2911.
35. Brown CB, Pihl CE, Murray EW. Oligomerization of the soluble granulocyte-macrophage colony-stimulating factor receptor: identification of the functional ligand-binding species. Cytokine. 1997; 9:219-225.
36. Rossjohn J, McKinstry WJ, Woodcock JM, et al. Structure of the activation domain of the GM-CSF/IL-3/IL-5 receptor common β chain bound to an antagonist. Blood. 2000;95:2491-2498.
37. Nicola NA, Cary D. Affinity conversion of receptors for colony stimulating factors: properties of solubilized receptors. Growth Factors. 1992;6: 119-129.
38. Bagley CJ, Woodcock JM, Stomski FC, Lopez AF. The structural and functional basis of cytokine receptor activation: lessons from the common β subunit of the granulocyte-macrophage colony-stimulating factor, interleukin-3 (IL-3) and IL-5 receptors. Blood. 1997;89:1471-1482.
39. Ward LD, Howlett GJ, Discolo G, et al. High affinity interleukin-6 receptor is a hexameric complex consisting of two molecules each of interleukin-6, interleukin-6 receptor, and gp-130. J Biol Chem. 1994;269:23286-23289.
40. Zhang JG, Owczarek CM, Ward LD, et al. Evidence for the formation of a heterotrimeric complex of leukaemia inhibitory factor with its receptor subunits in solution. Biochem J. 1997;325(pt 3):693-700.
41. Ronco LV, Silverman SL, Wong SG, Slamon DJ, Park LS, Gasson JC. Identification of conserved amino acids in the human granulocyte-macrophage colony-stimulating factor receptor α subunit critical for function: evidence for formation of a heterodimeric receptor complex prior to ligand binding. J Biol Chem. 1994;269:277-283.
42. Hage T, Sebald W, Reinemer P. Crystal structure of the interleukin-4/receptor α chain complex reveals a mosaic binding interface. Cell. 1999;97: 271-281.
43. Remy I, Wilson IA, Michnick SW. Erythropoietin receptor activation by a ligand-induced conformation change. Science. 1999;283:990-993.

Immunity, Vol. 2, 211–222, March, 1995, Copyright © 1995 by Cell Press

Mice Deficient for the IL-3/GM-CSF/IL-5 βc Receptor Exhibit Lung Pathology and Impaired Immune Response, While β_{IL3} Receptor-Deficient Mice Are Normal

Ryuichi Nishinakamura,*†§ Naoki Nakayama,† Yoko Hirabayashi,‡ Tohru Inoue,‡ Dee Aud,* Tom McNeil,* Sadahiro Azuma,† Shosei Yoshida,† Yutaka Toyoda,† Ken-ichi Arai,† Atsushi Miyajima,* and Richard Murray*
*DNAX Research Institute
of Molecular and Cellular Biology
901 California Avenue
Palo Alto, California 94304-1104
†Institute of Medical Science
University of Tokyo
Tokyo 108
Japan
‡Department of Pathology I
Yokohama City University
School of Medicine
Yokohama 236
Japan
§First Department of Internal Medicine
Faculty of Medicine
University of Tokyo
Tokyo 113
Japan

Summary

The receptors for IL-3, GM-CSF, and IL-5 share a common β subunit (βc), and mice have an additional IL-3 β subunit (β_{IL3}). We have independently generated mice carrying null mutations of each molecule. βc mutant bone marrow showed no response to GM-CSF or IL-5, whereas IL-3 stimulation of βc or β_{IL3} mutant bone marrow was normal. βc mutant mice showed lung pathology consisting of lymphocytic infiltration and areas resembling alveolar proteinosis, and also exhibited low basal numbers of eosinophils. Infection of βc mutant mice by Nippostrongylus brasiliensis resulted in the absence of blood and lung eosinophilia. Animals repopulated with βc mutant bone marrow cells showed slower leukocyte recovery and reduced eosinophil numbers. These data define the role of βc in vivo, and show a phenotype that is likely to be the cumulative effect of loss of GM-CSF and IL-5 stimulation.

Introduction

Although interleukin-3 (IL-3), granulocyte–macrophage colony-stimulating factor (GM-CSF), and IL-5 show no significant amino acid sequence homology with each other, they exhibit a number of similarities. IL-3 stimulates the development of various lineages of hematopoietic cells, at least in colony assays, by interacting with immature multipotential hematopoietic progenitors as well as with lineage-committed progenitors, and thus was originally referred to as multicolony-stimulating factor (multi-CSF) (Arai et al., 1990). GM-CSF was originally defined as a factor that stimulates colony formation of granulocytes and macrophages, and has subsequently been shown to share many of the properties of IL-3 stimulation of cells (Metcalf, 1991). While IL-5 was cloned as a B cell differentiation factor in mice (Kinashi et al., 1986), it appears to have a role in the development of eosinophils in both mice and humans, an activity shared by IL-3 and GM-CSF (Takatsu et al., 1988). These three cytokines are closely linked on human chromosome 5 and mouse chromosome 11, and are produced by activated T cells and mast cells (Arai et al., 1990). They induce protein phosphorylation of similar proteins (Isfort and Ihle, 1990; Kanakura et al., 1990) and compete with each other in binding to their high affinity receptors (Lopez et al., 1990; Taketazu et al., 1991; Lopez et al., 1991). Curiously, this cross-competition was observed only in human hematopoietic cells, but not in mouse cells.

Molecular cloning of the receptor subunits has explained at least some of these observations. The high affinity receptors for human IL-3, GM-CSF, and IL-5 are composed of two subunits, α and β (Hayashida et al., 1990; Kitamura et al., 1991; Tavernier et al., 1991). The α subunits are specific for each cytokine and bind their ligand with low affinity. The human has only one type of β subunit (βc), which has no binding capacity by itself but forms high affinity receptors for IL-3, GM-CSF, and IL-5 with their respective α subunits.

In contrast with the human, the mouse has two homologous β subunits, βc and β_{IL3}, which were previously termed AIC2B and AIC2A, respectively (Itoh et al., 1990; Gorman et al., 1990). They are 56% identical to the human βc. Like the human βc, the mouse βc is the common β subunit for mouse IL-3, GM-CSF, and IL-5 receptors. Although β_{IL3} has an extensive sequence homology with mouse βc (91% identical at the amino acid level), β_{IL3} does not form a high affinity receptor with the mouse IL-5 or mouse GM-CSF α receptors. β_{IL3}, originally cloned as a mouse IL-3-binding protein, binds mouse IL-3 with low affinity. When transfected into cells, both βc and β_{IL3} interact equally well with the mouse IL-3 α subunit in the presence of IL-3 to form high affinity IL-3 receptors and to transmit a proliferation signal. (Hara and Miyajima, 1992). The genes encoding these two β subunits are closely linked on mouse chromosome 15, and their exon–intron structures are almost identical (Gorman et al., 1992). Thus, they are likely products of a gene duplication event after the divergence of mouse and human. Why the mouse has two β subunits remains to be explained.

As many studies have examined the potential role of IL-3, GM-CSF, and IL-5 in hematopoietic development, as well as potential roles in infectious disease states and hematopoietic crises (Antman et al., 1988; Nemunaitis et al., 1988; Coffman et al., 1989), we reasoned that targeted disruption of the βc and β_{IL3} receptor chain genes in the mouse would allow us to evaluate collectively the functions of the cytokines in vivo. In this report, we describe the production and characterization of mutant mice for βc and

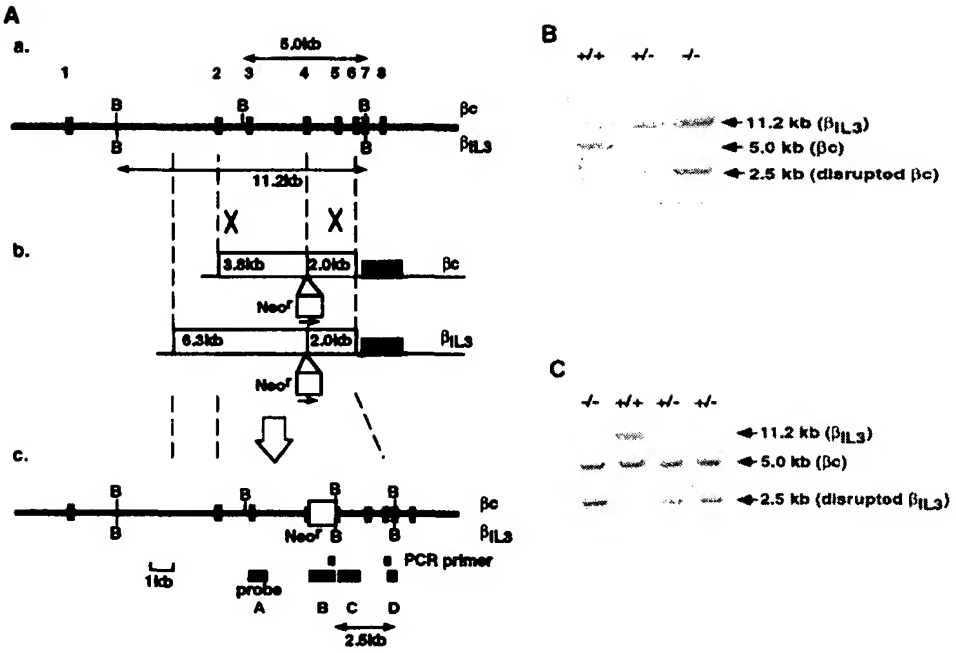

Figure 1. Targeting Strategy of βc and β_{IL3} Genes

(A) (a) Genomic structure and restriction maps of wild-type βc and β_{IL3} genes. The upper part of the central horizontal line is for βc and the lower part for β_{IL3}. B indicates BamHI sites. The closed squares show the exons. (b) Targeting vectors used to disrupt βc and β_{IL3}. The *neo*^{r} gene was inserted into exon 4. TK indicates herpes simplex virus thymidine kinase. (c) Predicted structure of the disrupted alleles. The upper part shows βc and the lower part β_{IL3}. Probe D was used for routine screening by Southern blot analysis.

(B) Southern blot analysis of wild-type (+/+), heterozygous (+/−), homozygous (−/−) βc mutant mice. Tail DNA was digested with BamHI and hybridized with probe D. Note that the band from βc gene disappeared in homozygous mutant mice, but the band from β_{IL3} remained intact.

(C) Southern blot analysis of wild-type (+/+), heterozygous (+/−), homozygous (−/−) β_{IL3} mutant mice. Tail DNA was digested with BamHI and hybridized with probe D. Note that the band from β_{IL3} gene disappeared in homozygous mutant mice, but the band from βc remained intact.

β_{IL3}. We examined intrinsic pathology of the mutants, cell lineage development in the mutant animals and in normal irradiated recipient animals receiving mutant bone marrow, and the response of the mutant animals to parasitic infections.

Results

Generation of Mice Homozygous for βc and β_{IL3} Mutations

The genes encoding βc and β_{IL3} were independently disrupted in E14.1 embryonic stem cells using conventional gene targeting techniques. A map of the βc and β_{IL3} locus and their representative gene-targeting vectors is shown in Figure 1A. In brief, the neomycin resistant gene (*neo*^{r}) was inserted into exon 4, which encodes the third and fourth cystein residues in the first repeat of the conserved motif of cytokine receptors. These constructs generate truncated molecules by introducing a stop codon and poly(A) addition signal. Alternative splicing from exon 3 to 5 would cause a frame shift mutation. A targeted disruption of the βc gene yielded a 2.5 kb BamHI fragment as opposed to a 5.0 kb wild-type fragment. β_{IL3} disruption yielded a 2.5 kb fragment as opposed to an 11.2 kb wild-type fragment (Figures 1B and 1C). Although the coding sequence of these two genes is 95% homologous, no evidence for a βc construct recombining at the β_{IL3} locus (or vice versa) was observed. Following injection of the homologous recombinants into blastocysts, we obtained chimeras able to transmit the mutations through the germline from two independent clones, both for βc and β_{IL3}. Heterozygous mice were intercrossed to obtain mice homozygous for the mutations (Figure 1B and 1C). Normal Mendelian segregation of the mutations was observed. Both βc and β_{IL3} mutants remained clinically healthy for 7 months of observation, and were fertile. The results described below were consistent in the two lines of mice, both for βc and β_{IL3} mutations.

To demonstrate that βc was disrupted, bone marrow cells from βc-deficient mice were stained with anti-βc-specific antibody (Figure 2A). As expected, βc was not detected. Staining of these same bone marrow cells with anti-β_{IL3}-specific antibody showed that expression of β_{IL3} was intact (data not shown). In the case of β_{IL3}-deficient mice, the results from FACS analysis were equivocal due to the weak background staining of anti-β_{IL3}-specific antibody. However, immunoblot analysis of bone marrow–derived mast cells showed no expression of β_{IL3} protein (Figure 2B). FACS analysis showed that expression of βc was intact in β_{IL3} mutant mice (data not shown).

Response of Mutant Cells to Cytokines

To investigate the response of βc- or β_{IL3}-deficient cells to various cytokines, methyl cellulose colony-forming unit

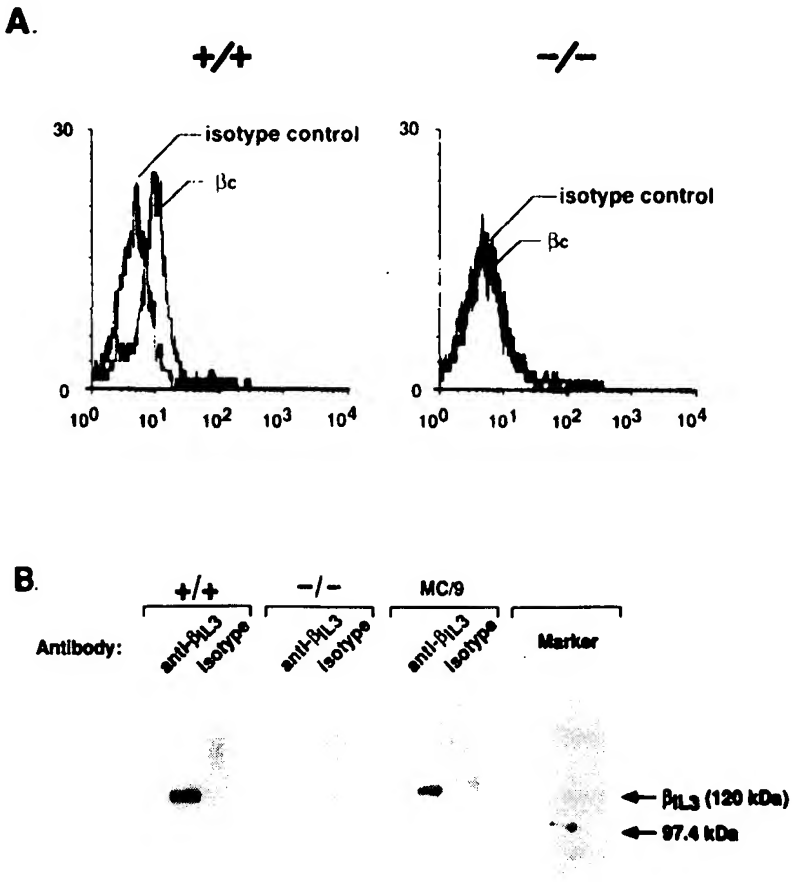

Figure 2. FACS Analysis and Immunoprecipitation of βc and β_{IL3}

(A) FACS analysis of bone marrow cells from wild-type (+/+) and βc-deficient (−/−) mice. Bone marrow cells were stained with either anti-βc-specific antibody or isotype control.

(B) Immunoblot analysis of bone marrow-derived mast cells. Bone marrow-derived mast cells from wild-type (+/+) or β_{IL3}-deficient mice (−/−) were lysed and immunoprecipitated with anti-β_{IL3}-specific antibody or isotype control, and blotted with anti-β_{IL3}-specific antibody. MC/9 cells were used as positive control.

(CFU) assays were performed using bone marrow cells (Table 1). βc-deficient cells did not respond to GM-CSF or IL-5, indicating that both GM-CSF and IL-5 receptors were disrupted functionally. However, βc-deficient cells did respond to IL-3 or IL-3 plus erythropoietin (EPO) normally. Colony types in IL-3 or IL-3 plus EPO plates were enumerated and no variations were seen, which indicates that β_{IL3} can transmit the IL-3 signal in the complete absence of βc. Eosinophil colonies were also detected in IL-3 or IL-3 plus EPO plates and were morphologically normal, suggesting that eosinophils were generated in vitro only by IL-3 in the absence of IL-5.

In contrast, β_{IL3}-deficient cells responded almost normally to IL-3, GM-CSF, and IL-5. This result showed that βc and β_{IL3} were redundant in terms of IL-3 stimulation, as well as confirming that β_{IL3} was not involved in the GM-CSF or IL-5 receptor system.

Normal multilineage colonies were formed from both βc and β_{IL3} mutant cells if a stimulus that is unrelated to the βc and β_{IL3} receptors, such as stem cell factor (SCF) was used.

Bone marrow cells were cultured in liquid media containing IL-3. Both βc- and β_{IL3}-deficient cells proliferated normally, and mast cells were generated after 35 days of culture. These mast cells were not different from wild-type cells in terms of proliferation in the presence of IL-3 and

Table 1. Colony-Forming Unit Assay from Mutant Bone Marrow

	Control	βc Mutant	Control*	β_{IL3} Mutant
GM-CSF	84.33 (12.58)	0.00 (0.00)	71.33 (7.51)	71.00 (7.94)
IL-5	6.00 (2.65)	0.00 (0.00)	10.00 (2.00)	9.00 (3.00)
IL-3	89.33 (12.58)	102.35 (18.90)	79.67 (12.01)	85.33 (6.66)
IL-3 plus EPO	102.67 (11.93)	93.00 (7.00)	91.00 (1.73)	90.67 (4.51)
SCF plus IL-6 plus EPO	65.67 (1.15)	66.33 (2.89)	56.00 (4.36)	67.00 (6.00)
EPO	1.67 (0.58)	0.67 (1.15)	4.33 (2.52)	4.67 (0.58)

Methyl cellulose colony assay to bone marrow cells from the mutant mice. Cells (2×10^4) were plated in each plate containing the cytokines indicated, and the total number of colonies was counted. Cells (4×10^4) were plated for IL-5 stimulation. Each type of stimulation was performed in triplicate and the mean (± standard deviation) is presented.

* The experiments for βc and β_{IL3} were performed independently, using their respective normal littermate controls. Three independent experiments were performed for both βc and β_{IL3}, and consistent results were obtained.

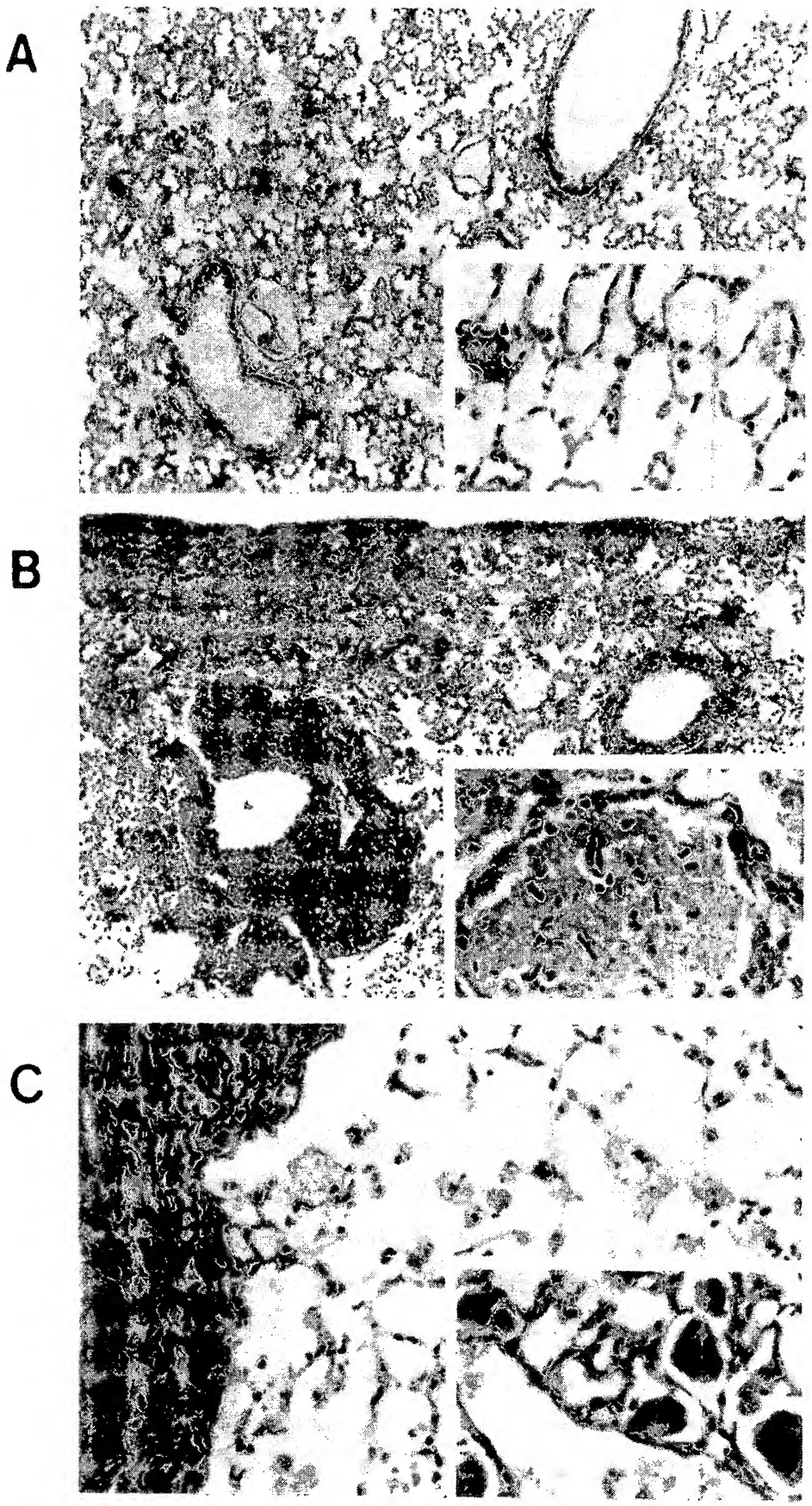

Figure 3. Pathologic Analysis of βc Mutant Lung Tissue

(A) Pulmonary tissue from the 10-week-old control mouse (84.6×). Inset, 338.4×.

(B) Pulmonary tissue from the 10-week-old βc mutant mouse. Note that peribronchovascular lymphocytic infiltration was seen along the two major bronchi and beneath the pleura next to the edematous alveoli with eosinophilic proteinous material (84.6×). Inset, an edematous area beneath the pleura with macrophages and necrotic cellular debris (338.4×).

(C) Pulmonary tissue from the 27-week-old βc mutant mouse. Foamy macrophages were seen in alveoli (338.4×). Inset, acellular PAS-positive proteinous material was observed in alveoli (338.4×).

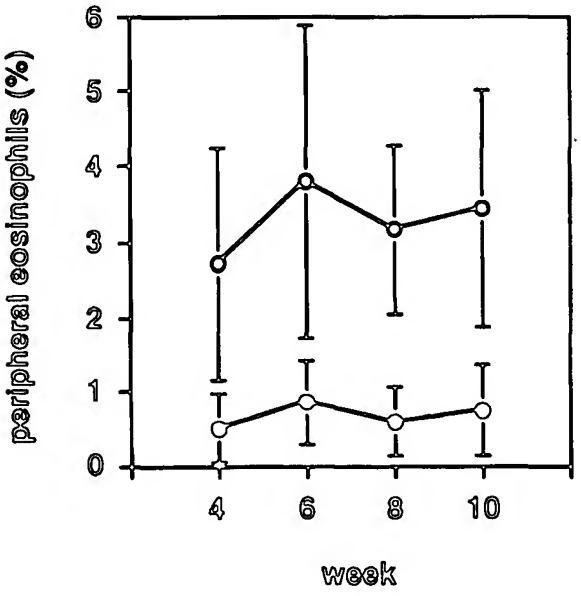

Figure 4. Eosinophils in βc-Deficient Mice

The percentage of eosinophils in the peripheral blood was examined over a 10 week period. The data represent the mean (± standard deviation) of eight mice in each group. Control, open circles; βc mutant, closed circles.

the staining patterns of granules (Wright–Giemsa, alcian blue, and safranin). There was no difference in connective tissue–type mast cells recovered from peritoneal washes, with respect to their frequency, proliferation in IL-3 plus IL-4, or staining patterns (data not shown).

Histological Characterization of Pulmonary Disease in βc-Deficient Mice

Pathologic examination of βc-deficient mice showed anomalous lung development, but no abnormalities were seen in β_{IL3}-deficient mice. Two seemingly separate findings were consistent in all βc-deficient animals: a focal but scattered intraalveolar proteinous substance and peribronchovascular lymphocytic infiltration of the tissue. Lungs from βc mutant mice were examined at 10 and 27 weeks of age to follow potential progression of the pathology.

The alveolar spaces of all βc mutants contained focal but scattered eosinophilic proteinous material with necrotic cellular debris and macrophages (Figure 3B), in clear contrast with control mice (Figure 3A). This pathology was often found beneath the pleura. Few inflammatory cells, such as neutrophils and lymphocytes, were observed directly in the focal lesions, suggesting that this disorder was not a secondary response to infections. In support of this, extensive pathogen screening revealed no bacterial, fungal, or viral infections in these animals (data not shown). Both 10- and 27-week-old mice showed intraalveolar material and this material was periodic acid Schiff's reaction (PAS) positive. In the older mice, the PAS-positive material was acellular (Figure 3C, inset). These findings resembled alveolar proteinosis (Rosen et al., 1958).

A second prominent finding in the lungs of βc mutants was peribronchovascular lymphocytic infiltration, and this infiltration was similar in mutant mice at both 10 and 27 weeks of age (Figure 3B). The infiltration was also detected in areas where no proteinosis was present, indicating that the infiltration was a primary event resulting from the βc mutation and not necessarily secondary to the proteinosis. In support of this, the infiltration was also seen in heterozygous mutant mice, to a milder extent and with no proteinosis (data not shown).

Additionally, there were many foamy macrophages in the alveoli of the 27-week-old mice (Figure 3C). In some cases, these cells contained PAS-positive material, suggesting that they could not degrade the ingested material (data not shown).

The findings of alveolar proteinosis-like disease and the lymphocytic infiltration are similar to the phenotype of GM-CSF-deficient mice (Dranoff et al., 1994; Stanley et al., 1994).

βc-Deficient Mice Had Impaired Eosinophil Development and Lacked Eosinophil Responses to Parasites

Examination of peripheral blood and bone marrow cells from βc- and β_{IL3}-deficient mice revealed that the βc mutants lacked normal numbers of eosinophils. Total peripheral leukocyte counts, differential counts (except for eosinophils), hemoglobin, and platelet counts were normal in both mutant mice. Bone marrow, spleen, and peritoneal cellularities were also normal (data not shown).

The percentage of eosinophils in the peripheral blood was examined from βc-deficient mice over a 10 week period and was significantly lower than that of wild-type mice (Figure 4). The few eosinophils found in βc mutants were morphologically normal.

Challenge to the immune system by parasitic organisms, such as Nippostrongylus brasiliensis, is characterized by marked eosinophilia and immunoglobulin E (IgE) production with well-defined kinetics (Urban et al., 1992). N. brasiliensis typically induces blood eosinophilia detectable at 7 days postinfection and subsiding by 21 days, as well as inducing lung granulomatous lesions composed of eosinophils, granulocytes, monocytes, and other cell types. As the βc-deficient mice exhibited low circulating numbers of eosinophils, we examined eosinophil response to N. brasiliensis in βc and β_{IL3} mutant mice. Animals were infected with 500 third-stage N. brasiliensis larvae and bled over a 3 week period to determine peripheral eosinophil counts. No eosinophil response was detected in the peripheral blood of βc mutant mice, whereas the response of β_{IL3}-deficient mice was not significantly different from that of the wild-type mice (Figure 5A). These data indicate that βc is not only essential for normal development of eosinophils but also for mounting a strong eosinophil response. The increase in serum IgE levels, another characteristic response to parasites, was similar in all three groups of animals (Figure 5B).

Lung tissue from both control and βc mutant mice infected with N. brasiliensis was examined. The lungs from control mice showed peribronchoalveolar lymphocytic infiltration and scattered granulomatous lesions with promi-

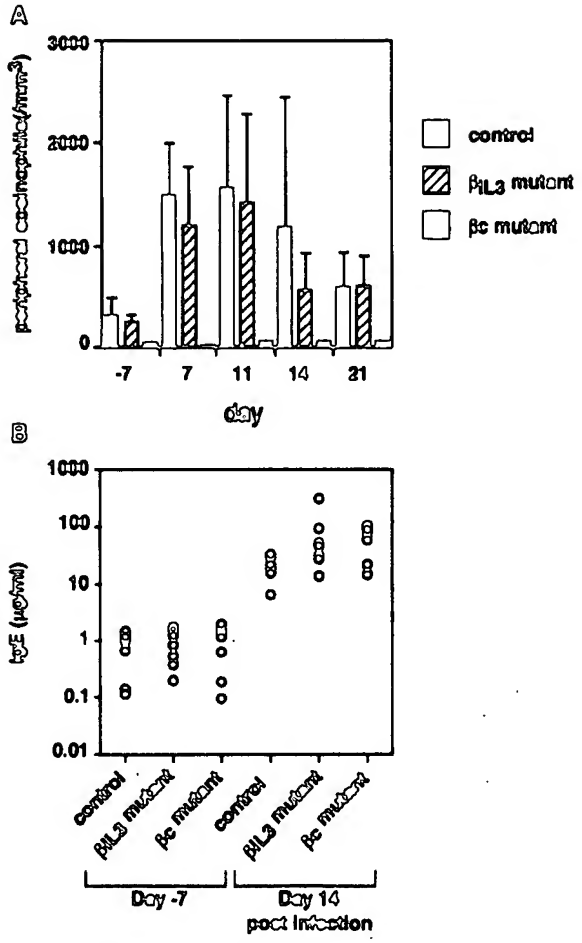

Figure 5. Response to Parasite Challenge

(A) Mice (11 weeks old) were infected with 500 third-stage N. brasiliensis larvae, and the absolute number of peripheral eosinophils was counted. The data represent the mean (± standard deviation) of 5 mice in each group.

(B) Serum IgE before and after the challenge of N. brasiliensis. In each group, 7 mice were analyzed from the same experiment as Figure 5A.

nent eosinophil infiltration and macrophages 14 days after infection (Figure 6A). However, the lungs from βc mutants showed severe edematous fluid accumulation and diffuse infiltration of mononuclear cells and neutrophils not only in peribronchial areas but also in most of the pulmonary airspace. There were no granulomatous lesions in the specimens and no eosinophils were detected (Figure 6B).

The lungs from control mice showed only remnant infectious lesions, where some scattered mononuclear cells were seen mixed with fibrous remnant tissue, 21 days after infection (Figure 6C). In contrast, there seemed to be a possible prolongation of inflammatory process in the lung tissue from βc mutants. Interestingly, some small granulomatous lesions were formed and they contained a small number of eosinophils (Figure 6D). These results suggested that the other signals, possibly IL-3 interacting through the β_{IL3} receptor, recruited eosinophils to a much lesser extent and at much slower kinetics.

Normal Irradiated Animals that Received βc-Deficient Bone Marrow Cells Showed Slower Kinetics of Leukocyte Repopulation and Lacked Normal Eosinophil Development

To evaluate further the intrinsic nature of the cellular defects in βc mutant animals, βc-deficient bone marrow was transferred into normal but irradiated recipient animals. To facilitate this transfer, we used 129/J (Ly5.1) × C57BL/SJL (Ly5.2) F1 recipient animals. The use of the F1 recipient animals allowed us to overcome graft-versus-host reaction from the 129 × C57BL/6 F2 mutant animals (Ly5.1), and to mark genetically the donor versus recipient repopulation. Bone marrow from three βc mutant animals was separately transferred into between 5 and 9 irradiated recipient animals. All recipient animals survived the hematopoietic crisis and repopulation and, to date, have shown no signs of graft-versus-host reaction. FACS analysis of recipient animals confirmed greater than 90% repopulation of donor cells (data not shown). The kinetics of leukocyte repopulation are shown in Figure 7A. βc mutant bone marrow consistently showed slightly slower repopulation in all recipient animals from multiple independent donors. However, spleen colony-forming unit (CFU-S) assays were performed, using control or βc mutant donor bone marrow. Day 8 and day 12 CFU-S were similar for both groups of animals (data not shown). These data indicate that the earliest donor-derived repopulating cells in the spleen are not dependent on signals through βc, but that the continued and efficient repopulation of cells to normal numbers in the peripheral blood is enhanced by stimulation through the βc receptor. As most repopulating cells were shown to be donor derived, differential smears were then evaluated to distinguish cell types during leukocyte recovery. Figure 7B shows that, by 5 weeks posttransfer, recipient animals had low recovery of eosinophils, similar to the reduced number of eosinophils in unmanipulated βc mutants. At 12 weeks posttransfer, peripheral donor-derived cells ($Ly5.1^+$, $Ly5.2^-$) were purified from any residual recipient cells ($Ly5.1^+$, $Ly5.2^+$) by cell sorting and the percentage of eosinophils in cytospun preparations were counted. The donor-derived eosinophil percentage in the animals grafted with βc mutant cells was 0.20% ± 0.20% (n = 3), significantly lower than that in the controls (2.23% ± 0.55%, n = 3). Thus, the lack of proper eosinophil development is clearly an autonomous defect for this cell lineage, owing to the absence of functional βc. Mutant bone marrow recipient animals have shown no obvious signs of pulmonary disease. This may be due to inefficient repopulation of hematopoietic lineages in the lung, or in contrast, may be due to other nonhematopoietic cell types in the lung that may be involved in the development of the pulmonary disease state.

Discussion

The receptors for IL-3, GM-CSF, and IL-5 share a common β subunit (βc), which explains many similar biological activities common to the three ligands. Mice have an additional β chain that is specific for IL-3 (β_{IL3}), but is not present in humans. To evaluate the roles of βc and β_{IL3} in vivo, and

the potential redundancies between them, we generated mice carrying null mutations for either of the two subunits.

The genes for βc and β_{IL3} reside on mouse chromosome 15 and are within 250 kb of each other (Gorman et al., 1992). The coding sequence of the two genes is 95% homologous, and restriction mapping indicates extensive homology in intron sequence as well. In this regard, it is interesting that neither targeting vector recombined with the other homologous gene, implying that strict conservation of sequence is necessary for optimal homologous recombination frequencies.

βc mutant cells were examined by methyl cellulose CFU assays and showed that GM-CSF and IL-5 receptors were functionally disrupted, reconfirming that βc is the common and the only β chain for both receptors. In contrast, the number and the types of colonies generated from βc mutant cells by IL-3 (functioning through the β_{IL3} receptor subunit) were not significantly different from those of the controls, indicating that β_{IL3} could transmit the IL-3 signal in the absence of βc. We also showed that β_{IL3}-deficient cells responded almost normally to IL-3. These results indicated that βc and β_{IL3} were redundant in terms of IL-3 stimulation. This redundancy was also confirmed in the proliferation of bone marrow cells in liquid culture, bone marrow–derived mast cells and connective tissue–type mast cells. As βc and β_{IL3} share only IL-3 as a ligand but not GM-CSF or IL-5, the phenotypes we described in βc-deficient animals are likely to be the cumulative effects of these two latter cytokines. The correlation of these defects to GM-CSF and IL-5 indicate that other uncharacterized cytokines probably do not interact through the βc receptor. Conversely, if such cytokines do exist and interact through the βc receptor, the associated phenotype of that individual cytokine must be minimal.

βc mutant mice exhibited lung abnormalities, including proteinous material in the alveolar spaces and peribronchovascular lymphocytic infiltration. Portions of this pathology resembled alveolar proteinosis. This lung disorder typically involves surfactant accumulation in alveoli and can also be influenced by infectious agents in the lung (Rosen et al., 1958). These findings were probably attributable to the loss of activity of GM-CSF, because this phenotype was very similar to that of GM-CSF-deficient mice (Dranoff et al., 1994; Stanley et al., 1994). GM-CSF is produced by many cell types present in the lungs, such as bronchial epithelial cells, macrophages, endothelial cells, and fibroblasts (Smith et al., 1990; Thorens et al., 1987; Seelentag et al., 1987; Zucali et al., 1987). Alveolar macrophages are responsive to GM-CSF (Bilyk and Holt, 1993), and may play a role in lung homeostasis by clearing surfactant and other debris from alveolar spaces (Wright and Dobbs, 1991). It is possible that alveolar macrophages could not function normally without GM-CSF, which led to the accumulation of material in the alveoli. In this sense, it was interesting that there were many alveolar macrophages that contained PAS-positive material in the 27-week-old βc mutants. This suggests that phagocytosis was occurring but subsequent degradation of this material may not have occurred effectively. Transfer of βc mutant bone marrow cells has not resulted in obvious lung pathology in recipient animals. This may be due either to the involvement of nonhematopoietic cells in the disease, or to inefficient repopulation in lung tissue by hematopoietic cells.

The etiology of the peribronchovascular lymphocytic infiltration is not known. This pathology was also found in GM-CSF-deficient mice (Dranoff et al., 1994; Stanley et al., 1994), in which both B and T cells ($B220^+$, $CD4^+$, and $CD8^+$ cells) accumulated. It has been reported that alveolar macrophages inhibited proliferation of lymphocytes, and that lymphocyte infiltration around blood vessels was observed after treatment of mice with liposomes containing a drug cytotoxic for alveolar macrophages and subsequent immunization (Bilyk and Holt, 1993; Thepen et al., 1989). One interpretation is that alveolar macrophages play a role in down-regulating lymphocytic infiltration. As suggested by Dranoff et al. (1994), the continual exposure of lungs to inhaled antigens may require a dampening of inappropriate immune responses, and this process may be regulated by GM-CSF signals through the βc receptor on alveolar macrophages.

Routine and extensive screening of mutant and control animals revealed the absence of specific pathogens. Comparisons of the severity of lung pathology between the βc mutants described here and GM-CSF-deficient mice may be as reflective of animal room conditions as genetic predisposition. Nevertheless, the basic observations between these mice are in good agreement, and suggest the possible clinical use of GM-CSF for some types of lung disease.

Eosinophilia is observed in a variety of clinical settings, such as parasite infections, asthma, allergic respiratory disease, hypereosinophilic syndrome, and eosinophilia–myalgia syndrome. IL-3, GM-CSF, and IL-5 have been shown to stimulate eosinophils in vitro. Unlike IL-3 and GM-CSF, IL-5 appears to affect the more mature eosinophil lineage (Yamaguchi et al., 1988a, 1988b).

The lower number of basal level peripheral eosinophils in βc-deficient mice could be attributed to the lack of IL-5 signaling, as this phenotype was not observed in GM-CSF-deficient mice. This leads to the suggestion that IL-5 is important for maintaining basal levels of eosinophils in steady-state hematopoiesis, perhaps produced from activated T cells. Although eosinophils were greatly reduced in βc mutants, the few remaining eosinophils were morphologically normal. The in vitro CFU assays indicated that IL-3 stimulation could produce eosinophils from βc mutant cells. Collectively, these data indicate that factors other than IL-5 may be capable of generating eosinophils to some extent, but that IL-5 is of primary importance in vivo.

N. brasiliensis is a nematode parasite that has been widely used as a model in studying host immunity. The third-stage larvae of N. brasiliensis typically infect an animal by penetration through the skin, followed by migration to the lungs. Numerous studies have shown that the normal response to N. brasiliensis is driven by a Th2 cell response: that is, strong production of IL-4 and IL-5. The resulting immune response includes blood and tissue eosinophilia and IgE production (for review see Urban et al., 1992).

The fact that βc mutants lacked eosinophilia in response

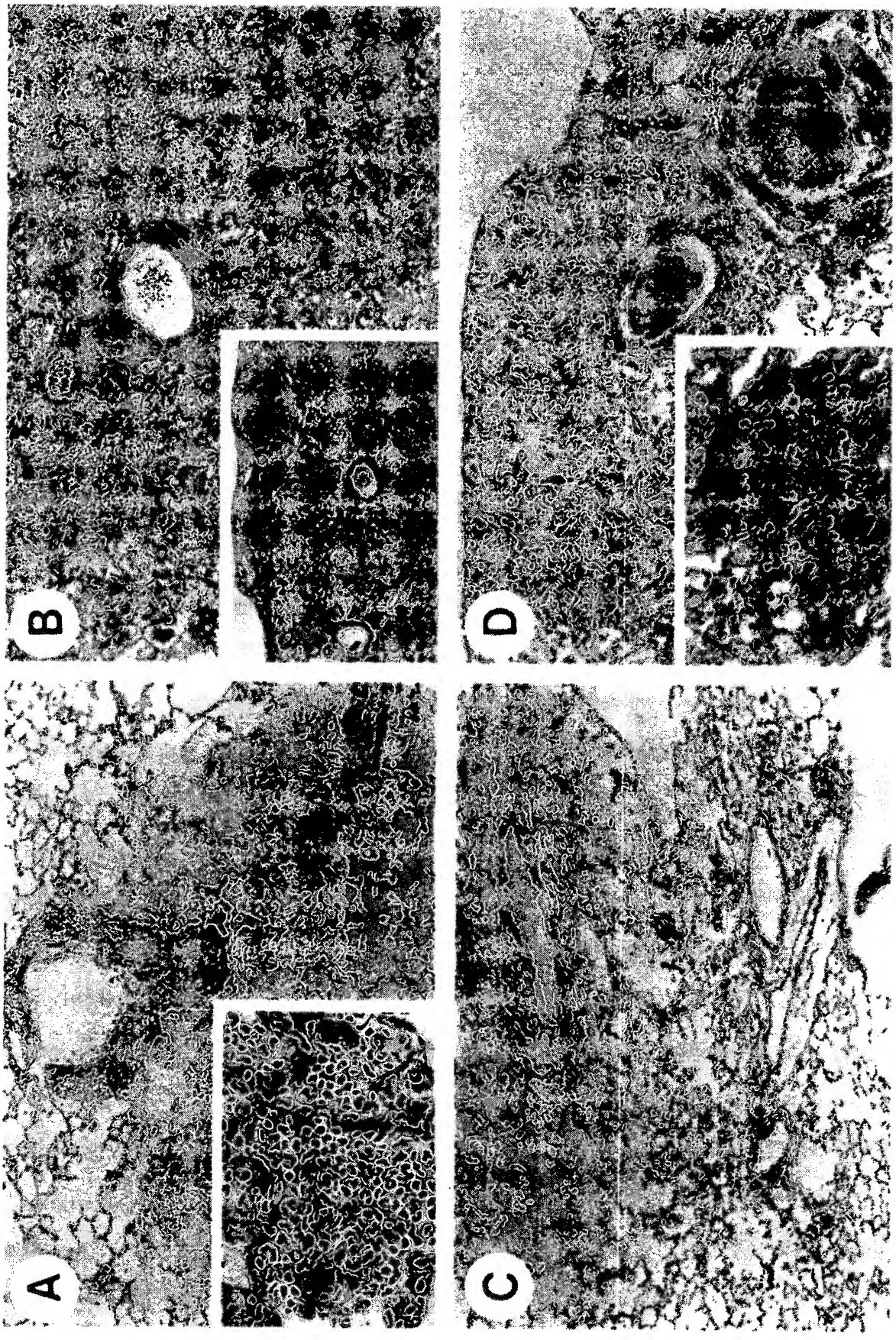
A
B
C
D

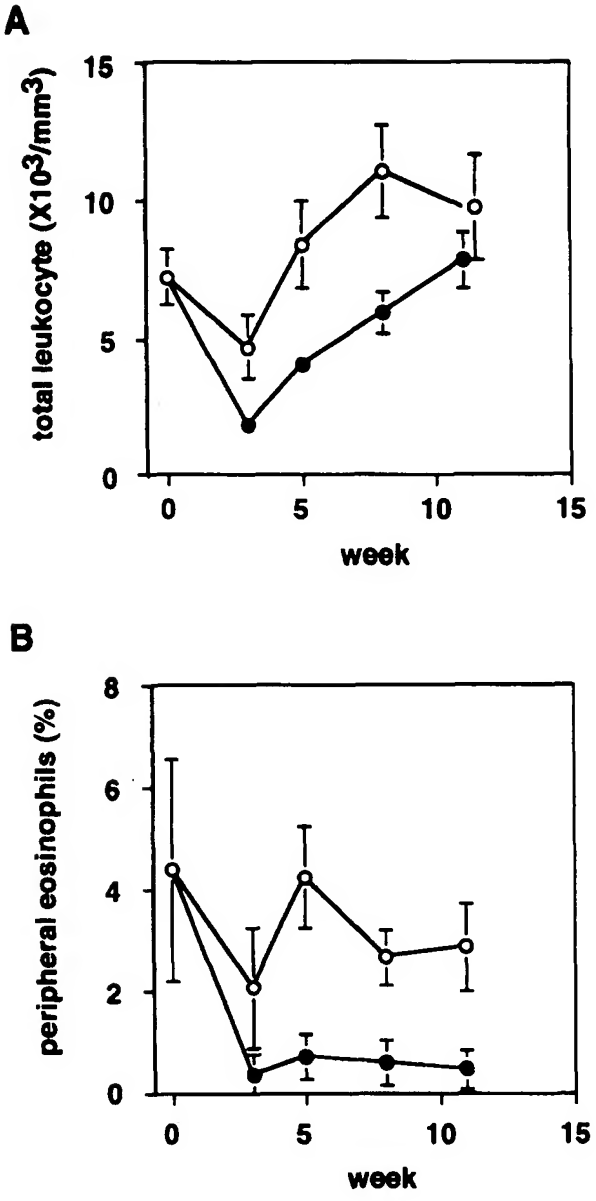

Figure 7. Bone Marrow Transfer

(A) The total number of peripheral leukocytes after bone marrow transplantation. The data represent the mean (± standard deviation) of 5 mice in each group. Open circles indicate animals grafted with control donor cells and closed circles indicate animals grafted with βc mutant donor cells. Three independent donors were used both for controls and βc mutants, and consistent results were obtained.

(B) The percentage of peripheral eosinophils after bone marrow transplantation. The same mice from (A) were evaluated, and are represented as in (A).

to parasitic infections indicated that the signal through βc, probably IL-5, was indispensable for evoking a normal immune response. Blood analysis from parasite-infected βc mutants, followed to 21 days postinfection, showed no detectable eosinophilia. Similar to the conclusions from the blood data, βc mutant lung tissue at day 14 postinfection showed no eosinophils. These observations were consistent with a study using an anti-IL-5 antibody (Coffman et al., 1989). However, in contrast with the anti-IL-5 antibody study, these lungs showed signs of severe edematous fluid accumulation and massive infiltration of mononuclear cells and neutrophils without any granulomatous lesions, whereas clearly defined granulomatous lesions were formed in the controls. This additional pathologic condition may have been related to the preexisting lung pathology in the mutant animals, or due to the lack of the response to GM-CSF during the parasitic infection. Interestingly, at day 21 postinfection, the βc mutants showed small granulomatous lesions with a disproportionately low number of eosinophils, whereas control animals had resolved the lung response at this timepoint. These data indicate that other signals, possibly IL-3 interacting through β_{IL3}, could recruit eosinophils to a much lesser extent and at much slower kinetics. The normal increase in serum IgE levels during the parasite response was consistent with other reports indicating that IgE was controlled by IL-4 (Finkelman et al., 1988; Kuhn et al., 1991). Therefore, IL-4 production must be normal during the parasite challenge, indicating that the overall Th2 response is not likely to be affected in the βc mutant animals. As GM-CSF has been implicated in dendritic cell differentiation and function (Inaba et al., 1992), it will be worthwhile to isolate this cell type and test them functionally despite the fact the IgE response induced by N. brasiliensis implies functional antigen presentation. Despite the abnormalities described above, βc mutants survived the infections. The strain of N. brasiliensis used in this study was adapted to rats and, thus, the parasites did not adhere to the intestinal walls of mice. This study, therefore, did not address the parasite burden.

The bone marrow transfer experiment showed that βc mutant cells could not repopulate lethally irradiated recipients as efficiently as the wild-type cells. Although unmani-

Figure 6. Lung Pathology in Response to N. brasiliensis Challenge

(A) Pulmonary tissue from the control mouse 14 days after infection of N. brasiliensis. Note the prominent peribronchoalveolar lymphocytic infiltration and scattered granulomatous lesions (85.5×). Inset, prominent eosinophil infiltration and macrophages in granulomatous lesions (342×).

(B) Pulmonary tissue from the βc mutant mouse 14 days after infection of N. brasiliensis. Note the infiltration of inflammatory cells was not only in the peribronchial areas but also in most of the pulmonary airspace (85.5×). Lower magnification (inset) showed an infiltration of inflammatory cells in the entire pulmonary lobe (28.5×). There were no granulomatous lesions in the specimen.

(C) Pulmonary tissue from the control mouse 21 days after infection of N. brasiliensis. There were remnant infectious lesions where some mononuclear cells were seen (85.5×).

(D) Pulmonary tissue from the βc mutant mouse 21 days after infection of N. brasiliensis. Low magnification showed prolongation of inflammatory process with some small granulomatous lesions (85.5×). Inset, higher magnification of the granulomatous lesions where infiltration of eosinophils was occasionally observed (342×).

pulated βc mutant mice had normal leukocyte counts, except for eosinophils, signals through βc increased the kinetics of recovery during a hematopoietic crisis. However, animals repopulated with βc mutant cells did not show an increase in mortality under our experimental conditions and eventually regained leukocyte counts comparable to animals repopulated by normal bone marrow. This is consistent with the therapeutic use of GM-CSF to enhance leukocyte recovery postchemotherapy, bone marrow transplantation, or both (Antman et al., 1988; Nemunaitis et al., 1988). The percentage of peripheral eosinophils was also reduced in the animals grafted with βc-deficient deficient cells, and confirms the autonomous requirement for βc signaling on this cell type.

IL-5 is an IgA-enhancing factor (Bond et al., 1987). Steady-state levels of serum IgA were examined in βc mutant mice and found to be normal, as were IgM and IgG1 levels (data not shown). Additionally, peritoneal Ly-1 (CD5) B cells, which were reported to express functional IL-5 receptor complexes (Hitoshi et al., 1990) (Wetzel, 1989), were present in close to normal numbers. A tendency toward fewer of these cells was observed in βc mutants but, due to animal to animal variation, was not statistically significant (data not shown).

To address the role of the entire IL-3/GM-CSF/IL-5 system, it would be necessary to generate mice lacking both βc and β_{IL3}. This necessitates a double mutation in embryonic stem cells, because these two genes are closely linked on chromosome 15, making intercrossing the two mutant mice impractical.

The description of βc-deficient mice presented here suggests that these animals will be useful models for other studies of infectious diseases and recovery from hematopoietic crisis. Owing to the complexities of cytokine binding to common receptor molecules, comparisons of mutant mice for both cytokines and their receptors will ultimately allow for a full understanding of these molecules in vivo.

Experimental Procedures

Generation of βc and β_{IL3}-Deficient Mice

βc and β_{IL3} genomic DNA were cloned from a C57BL/6N genomic library (Gorman et al., 1992). The targeting vectors for βc and β_{IL3} were constructed by incorporating a 5.8 kb SmaI–SmaI fragment and a 8.3 kb BglII–FspI fragment, respectively, which contain exon 2 to exon 6, into a vector that contained the neomycin-resistant (*neo*) gene (*PMC1–neo* poly(A)$^+$) and a herpes simplex virus thymidine kinase (HSV–tk) in tandem. The 5′ genomic fragment upstream of a SacI site in exon 4 was subcloned into an XhoI site 5′ of *neo* gene, and the 3′ downstream fragment was cloned into a BamHI site 3′ of *neo* gene, resulting in an insertion of *neo* gene in the same transcriptional direction as that of βc and β_{IL3}. The constructs were linealized by ClaI and used to electroporate E14.1 cells. The cells were plated on mitomycin C–treated primary embryonic fibroblasts, and clones resistant to G418 (350 μg/ml) and gancyclovir (GANC) (2 μM) were screened by polymerase chain reaction (PCR) and Southern blot analysis. Pools of 8 clones were analyzed by PCR, using a 5′ primer in the coding region of the *neo* gene and a 3′ primer in exon 6 downstream of 3′ homology. 5′ primer: GCGTTGGCTACCCGTGATAT: 3′ primer: GGTCTCCCAGACAAGCTTGAACC. For Southern blot analysis, the genomic DNA from the PCR-positive clones was digested with BamHI, electrophoresed through 0.7% agarose gels, transferred to nylon membranes (Hybond N$^+$, Amersham), and hybridized to a radioactive probe. The probe used to screen the samples was a HindIII–BamHI 600 bp fragment of β_{IL3} downstream of 3′ homology (probe D). The samples were also digested with EcoRI, HindIII, or BglII and hybridized with the other three probes (probes A, B, and C). A probe corresponding to the *neo* sequence (probe B) was used to verify that only one copy of the vector was integrated into the genome. Of 1034 clones, 25 were correctly targeted for βc, and 12 out of 471 were targeted for β_{IL3}. Recipient blastocysts were from C57BL/6N mice. Chimeric animals were bred with C57BL/6N females. All mutant animals studied were of the F2 generation.

FACS Analysis and Immunoprecipitation

Anti-βc-specific monoclonal antibody (gift from Dr. S. Yonehara) and 9D3, an anti-β_{IL3}-specific monoclonal antibody, were used for FACS analysis (Ogorochi et al., 1992). Both recognized the extracellular domain of βc and β_{IL3}, respectively.

Monoclonal antibody 3D1, which recognized the second extracellular repeat of conserved cytokine receptor motif of β_{IL3}, was used for immunoprecipitation (Ogorochi et al., 1992). Affinity-purified rabbit antibody, which recognized the amino-terminal 15 aa of β_{IL3} but not of βc, was used for immunoblotting (Mui et al., 1992). Rat IgG2 was used as an isotype control.

Immunoprecipitation and Western blotting were performed as described previously (Mui et al., 1992). In brief, 1 × 10^7 bone marrow–derived mast cells were lysed and incubated with 10 μg of 3D1 or isotype control for 2 hr at 4°C, followed by incubation with anti-rat IgG agarose beads for 1 hr at 4°C. The samples were electrophoresed on 10% SDS–polyacrylamide gels and transferred to Immobilon-P membrane (Millipore). The blot was incubated with affinity-purified anti-β_{IL3} rabbit antibody and subsequently with horseradish peroxydase–conjugated anti-rabbit antibody. The development was performed by the enhanced chemiluminescence detection system (Amersham).

Hematological Analysis

Total leukocyte, hemoglobin, and platelet estimates were performed on tail-bled samples using a System 9010 CP blood analyzer (Serono). Manual 500-cell leukocyte differential counts were performed on Wright–Giemsa-stained smears. Methyl cellulose colony assays were performed as described (Nakahata and Ogawa, 1982). The cells were stimulated by the following recombinant growth factors: murine IL-3 (10 ng/ml), murine GM-CSF (10 ng/ml), murine IL-5 (100 ng/ml), human erythropoietin (2 U/ml), human IL-6 (100 ng/ml), and mouse stem cell factor (100 ng/ml).

Infection of *N. brasiliensis*

Mice (11 weeks old) were injected subcutaneously with 500 third-stage *N. brasiliensis* larvae, as described (Urban et al., 1992). Animals were bled from the tail vein on the days indicated, and the eosinophils were counted by multiplying their percentage in smears by the total number of leukocytes. The data represent the mean (± standard deviation) eosinophil counts per cubic millimeter in groups of 5 mice. Serum IgE was determined by an IgE-specific enzyme-linked immunosorbent assay (Coffman and Carty, 1986).

Bone Marrow Transplantation

Bone marrow cells (1 × 10^6) were injected intravenously into lethally irradiated (1300 rads) recipients. Bone marrow from three βc mutant animals and from three control animals was separately transferred into between 5 and 9 irradiated recipient animals. 129/J (Ly 5.1) × C57BL/SJL (Ly 5.2) F1 were used as hosts. The cells of hosts express Ly 5.1 and Ly 5.2, while donor cells express only Ly 5.1. FACS analysis of transplanted animals confirmed repopulation of donor cells. Cell sorting experiments were performed on a FACstar Plus (Becton Dickinson) and gave 99% purity of the sorted populations.

CFU-S Assay

Bone marrow cells were injected intravenously into lethally irradiated (1100 rads) C57BL/6N recipients. Cells (10^6) and 5 × 10^4 cells were used for day 8 CFU-S and day 12 CFU-S, respectively.

Pathological Examination

Mice were fixed with 3% formaldehyde, and visceral organs were processed for paraffin-embedded sectioning at 5 μm in thickness, followed

by double staining with hematoxylin and eosin. Complete serial sectioning was made for pulmonary tissues to ensure the degree and spread of each pulmonary lesion, and every third section was stained with PAS reaction to evaluate the possible deposition of mucopolysaccharides.

Acknowledgments

We would like to thank Drs. M. Takagi and T. Hara for their invaluable advice and technical support, and Drs. R. Coffman and B. Seymour for help with parasite infections. We are also grateful to Drs. F. Nolzat-Pirenne and J. Cupp for technical assistance, D. Wylie for critical reading of the manuscript, and Dr. K. Kurokawa for encouragement. DNAX Research Institute is supported by Schering-Plough Corporation.

Received November 23, 1994; revised January 18, 1995.

References

Antman, K. S., Griffin, J. D., Elias, A., Socinski, M. A., Ryan, L., Cannistra, S. A., Oette, D., Whitley, M., Frei, E. I., and Schnipper, L. E. (1988). Effect of recombinant human granulocyte–macrophage colony-stimulating factor on chemotherapy-induced myelosuppression. N. Engl. J. Med. *319*, 593–598.

Arai, K., Lee, F., Miyajima, A., Miyatake, S., Arai, N., and Yokota, T. (1990). Cytokines: coordinators of immune and inflamatory responses. Annu. Rev. Biochem. *59*, 783–836.

Bilyk, N., and Holt, P. G. (1993). Inhibition of the immunosuppressive activity of resident pulmonary alveolar macrophages by granulocyte/macrophage colony-stimulating factor. J. Exp. Med. *177*, 1773–1777.

Bond, M. W., Schrader, B., Mosmann, T. R., and Coffman, R. L. (1987). A mouse T cell product that preferentially enhances IgA production. II. Physicochemical characterization. J. Immunol. *139*, 3691–3698.

Coffman, R. L., and Carty, J. (1986). A T cell activity that enhances polyclonal IgE production and its inhibition by interferon-gamma. J. Immunol. *136*, 949–954.

Coffman, R. L., Seymour, B. W., Hudak, S., Jackson, J., and Rennick, D. (1989). Antibody to interleukin-5 inhibits helminth-induced eosinophilia in mice. Science *245*, 308–310.

Dranoff, G., Crawford, A. D., Sadelain, M., Ream, B., Rashid, A., Bronson, R. T., Dickersin, G. R., Bachurski, C. J., Mark, E. L., Whitsett, J. A., and Mulligan, R. C. (1994). Involvement of granulocyte–macrophage colony-stimulating factor in pulmonary homeostasis. Science *264*, 713–716.

Finkelman, F. D., Katona, I. M., Urban, J., Jr., Holmes, J., Ohara, J., Tung, A. S., Sample, J. V., and Paul, W. E. (1988). IL-4 is required to generate and sustain in vivo IgE responses. J. Immunol. *141*, 2335–2341.

Gorman, D. M., Itoh, N., Kitamura, T., Schreurs, J., Yonehara, S., Yahara, I., Arai, K., and Miyajima, A. (1990). Cloning and expression of a gene encoding an interleukin 3 receptor-like protein: identification of another member of the cytokine receptor gene family. Proc. Natl. Acad. Sci. USA *87*, 5459–5463.

Gorman, D. M., Itoh, N., Jenkins, N. A., Gilbert, D. J., Copeland, N. G., and Miyajima, A. (1992). Chromosomal localization and organization of the murine genes encoding the β subunits (AIC2A and AIC2B) of the interleukin 3, granulocyte/macrophage colony-stimulating factor and interleukin 5 receptors. J. Biol. Chem. *267*, 15842–15848.

Hara, T., and Miyajima, A. (1992). Two distinct functional high affinity receptors for mouse interleukin −3 (IL-3). EMBO J. *11*, 1875–1884.

Hayashida, K., Kitamura, T., Gorman, D. M., Arai, K., Yokota, T., and Miyajima, A. (1990). Molecular cloning of a second subunit of the receptor for human granulocyte–macrophage colony-stimulating factor (GM-CSF): reconstitution of a high-affinity GM-CSF receptor. Proc. Natl. Acad. Sci. USA *87*, 9655–9659.

Hitoshi, Y., Yamaguchi, N., Mita, S., Sonoda, E., Takaki, S., Tominaga, A., and Takatsu, K. (1990). Distribution of IL-5 receptor-positive B cells: expression of IL-5 receptor on Ly-1(CD5)$^+$ B cells. J. Immunol. *144*, 4218–4225.

Inaba, K., Inaba, M., Romani, N., Aya, H., Deguchi, M., Ikehara, S., Muramatsu, S., and Steinman, R. M. (1992). Generating of large numbers of dendritic cells from mouse bone marrow cultures supplemented with granulocyte/macrophage colony-stimulating factor. J. Exp. Med. *176*, 1693–1702.

Isfort, R. J., and Ihle, J. N. (1990). Multiple hematopoietic growth factors signal through tyrosine phosphorylation. Growth Factors *2*, 213–220.

Itoh, N., Yonehara, S., Schreurs, J., Gorman, D. M., Maruyama, K., Ishii, A., Yahara, I., Arai, K., and Miyajima, A. (1990). Cloning of an interleukin-3 receptor: a member of a distinct receptor gene family. Science *247*, 324–327.

Kanakura, Y., Druker, B., Cannistra, S. A., Furukawa, Y., Torimoto, Y., and Griffin, J. D. (1990). Signal transduction of the human granulocyte–macrophage colony-stimulating factor and interleukin-3 receptors involves tyrosine phosphorylation of a common set of cytoplasmic proteins. Blood *76*, 706–715.

Kinashi, T., Harada, N., Severinson, E., Tanabe, T., Sideras, P., Konishi, M., Azuma, C., Tominaga, A., Bergstedt-Lindqvist, S., Takahashi, M., Matsuda, F., Yaoita, Y., Takatsu, K., and Honjo, T. (1986). Cloning of complementary DNA encoding T-cell replacing factor and identity with B-cell growth factor II. Nature *324*, 70–73.

Kitamura, T., Sato, N., Arai, K., and Miyajima, A. (1991). Expression cloning of the human IL-3 receptor cDNA reveals a shared beta subunit for the human IL-3 and GM-CSF receptors. Cell *66*, 1165–1174.

Kuhn, R., Rajewsky, K., and Muller, W. (1991). Generation and analysis of interleukin-4 deficient mice. Science *254*, 707–710.

Lopez, A. F., Eglinton, J. M., Lyons, A. B., Tapley, P. M., To, L. B., Park, L. S., Clarke, S. C., and Vadas, M. A. (1990). Human interleukin-3 inhibits the binding of granulocyte–macrophage colony-stimulating factor and interleukin-5 to basophils and strongly enhances their functional activity. J. Cell. Physiol. *145*, 69–77.

Lopez, A. F., Vadas, M. V., Woodcock, J. M., Milton, S. E., Lewis, A., Elliott, M. J., Gillis, D., Ireland, R., Olwell, E., and Park, L. S. (1991). Interleukin-5, interleukin-3, and granulocyte–macrophage colony-stimulating factor cross-compete for binding to cell surface receptors on human eosinophils. J. Biol. Chem. *266*, 24741–24747.

Metcalf, D. (1991). Control of granulocytes and macrophages: molecular, cellular, and clinical aspects. Science *254*, 529–533.

Mui, A. L., Kay, R. J., Humphries, R. K., and Krystal, G. (1992). Purification of the murine interleukin 3 receptor. J. Biol. Chem. *267*, 16523–16530.

Nakahata, T., and Ogawa, M. (1982). Clonal origin of murine hematopoietic colonies with apparent restriction to granulocyte–macrophage–megakaryocyte (GMM) differentiation. J. Cell. Physiol. *111*, 239–246.

Nemunaitis, J., Singer, J. W., Buckner, C. D., Hill, R., Storb, R., Thomas, E. D., and Applegaum, F. R. (1988). Use of recombinant granulocyte-macrophage colony-stimulating factor in autologous marrow transplantation for lymphoid malignancies. Blood *72*, 834–836.

Ogorochi, T., Hara, T., Wang, H. M., Maruyama, K., and Miyajima, A. (1992). Monoclonal antibodies specific for low-affinity interleukin-3 (IL-3) binding protein AIC2A: evidence that AIC2A is a component of a high-affinity IL-3 receptor. Blood *79*, 895–903.

Rosen, S. H., Castleman, B., and Liebow, A. A. (1958). Pulmonary alveolar proteinosis. N. Engl. J. Med. *258*, 1123–1142.

Seelentag, W. K., Mermod, J. J., Montesano, R., and Vassalli, P. (1987). Additive effects of interleukin 1 and tumour necrosis factor-alpha on the accumulation of the three granulocyte and macrophage colony-stimulating factor mRNAs in human endothelial cells. EMBO J. *6*, 2261–2265.

Smith, S. M., Lee, D. K., Lacy, J., and Coleman, D. L. (1990). Rat tracheal epithelial cells produce granulocyte/macrophage colony-stimulating factor. Am. J. Respir. Cell. Mol. Biol. *2*, 59–68.

Stanley, E., Lieschke, G. J., Grail, D., Metcalf, D., Hodgson, G., Gall, J. A., Maher, D. W., Cebon, J., Sinickas, V., and Dunn, A. R. (1994). Granulocyte/macrophage colony-stimulating factor-deficient mice

show no major perturbation of hematopoiesis but develop a characteristic pulmonary pathology. Proc. Natl. Acad. Sci. USA *91*, 5592–5596.

Takatsu, K., Tominaga, A., Harada, N., Mita, S., Matsumoto, M., Takahashi, T., Kikuchi, Y., and Yamaguchi, N. (1988). T cell–replacing factor (TRF)/interleukin 5 (IL-5): molecular and functional properties. Immunol. Rev. *102*, 107–135.

Taketazu, F., Chiba, S., Shibuya, K., Kuwaki, T., Tsumura, H., Miyazono, K., Miyagawa, K., and Takaku, F. (1991). IL-3 specifically inhibits GM-CSF binding to higher affinity receptor. J. Cell. Physiol. *146*, 251–257.

Tavernier, J., Devos, R., Cornelis, S., Tuypens, T., Van der Heyden, J., Fiers, W., and Plaetinck, G. (1991). A human high affinity interleukin-5 receptor (IL5R) is composed of an IL5-specific α chain and a β chain shared with the receptor for GM-CSF. Cell *66*, 1175–1184.

Thepen, T., Van Rooijen, N., and Kraal, G. (1989). Alveolar macrophage elimination in vivo is associated with an increase in pulmonary immune response in mice. J. Exp. Med. *170*, 499–509.

Thorens, B., Mermod, J.-J., and Vassali, P. (1987). Phagocytosis and inflammatory stimuli induce GM-CSF mRNA in macrophages through posttranscriptional regulation. Cell *42*, 889–902.

Urban, J., Jr., Madden, K. B., Svetic, A., Cheever, A., Trotta, P. P., Gause, W. C., Katona, I. M., and Finkelman, F. D. (1992). The importance of Th2 cytokines in protective immunity to nematodes. Immunol. Rev. *127*, 205–220.

Wetzel, G. D. (1989). Interleukin 5 regulation of peritoneal Ly-1 B lymphocyte proliferation, differentiation and autoantibody secretion. Eur. J. Immunol. *19*, 1701–1707.

Wright, J. R., and Dobbs, L. G. (1991). Regulation of pulmonary surfactant secretion and clearance. Annu. Rev. Physiol. *53*, 395–414.

Yamaguchi, Y., Hayashi, Y., Sugama, Y., Miura, Y., Kasahara, T., Kitamura, S., Torisu, M., Mita, S., Tominaga, A., and Takatsu, K. (1988a). Highly purified murine interleukin 5 (IL-5) stimulates eosinophil function and prolongs in vitro survival: IL-5 as an eosinophil chemotactic factor. J. Exp. Med. *167*, 1737–1742.

Yamaguchi, Y., Suda, T., Suda, J., Eguchi, M., Miura, Y., Harada, N., Tominaga, A., and Takatsu, K. (1988b). Purified interleukin 5 supports the terminal differentiation and proliferation of murine eosinophilic precursors. J. Exp. Med. *167*, 43–56.

Zucali, J. R., Broxmeyer, H. E., Dinarello, C. A., Gross, M. A., and Weiner, R. S. (1987). Regulation of early human hematopoietic (BFU-E and CFU-GEMM) progenitor cells in vitro by interleukin 1-induced fibroblast-conditioned medium. Blood *69*, 33–37.

Structure of the activation domain of the GM-CSF/IL-3/IL-5 receptor common β-chain bound to an antagonist

Jamie Rossjohn, William J. McKinstry, Joanna M. Woodcock, Barbara J. McClure, Timothy R. Hercus, Michael W. Parker, Angel F. Lopez, and Christopher J. Bagley

Heterodimeric cytokine receptors generally consist of a major cytokine-binding subunit and a signaling subunit. The latter can transduce signals by more than 1 cytokine, as exemplified by the granulocyte-macrophage colony-stimulating factor (GM-CSF), interleukin-2 (IL-2), and IL-6 receptor systems. However, often the signaling subunits in isolation are unable to bind cytokines, a fact that has made it more difficult to obtain structural definition of their ligand-binding sites. This report details the crystal structure of the ligand-binding domain of the GM-CSF/IL-3/IL-5 receptor β-chain (β_c) signaling subunit in complex with the Fab fragment of the antagonistic monoclonal antibody, BION-1. This is the first single antagonist of all 3 known eosinophil-producing cytokines, and it is therefore capable of regulating eosinophil-related diseases such as asthma. The structure reveals a fibronectin type III domain, and the antagonist-binding site involves major contributions from the loop between the B and C strands and overlaps the cytokine-binding site. Furthermore, tyrosine^{421} (Tyr^{421}), a key residue involved in receptor activation, lies in the neighboring loop between the F and G strands, although it is not immediately adjacent to the cytokine-binding residues in the B-C loop. Interestingly, functional experiments using receptors mutated across these loops demonstrate that they are cooperatively involved in full receptor activation. The experiments, however, reveal subtle differences between the B-C loop and Tyr^{421}, which is suggestive of distinct functional roles. The elucidation of the structure of the ligand-binding domain of β_c also suggests how different cytokines recognize a single receptor subunit, which may have implications for homologous receptor systems. (Blood. 2000;95:2491-2498)

Introduction

Cytokine receptors exist largely as homodimers or heterodimers.[1-3] Homodimeric receptors, of which the human growth hormone receptor (GH) is the prototype, bind to a single cytokine that bridges 2 identical subunits and causes receptor activation.[2] In contrast, heterodimeric receptors comprise 2 or 3 subunits that subserve distinct and specialized functions: a major ligand-binding subunit (the α subunit) and a signaling subunit (the β or γ subunit). Importantly, a signaling subunit is able to recognize several cytokines complexed to the appropriate α-chain and to transduce their signals. This is exemplified by the common β-chain (β_c) of the granulocyte-macrophage colony-stimulating factor (GM-CSF), interleukin-3 (IL-3), and IL-5 receptors; the common IL-2 receptor γ-chain (shared by the IL-2, IL-4, IL-7, IL-9, and IL-15 receptors); and gp130 (shared by the receptors for IL-6, IL-11, Leukemia Inhibitory Factor (LIF), ciliary neurotrophic factor, oncostatin M, and cardiotrophin).

The GM-CSF, IL-3, and IL-5 receptors are the only receptors known to transduce signals leading to eosinophil production and, significantly, the corresponding cytokines can be found concomitantly at elevated levels in lungs affected by allergic inflammation. The simultaneous elevation of the GM-CSF, IL-3, and IL-5 receptors may increase eosinophil numbers, contribute to the overall degree of eosinophil activation, cause the different phases of eosinophil infiltration, and determine a localized versus a generalized eosinophil-mediated inflammation.[4-6] This may be particularly important in the pathology of certain diseases, such as asthma, where the eosinophil plays a major effector role. Thus, an antagonist directed against β_c would simultaneously inhibit the function of all 3 eosinophilopoietic cytokines and may prove a useful therapeutic agent.

The extracellular part of β_c comprises 2 pairs of a conserved cytokine receptor module (CRM),[3] a membrane-spanning region,

From the Ian Potter Foundation Protein Crystallography Laboratory, St. Vincent's Institute of Medical Research, Fitzroy, Victoria, Australia; the Cytokine Receptor Laboratory and the Protein Laboratory, Hanson Centre for Cancer Research, Institute of Medical and Veterinary Science, Adelaide, South Australia, Australia; and the Royal Adelaide Hospital, Adelaide, South Australia, Australia.

Submitted September 17, 1999; accepted December 15, 1999.

Supported in part by a grant from the National Health and Medical Research Council of Australia, Canberra, Australia, and a grant from the Australian Synchrotron Research Program, Australian Nuclear Science and Technology Organisation, Menai, Australia, which is funded by the Commonwealth of Australia under the Major National Research Facilities Program, Australia. Use of the Advanced Photon Source was supported under contract W-31-109-Eng-38 from the U.S. Department of Energy, Basic Energy Sciences, Office of Science, Washington DC. Use of the BioCARS Sector 14 (Advanced Photon Source, Argonne National Laboratory, 9700 South Cass Ave, Argonne, IL) was supported by grant RR07707 from the National Institutes of Health, National Center for Research Resources, Bethesda, MD.

J.R. and W.J.M. contributed equally to the structural biology aspects of this work. J.R. is a postdoctoral fellow of the Australian Research Council, Canberra, Australia. J.M.W. is a fellow of the Anti-Cancer Foundation of South Australia, Adelaide, South Australia, Australia; M.W.P. is a senior research fellow of the Australian Research Council, Canberra, Australia; and C.J.B. is a Florey fellow of the Royal Adelaide Hospital, Adelaide, South Australia, Australia.

Reprints: Angel F. Lopez, Cytokine Receptor Laboratory, Hanson Centre for Cancer Research, Institute of Medical and Veterinary Science, Frome Rd, Adelaide, South Australia 5000, Australia; e-mail: angel.lopez@imvs.sa.gov.au; or Michael W. Parker, The Ian Potter Foundation Protein Crystallography Laboratory, St Vincent's Institute of Medical Research, 41 Victoria Parade, Fitzroy, Victoria 3065, Australia; e-mail: mwp@rubens.its.unimelb.edu.au.

The publication costs of this article were defrayed in part by page charge payment. Therefore, and solely to indicate this fact, this article is hereby marked "advertisement" in accordance with 18 U.S.C. section 1734.

and a cytoplasmic domain. Each CRM comprises 2 domains of a fibronectin type III structure with features especially conserved among cytokine receptors.[3] Although β_c does not bind cytokines by itself, its coexpression with the α-chains enhances the affinity of cytokine binding, a process termed affinity conversion. Extensive mutational analysis has localized the affinity-converting (cytokine-binding) region to residues in the fourth extracellular domain ($D4\beta_c$) and has shown that this domain and in particular the residues Tyr^{365}, His^{367}, Ile^{368}, and Tyr^{421} within it are crucial for receptor activation.[7-9]

A major problem in seeking structural data of the binding site of a communal subunit complexed to cytokines is that, unlike homodimeric receptors or isolated α-chains of heterodimeric receptors that can bind directly to cytokines, communal subunits often cannot bind to cytokines by themselves. We therefore used an antagonistic monoclonal antibody (mAb), BION-1, which we have shown to reciprocally inhibit cytokine binding to β_c[10], to form a complex for crystallographic studies. BION-1, which was raised against $D4\beta_c$, has been shown to inhibit the high-affinity binding of GM-CSF, IL-3, and IL-5 to human eosinophils and their production and functional activation in vitro.[10] Within β_c, residues Glu^{366}, Arg^{418}, and Met^{363} or Arg^{364} were found to be required for binding BION-1.[10]

BION-1 thus represents the first common antagonist of the GM-CSF, IL-3, and IL-5 receptors, and it is a unique tool with which to explore the cytokine-binding site in the common β_c. Here we report the crystal structure of the activation domain of the GM-CSF/IL-3/IL-5 receptor signaling subunit bound to the mAb antagonist, BION-1. The structure provides a molecular basis for understanding ligand recognition and receptor assembly. Furthermore, the structure of the complex provides leads for the design of novel therapeutics against allergic diseases.

Materials and methods

Crystallization and data collection

$D4\beta_c$ (residues 338-438 with an additional amino-terminal Met) was expressed using the pEC611 vector in *Escherichia coli* and purified by reverse-phase high-performance liquid chromatography (HPLC). The expressed protein was insoluble, but it could be recovered from the bacteria by dissolution in 6 mol/L guanidine hydrochloride and 50 mmol/L sodium acetate buffer (pH 4.0). After HPLC the protein was dialyzed exhaustively against 5 mmol/L 2-[N-morpholino]ethanesulfonic acid (MES) buffer (pH 6.0). The BION-1 mAb was raised against $D4\beta_c$,[10] and Fab fragments were generated and purified by standard methods. The complex was produced by mixing BION-1 Fab and $D4\beta_c$ to give a 1:1 (mol/mol) complex, which was purified on a gel filtration column (Superdex 75; Amersham Pharmacia, Little Chalfont, England).

Crystals of the complex were grown by the hanging-drop vapor diffusion method at 22°C. We mixed 2-μL droplets of protein solution (protein concentration of 5-7 mg/mL) with 1.5 μL of the reservoir solution. The solution was then equilibrated against a 1-mL reservoir consisting of 100 mmol/L citrate buffer (pH 5.5) containing 12% (wt/vol) polyethylene glycol 4000. The crystals reached maximum size of approximately 0.6 mm × 0.2 mm × 0.2 mm over 10 days. The crystals belonged to space group $P4_1\,2_1\,2$ and had the following cell dimensions: *a* and *b* were 7.76 nm, and *c* was 29.49 nm. The crystals were micromanipulated, washed several times in reservoir buffer, and dissolved in sodium dodecyl sulfate–N-tris[hydroxymethyl]methylglycine (SDS-Tricine) sample buffer. Polyacrylamide gel electrophoresis (PAGE) was performed to confirm that the crystals were of the intact complex. The crystals proved to be sensitive to radiation, and hence, cryocooling was essential. However, they were fragile, and an array of commonly used cryoprotectants caused disordering of the crystals. A flash-freezing protocol was finally established. This involved soaking the crystals in 5% (vol/vol) increments of 2-methyl-2,4-pentanediol for 2 minutes to a final concentration of 15% (vol/vol).

A native data set was initially collected in-house on an imaging plate area detector (MARResearch, marUSA, Evanston, IL) with Cu $K\alpha$ x-rays generated by a rotating anode generator (Rigaku RU-200, Molecular Structure Corp., The Woodlands, TX). A better native data set was subsequently collected from a single crystal frozen to −273°C using synchrotron radiation (BioCARS beamline, 14-BM-C; Advanced Photon Source, Chicago, IL). The diffraction data were processed and analyzed using DENZO and SCALEPACK[11] and programs in the CCP4 suite[12] (Table 1).

Structure determination

The crystal structure was solved by molecular replacement using AmoRe[14] and the in-house native data set. Nonredundant Fab fragments were downloaded from the protein databank (PDB) and systematically tested as molecular replacement search probes. The second search probe tested, a mouse Fab fragment with PDB identifier 1YEC,[15] proved successful. The 10th peak in the rotation function (peak height of 3.3 σ) produced the highest peak in the translation function (with a correlation coefficient of 27.9 and an R_{factor} of 54.1% compared with the next highest peak, which had a correlation coefficient of 17.3 and an R_{factor} of 57.5%). The statistics indicated that $P4_1\,2_1\,2$ was the correct enantiomorphic space group. Rigid body refinement of the initial solution lead to a model with a correlation coefficient of 28.7 and an R_{factor} of 49.9% (resolution range, 1.0-0.45 nm). Further refinement, in which the Fab domains were treated as separate rigid bodies, resulted in further improvement of the statistics (an R_{factor} of 46.1% and a drop of R_{free} from 50.9% to 43.8%). Maps calculated from this solution yielded readily interpretable density for $D4\beta_c$.

The model of the complex was then built with the help of skeletonized maps using the program O[16] and refined using the maximum likelihood target in the program package CNS.[17] The refinement was completed with the synchrotron native data set (Table 1). In the final stages a bulk solvent correction and restrained individual isotropic B-factors were applied. The quality of the final map was very good, with no breaks in the main-chain connectivity, and the real space fit[16] of residues into the map never fell below 0.7. The final model comprises residues 338-438 for $D4\beta_c$; all residues for the Fab fragment; 124 solvent molecules; and 1 carbohydrate unit, an N-acetylglucosamine unit off the BION-1 residue Asn^{26L}.

The choice of solvent molecules was conservative. The molecules were only accepted if they appeared as peaks, with a signal of more than 3 times

Table 1. Crystallographic analysis

Data collection			
Temperature of collection (°C)	173	Multiplicity	2.8
Resolution limit (nm)	0.28	I/σ_I	11.4
Observations	58 732	No. of data > $2\sigma_I$ (%)	66.2
Unique reflections	21 211	*R_{merge} (%)	9.8
Completeness (%)	88.1		
Refinement statistics			
Resolution range (nm)	∞ − 0.28	SD from ideality	
†R_{factor} (%)	22.8	Bond lengths (nm)	0.0010
†R_{free} (%)	28.8	Bond angles (°)	1.55
		Impropers (°)	0.95
		Dihedrals (°)	27.1
Atoms in model			
Protein (nonhydrogen)	4146		
Water	124		
Carbohydrate	14		
Residues in most favored regions[13] of Ramachandran plot (%)			80
Residues in additionally allowed regions[13] of Ramachandran plot (%)			19

*R_{merge} indicates $\Sigma_{hkl}\Sigma_i|I_i - \langle I\rangle|/|\langle I\rangle|$, where I_i is the intensity for the i^{th} measurement of an equivalent reflection, with indices *h*, *k*, and *l*.

†R_{factor} indicates $100(\Sigma||F_o| - |F_c||/\Sigma|F_o|)$ using all data except 6%, which were used for the R_{free} calculation.

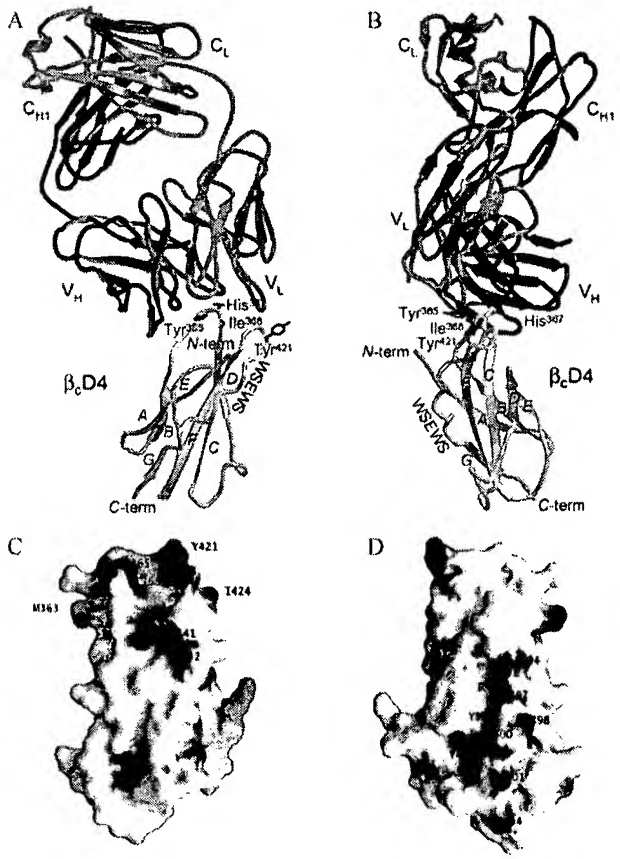

Figure 1. Structure of D4β_c. (A) Structure of the Fab receptor D4β_c complex shown in ribbon representation. The mAb light chain is shown in cyan blue, the heavy chain in blue, and the receptor in yellow. The major structural features of D4β_c are labeled, and the locations of key residues are denoted by stick representation. These pictures were produced using the Molscript[20] and Raster3D[21] programs. (B) Structure as for (A) but reoriented 90° about the vertical axis. (C) Surface representation of the receptor using the program GRASP.[22] The green surface indicates the location of hydrophobic-aromatic patch H1. The molecule is tilted approximately 20° counterclockwise relative to (A). (D) View of hydrophobic-aromatic patch H2 prepared as for (C). The molecule is tilted approximately 20° clockwise and rotated approximately 60° clockwise from above, about a vertical axis relative to (B).

the SD error in difference maps; reappeared in subsequent $2F_o$-F_c maps; took part in at least 1 hydrogen-bonding interaction; and had temperature factors of less than 0.8 nm^2. The stereochemical quality of the final model is good (Table 1), and other stereochemical parameters, such as side-chain chi angle values, peptide bond planarity, alpha-carbon tetrahedral distortions, and nonbonded interactions, are all significantly better than the ranges allowed according to the program PROCHECK.[13] The correctness of the tracing is supported by residue omit maps in which 10% of the model was deleted, a round of simulated annealing was performed to reduce bias, and the resultant map was examined in the region of omission. The tracing is also supported by 3D-1D scores that never fall below 0.2, which indicates that there are no residues in chemically unreasonable environments.[18]

Functional studies

Human Embryonal Kidney 293T (HEK293T) cells were grown in RPMI-1640 (GIBCO Laboratories, Glen Waverly, Vic., Australia) containing 10% fetal calf serum (FCS) and were cotransfected with expression constructs encoding IL-3 receptor α-chain, βc, and Janus kinase (JAK-2) using a calcium-phosphate precipitation procedure. Briefly, 1.4×10^6 cells were plated onto 6-cm plastic tissue culture dishes the day before transfection and left to adhere overnight. Four hours after a medium change, 10 μg DNA was added in the form of a calcium phosphate precipitate, which was left on the cells for a further 4 hours. The expression constructs used per transfection were 6 μg wild-type or mutant β_c complementary DNA (cDNA) cloned into pcDNA1 (Invitrogen, Groningen, The Netherlands), 3 μg IL-3 receptor α-chain cDNA in pCDM8, and 1 μg JAK-2 in pRcCMV (Invitrogen). The cells were then released from the plates, replated in flasks, and incubated for a further 40 hours before use in an activation assay. On the day of the functional experiment, the cells were released and washed in cold phosphate-buffered saline (PBS) and subsequently stimulated with IL-3 at the concentration specified for 5 minutes on ice. Lysates were prepared, precleared and immunoprecipitation was carried out with an anti-β_c mAb, 8E4, essentially as described previously.[19] After extensive washing, immunoprecipitates were separated on a 7.5% SDS-PAGE gel under reducing conditions, transferred to nitrocellulose, and immunoblotted with antiphosphotyrosine antibody, PY20 (Transduction Laboratories, Lexington, KY). The blot was developed by enhanced chemiluminescence (ECL) (Amersham, Pharmacia) and then stripped and reprobed with anti-β_c antibody 1C1 to control the amount of β_c present.

Epitope mapping

African green monkey COS cells were maintained in RPMI with 10% FCS and transfected with 10 μg of wild-type or mutant β_c expression construct by electroporation essentially as described previously.[8] The cells were washed in PBS and lysed as detailed elsewhere[19] 48 hours after transfection. Lysates were run on a 7.5% SDS-PAGE under reducing conditions, and immunoblotting was carried out after electro-blot transfer using either

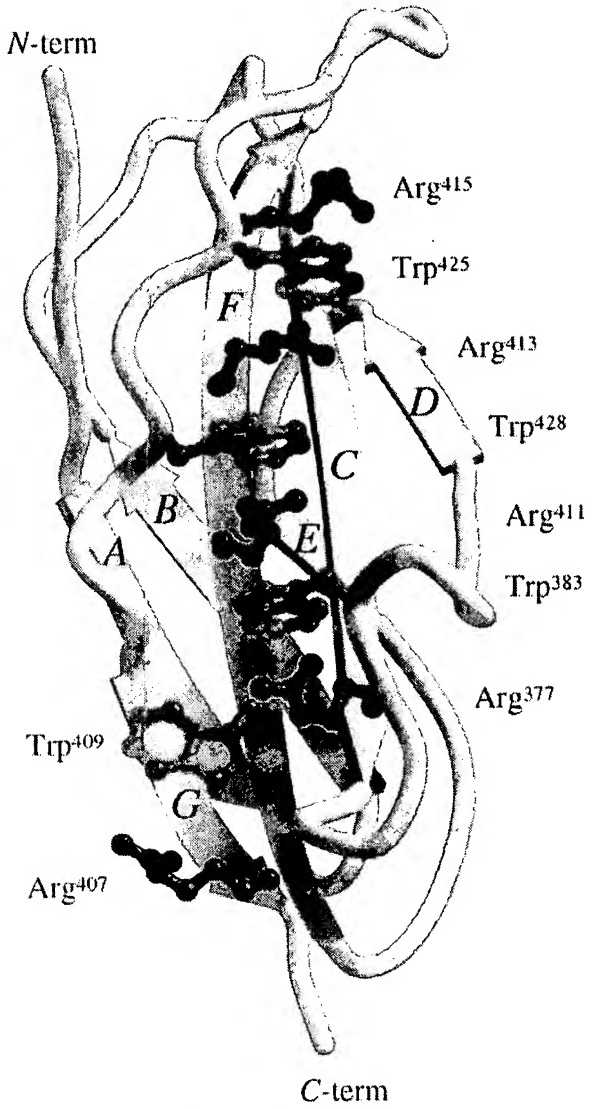

Figure 2. View of the Trp/Arg "ladder." Structure of the D4β_c shown in ribbon representation with the side chains of the Trp/Arg stack shown as ball and stick. The molecular graphics were produced using the Molscript[20] and Raster3D[21] programs.

the antagonistic mAb, BION-1, or anti-β_c mAb, 1C1, at 1 μg/mL. This was followed by the addition of antimouse Ig coupled to horseradish peroxidase (Pierce, Rockford, IL). Blots were developed by ECL (Amersham) following manufacturer's instructions.

Results

Crystal structure of the GM-CSF/IL-3/IL-5 receptor β_c activation domain

We expressed D4β_c in *E coli* and purified it to homogeneity by reverse-phase HPLC. BION-1 mAb was digested with ficin to generate Fab fragments that were purified by chromatography on protein A sepharose. Titration of D4β_c and the BION-1 Fab produced a stoichiometric 1:1 complex that subsequently formed crystals. These crystals diffracted well enough to allow a full crystallographic structure determination to proceed.

We determined the structure of the BION-1/D4β_c complex to a resolution limit of 0.28 nm. The structure showed that the D4β_c molecule has a compact globular shape with overall dimensions of 4.5 nm × 2.5 nm × 2.0 nm (Figure 1). The amino-terminus and carboxy-terminus represent the sites of attachment for the remainder of the extracellular region and the membrane-spanning domain, respectively. The molecule adopts the topology of a fibronectin type III module with 2 antiparallel β-sheets (42% sheet) packing against each other via a multitude of hydrophobic interactions including 2 clusters of aromatic residues Trp^{434}, Tyr^{354}, and Tyr^{376}; Trp^{358}, Phe^{372}, and His^{370}). Sheet A consists of 3 beta-strands: strand A is comprised of residues 344-350, B of residues 353-359, and E of residues 396-398. Sheet B consists of 4 strands: strand C is comprised of residues 369-378, D of residues 389-392, F of residues 406-417, and G of residues 432-436). The longest strand, F, almost spans the entire length of the molecule.

The amino acid sequence motif WSXWS (tryptophan-serine-any residue-tryptophan-serine) is a characteristic feature of many cytokine receptors. WSXWS is located between F and G strands and adopts a double β-bulge structure (Figure 2) with the tryptophan side chains interdigitated between the arginine side chains from the adjacent F strand. In D4β_c, this ladder of alternating basic and aromatic residues is extended and consists of the following side chain: Arg^{415}-Trp^{425}-Arg^{413}-Trp^{428}-Arg^{411}-Trp^{383}-Arg^{377}-Trp^{409}-Arg^{407}. There is a "sidestep" in the ladder at Arg^{377}-Trp^{409}. This 9-rung ladder, measuring 2.9 nm long with rungs of about 0.5 nm wide, represents the only significant electropositive patch on the surface of the molecule.

There are 2 large hydrophobic patches on the surface of D4β_c: H1 and H2. The first, H1, forms part of a lip at the end of a pronounced groove on the surface of the molecule (Figure 1C). This patch is made up of residues Ile^{338}, Met^{340}, Ala^{341}, Pro^{342}, Met^{361}, Tyr^{365}, the aliphatic moiety of Lys^{362}, Ile^{368}, and Tyr^{421}. The groove is located at the N-terminal end of the molecule, where one wall is formed by the B-C loop and part of the F-G loop, and the other wall is formed by the N-terminus (residues 338-342) (Figure 1C). The second hydrophobic patch, H2, located on the opposite face to the first, is a dense strip of hydrophobic residues located at one edge of the β-sandwich defined by the D and E strands. It measures 2.7 nm × 0.6 nm (Figure 1D).

Of the interstrand loops, only the B-C and F-G loops protrude significantly from the body of the protein; both have been implicated in cytokine binding.[3,7-9] The B-C loop adopts significant regular structure with residues 365-368, forming a type I β-turn (Figure 1A). Significant features of the B-C loop of D4β_c include residues Tyr^{365} and His^{367}, both of which project out into the solution (Figure 1A, B). The F-G loop adopts a type I′ β-turn at its tip, and the most significant features in this region are Arg^{418} and Tyr^{421}, both of which project away from the body of D4β_c (Figure 1A, B).

Functional roles of the B-C loop and Tyr^{421}

Although the structure of D4β_c revealed that Tyr^{421} is in close proximity to the 3 residues in the B-C loop involved in cytokine binding (Tyr^{365}, His^{367}, and Ile^{368}), the side chain is oriented away from these, possibly reflecting different functional roles. Previous experiments[9] suggested that high-affinity binding of IL-3 was sensitive to mutation of Tyr^{421} but not to replacement of individual residues in the B-C loop.[8] We examined whether a multiple mutation in the B-C loop of the residues implicated in binding GM-CSF and IL-5 would affect IL-3 high-affinity binding. The results showed that alanine substitution of residues 365-368 in the B-C loop abrogated high-affinity binding of both GM-CSF and IL-3 (Figure 3A). We next examined phosphorylation of cytoplasmic tyrosine residues, as this is a very sensitive measure of recruitment of β_c to a ligand/α-chain complex. Some analogs of β_c are unable to affinity-convert due to the affinity of the α-β complex for cytokine being less than or equal to that of the α-chain alone. These same analogs may nevertheless exhibit differences in tyrosine phosphorylation (see "Discussion"). We examined the effects of mutating the B-C loop or Tyr^{421}, either separately or in combination, on the ability of β_c to undergo tyrosine phosphorylation in response to IL-3. We found that substitution of Tyr^{421} had a pronounced effect, with high levels of tyrosine phosphorylation of β_c being achieved only at 3 μmol/L IL-3, a concentration about 500-fold higher than that required by the native receptor (6 nmol/L). In contrast, mutation of the B-C loop alone did not impair IL-3–induced phosphorylation of β_c at the high concentration used. Nevertheless, a role for the B-C loop in β_c activation was demonstrated by a combined mutant of the B-C loop and Tyr^{421} (Figure 3B), which abrogated IL-3–induced tyrosine phosphorylation of β_c.

Antagonist interactions with the β_c activation domain

A detailed analysis of the structure of the BION-1/D4β_c complex confirmed and extended the observations that BION-1 appeared to form extensive and intimate interactions with the receptor activation domain (Figure 1A, B and Figure 4). The total surface area buried on complex formation is 15 nm^2, which is in the range reported for other antibody-protein antigen complexes.[24] In total, there are 2 salt bridges (Lys^{362}/Asp^{L94} and Glu^{366}/Lys^{H35}), 8 potential hydrogen bonds, and 124 van der Waals (vdw) interactions (Table 2). The B-C loop of D4β_c is nestled in the shallow antigen-binding groove between the V_H and V_L domains, whereas the F-G loop forms a more peripheral interaction with complementarity determining region one of the light chain (CDR L1) of BION-1 (Figure 1A, B and Figure 4). The contact surface comprises 14 residues from BION-1, with 9 residues from V_H and 5 residues from V_L. The majority of contacts are roughly shared between 4 of the CDRs: CDR L1 (1 hydrogen bond and 29 vdw contacts); CDR L3 (1 salt bridge, 3 hydrogen bonds, and 28 vdw contacts); CDR H1 (1 salt bridge, 3 hydrogen bonds, and 36 vdw contacts); and CDR H3 (1 hydrogen bond and 23 vdw contacts). In addition, CDR H2 provides 8 vdw contacts, but CDR L2 makes no contacts with the receptor domain.

In total, 6 residues from the B-C loop (between residues 362-368) and 3 residues from the F-G loop (between residues 416-422) of D4β_c are involved in antibody interactions with those

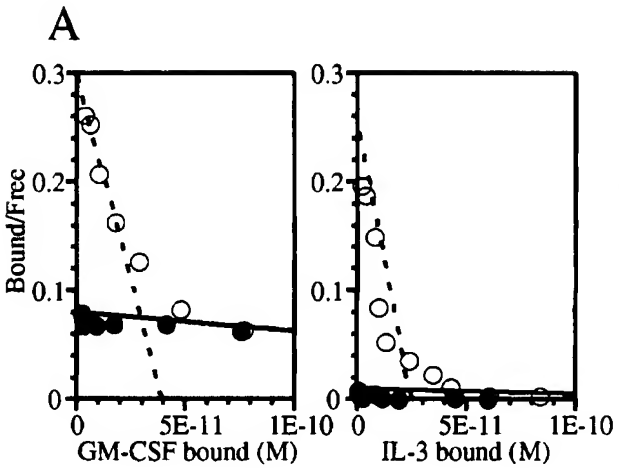

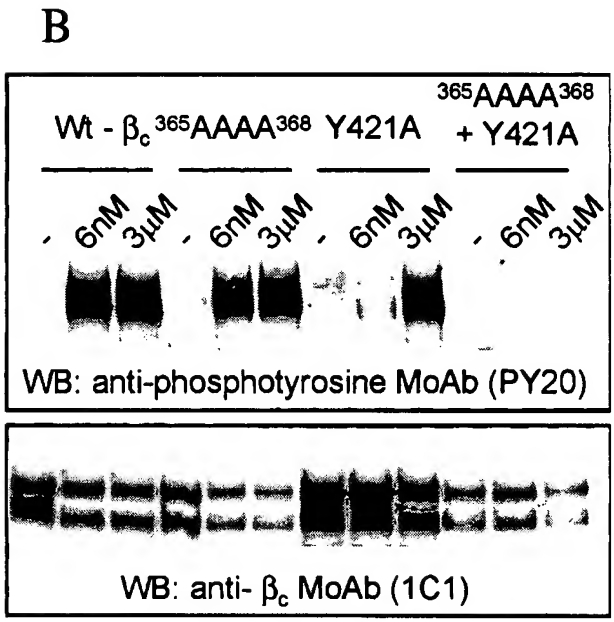

Figure 3. Differential effects of mutating the B-C loop and/or Tyr^{421} of the F-G loop in receptor activation. (A) Scatchard plot transformation of binding isotherms for ^{125}I-GM-CSF and ^{125}I-IL-3 to cells transfected with wild-type β_c (O) or ^{365}AAAA^{368} mutant β_c (●). (B) Western blot of wild-type and mutant β_c after stimulation with various concentrations of IL-3. The blot was probed for phosphotyrosine (upper panel) and β_c (lower panel). The double bands in each lane of the gels represent glycosylation variants of β_c.[23]

from the B-C loop, accounting for 75% of the total. The B-C loop interacts with CDRs H1, H2, H3, L1, and L3, whereas the F-G loop interacts only with CDRs H3 and L1 (Figure 4). There is one small cavity of 0.0099 nm^3 in the antibody-antigen interface. The cavity is lined by residues Tyr^{365}, His^{367}, and Ile^{368} of the receptor and residues Val^{27}, Tyr^{28}, Phe^{32}, and Asn^{92} of the antibody light chain. Not all of the potential salt bridges and hydrogen bonds identified above are likely to contribute productively to complex formation because substitution analysis has only identified Glu^{366}, Arg^{418}, and Met^{363} or Arg^{364} in D4β_c as contributing to the epitope for binding BION-1[10] (Table 2).

Discussion

We describe here the structure of the activating domain of the common β_c of the GM-CSF/IL-3/IL-5 receptors complexed with

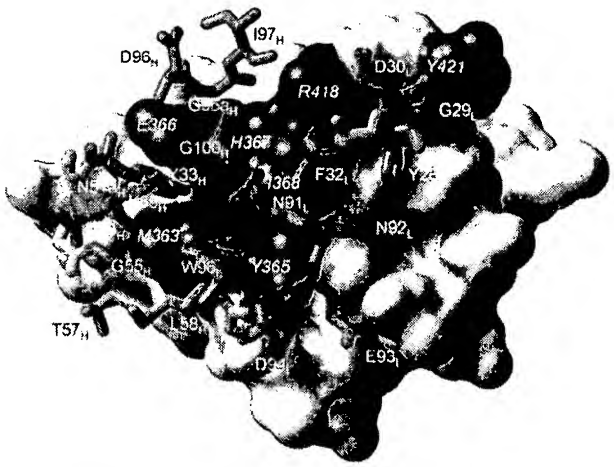

Figure 4. The BION-1/D4β_c Interface. D4β_c is shown as a surface representation colored according to the functional effect of residue substitution. Blue represents residues whose substitution abrogates binding of BION-1 but does not affect affinity-conversion. Red represents residues whose substitution reduces affinity-conversion but does not affect binding of BION-1. Yellow represents residues whose substitution does not affect binding of BION-1 or cytokines. Gray represents residues that have not been examined by mutation and do not contact BION-1. The identities of key D4β_c residues are shown in italics. Residues in BION-1 that contact D4β_c are shown in stick representation and colored cyan blue (hydrophilic) or brown (hydrophobic-aromatic). The backbone atoms of residues colored gray show the connectivity of the loops.

the Fab fragment of the antagonistic mAb, BION-1. The structure shows general features typical of the cytokine receptor superfamily as well as unique features that reveal how a single receptor subunit can interact with 3 different cytokines. Functional analyses show the separate but cooperative interplay of the B-C loop and Tyr^{421} in the F-G loop in receptor activation.

A number of related (class 1) cytokine receptor structures are known: growth hormone receptor (GHR),[26] prolactin receptor (PRLR),[27] erythropoietin receptor (EPOR),[28] G-CSF receptor (G-CSFR),[29] gp130,[30] and the IL-4 receptor α-chain (IL-4Rα-

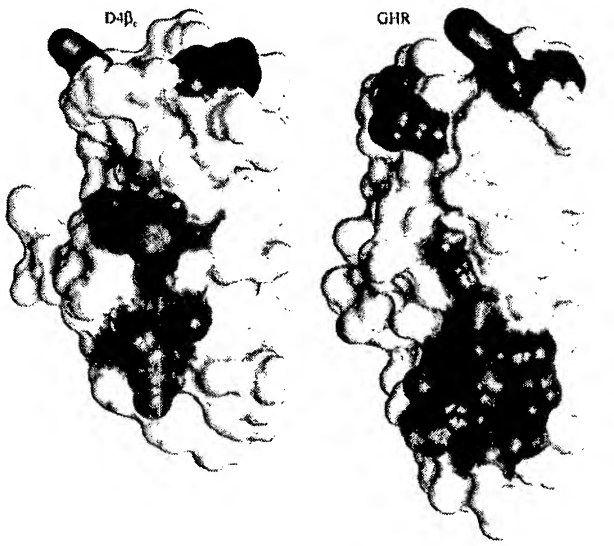

Figure 5. Comparison of D4β_c with the membrane-proximal domain of GHR. D4β_c and domain 2 of the subunit of the GHR, which interacts with the helix A/helix C face of GH, were aligned structurally via their core residues and are shown as surface representations using the program InsightII (MSI, San Diego, CA). The hydrophobic-aromatic patch, H2, of D4β_c and the location of GHR that interacts with the opposing receptor molecule are indicated by green surfaces. The red surfaces of D4β_c indicate the residues required for affinity-conversion, and the blue surfaces of GHR indicate the region known to interact with GH.

Table 2. Interactions between D4β_c and BION-1 or cytokines

Residue identity	Residue type	Vdw contact	Buried area polar interactions (nm^2)		Required for binding BION-1	Required for affinity conversion
D4β_c						
β_c 361	Met	No	0		No	No
β_c 362	Lys	Yes	0.45	Nζ → L94:Oδ	No	No
β_c 363	Met	Yes	1.21	Sδ → H57:N	?	No
β_c 364	Arg	Yes	0.33	Nη → H33:Oη O → H33:Oη	?	No
β_c 365	Tyr	Yes	0.87	Oη → L94:Oδ	No	Yes
β_c 366	Glu	Yes	1.65	Oε → H35:Nζ Oε → H33:N	Yes	No
β_c 367	His	Yes	0.99	Nε → L91:O	No	Yes
β_c 368	Ile	No	0.16		No	Yes
β_c 369	Asp	No	0		No	No
β_c 370	His	No	0		No	No
β_c 395	His	No	0.26		ND	ND
β_c 416	Thr	Yes	0.29	Oγ → L28:Oη	ND	ND
β_c 418	Arg	Yes	1.01	Nη → H97:O	Yes	No
β_c 419	Thr	No	0.15		No	No
β_c 420	Gly	No	0		No	No
β_c 421	Tyr	Yes	0.45		No	Yes
β_c 422	Asn	No	0		No	No
BION-1 light chain						
L 28	Tyr	Yes	1.62	Oη → β_c416:Oγ		
L 29	Gly	No	0.21			
L 30	Asp	No	0.18			
L 32	Phe	Yes	0.39			
L 91	Asn	Yes	0.17	O → β_c367:Nε		
L 92	Asn	No	0.14			
L 93	Glu	No	0.13			
L 94	Asp	Yes	0.48	Oδ → β_c362:Nζ Oδ → β_c365:Oη		
L 96	Trp	Yes	0.31			
BION-1 heavy chain						
H 32	Tyr	Yes	0.60			
H 33	Tyr	Yes	1.00	Oη → β_c364:Oη Oη → β_c364:O N → β_c366:Oε		
H 35	Lys	No	0	Nζ → β_c366:Oε		
H 51A	Asn	Yes	0.21			
H 53	Asn	No	0.37			
H 55	Gly	Yes	0.09			
H 57	Thr	Yes	0.18	Oγ → β_c363:Sδ		
H 58	Leu	No	0.52			
H 96	Asp	Yes	0.06			
H 96A	Gly	Yes	0.51			
H 97	Ile	Yes	0.13	O → β_c418:Nη		
H 100A	Gly	Yes	0.16			

vdw contacts are β_c with BION-1 or vice versa. The buried area (solvent exposure lost) on formation of the D4β_c/BION-1 complex was calculated using dssp.[25] The polar interactions include salt bridges and hydrogen bonds and are based on the distance and geometric criteria of Kabsch and Sander.[25] The requirement for binding BION-1[10] and the requirement for affinity conversion[8,9] are based on mutations to alanine. ND indicates not determined.

chain).[31] The pair-wise sequence identities between D4β_c and these receptors, after structure-based alignment, range from 12% (G-CSF) to 27% (gp130). There are only 7 residues (Pro^{343}, Trp^{358}, Leu^{402}, Tyr^{408}, Arg^{413}, Gly^{423}, and Ser^{426}) that are strictly conserved across the receptors; all appear to play structural roles. The structural importance of Trp^{358} is highlighted by the observation that its substitution or the substitution of neighboring Tyr^{356} by Asn abrogates affinity conversion by β_c.[32] A structural superposition indicates that D4β_c is most closely related to PRLR (0.16 nm studies on 88 Cα atoms, 20% sequence identity) followed by GHR (0.19 nm on 81 Cα atoms, 23% sequence identity). The root mean square deviation of other receptors indicates that (1) the membrane-distal B-C loop of the second domain within a CRM is normally involved in cytokine-binding and (2) the neighboring F-G loop of this domain and the A-B and E-F loops of the first domain also make contributions to cytokine-binding. The B-C loop of D4β_c, in particular Tyr^{365} and His^{367}, has been found to be involved in cytokine binding (Figure 3).[7,8] G-CSFR, GHR, PRLR, and IL-4Rα-chain have an aromatic residue in an equivalent position to Tyr^{365}, whereas only the IL-4Rα-chain has an aromatic residue (tyrosine) similar to His^{367} of β_c. The IL-4Rα-chain is also the only receptor of known structure that has an aromatic residue (tyrosine) equivalent to Tyr^{421} in the F-G loop.

The most salient features of the D4β_c crystal structure are the 2 hydrophobic-aromatic patches and the distinct groove, which is formed in part by the B-C and F-G loops and hence located at the putative cytokine-binding site. The hydrophobic-aromatic surface patches, H1 and H2 (Figure 1C, D), have corresponding features in most of the other receptors. With the exception of gp130, all the receptors possess significant hydrophobic-aromatic patches equivalent to the location of H2 (centered about the D-E strand connection), although the degree and extent of hydrophobicity varies greatly. The corresponding H2 patch of GHR (Figure 5) forms part of the surface involved in subunit contacts.[26] This is suggestive of a role for the H2 of D4β_c in association with α-chains, particularly the GMRα with which it associates spontaneously.[23] The equivalent region to H1 is conserved in all but gp130. By analogy with the other receptors, the H1 patch of D4β_c might interact with the A-B loop from domain 3 of the intact receptor. The groove is only present in G-CSFR, whereas the N-terminal ends of the equivalent domains of EPOR and gp130 are rather flat, and those of GHR and PRLR are mostly flat, with the exception of a tryptophan residue that protrudes into the solution.

There are considerable amounts of mutagenesis data available that indicate which regions of the receptor and the cytokine interact with each other. In the cytokines there is an essential glutamate (Glu^{21} of GM-CSF, Glu^{22} of IL-3, and Glu^{13} of IL-5) involved in binding to β_c.[33-35] The loops of domains 3 and 4 of β_c have been the subject of extensive mutagenesis that has led to the following conclusions: (1) Tyr^{365}, His^{367}, and Ile^{368} of the B-C loop are implicated in cytokine interaction, whereas mutations of other residues in this loop have little or no effect on binding.[7,8] Substitution of any of these residues by alanine led to a loss of affinity-conversion of GM-CSF and IL-5 binding,[8] whereas the Phe^{365} mutant retained affinity-conversion of GM-CSF binding.[7] (2) The major residue in the F-G loop that has been implicated in binding[9] is Tyr^{421}. (3) To date, there have been no residues in domain 3 implicated in binding.[3]

The crystal structure of D4β_c provides a molecular explanation of how each cytokine, with less than 15% pair-wise sequence identity, can recognize the signaling subunit. The side-chains of the 3 key residues in the B-C loop that interact with a cytokine, as identified by the mutagenesis studies, are seen to converge closely at their tips (Figure 1A). Thus Tyr^{365}, His^{367}, and Ile^{368} may play a pivotal role by promoting an interaction with the essential glutamate residue in all 3 cytokines. This may involve formation of a hydrogen bond between the glutamate residue and Tyr^{365} or His^{367} or the cooperative formation of part of the cytokine-binding

surface. In this context it is worth noting that in the IL-4 receptor system, the homologous Tyr^{127} is close to Glu^{9} but does not form a hydrogen bond with it.[31] All other residues of the B-C loop are orientated in a different direction from the binding triad, which is consistent with their not taking part in binding cytokines. On the other hand, Tyr^{421} in the neighboring F-G loop is positioned to contribute directly or indirectly to binding cytokines. Directly, through its hydroxyl group, Tyr^{421} may form a hydrogen bond with the conserved glutamate. This would be akin to the known interaction of Tyr^{183} in a homologous position in IL-4Rα-chain and Glu^{9} of IL-4.[31] Indirectly, Tyr^{421} may interact with the A-B loop of domain 3 of β_c, as seen with Phe^{205} of EPOR,[28] and thus support an appropriate orientation of this domain, or Tyr^{421} may facilitate receptor assembly. Given that the active receptor probably has a stoichiometry of 2 α-chains : 2 β_c : 2 ligands, Tyr^{421} may directly interact with either a second β_c subunit or α-chain subunit in the hexameric complex.[3]

The separate and combined mutagenesis of the B-C loop and Tyr^{421} revealed that both sites are involved in high-affinity binding and receptor activation of all 3 cytokines, GM-CSF, IL-3, and IL-5, albeit in subtly different ways. The observation that the tetra-alanine substitution of the B-C loop abrogated IL-3 high-affinity binding (Figure 3A) is particularly interesting because single or paired alanine substitutions along this loop have marginal or no effect on IL-3 high-affinity binding.[8] The latter is in contrast to GM-CSF and IL-5, where substitution of either Tyr^{365}, His^{367}, or Ile^{368} completely eliminates high-affinity binding.[7,8] Conversely, substitution of Tyr^{421}, while abrogating high-affinity binding of all 3 cytokines, has a profound effect on IL-3 receptor activation, as measured by phosphorylation of cytoplasmic tyrosine residues of β_c (Figure 3B), but a minor effect on the activation of the GM-CSF receptor.[9] These differences in receptor activation probably reflect the different abilities of mutated β_c to be recruited to IL-3/IL-3Rα-chain complexes and suggest that, in the case of Y421A, the stability of the active IL-3/IL-3Rα-chain/β_c complex is considerably lower than even that of an IL-3/IL-3Rα-chain complex.

The combination of substitutions within the B-C loop and Tyr^{421} caused a complete loss of tyrosine-phosphorylation of β_c. This suggests that even in the presence of concentrations of IL-3 that saturate the IL-3Rα-chain, β_c is not recruited significantly (Figure 3B). These functional observations in the context of the structure support the notion of a central cytokine-binding "hot spot" in D4β_c, with a structural plasticity that allows it to accommodate 3 cytokines of significant diversity as well as monomeric (GM-CSF and IL-3) and dimeric (IL-5) structure. In this model, GM-CSF may interact more closely with the B-C loop, while the orientation of IL-3 may be slightly different and more dependent on Tyr^{421} for its interaction with β_c. Comparison of the cytokine-binding surface of D4β_c with the corresponding surface of GHR reveals substantial similarity in terms of the parts of the B-C and F-G loops involved (Figure 5), although the contributions to cytokine binding of these GHR residues have not been assessed by mutational analysis for this homodimeric receptor. The location of these cytokine-binding residues of β_c relative to the hydrophobic patch, H2, which may interact with α-chains, is similar to the intermolecular contacts seen in the GH:GHR complex.[26] Ultimately, solving the structures of the GM-CSF and IL-3 receptor complexes may provide a definitive answer to the relative positioning of GM-CSF, IL-3, and their α-chains in respect to β_c.

The epitope of D4β_c that interacts with cytokines, largely overlaps the surface that is recognized by BION-1. Although several residues that are required for affinity-conversion (Tyr^{365} and His^{367} and others such as Lys^{362} make intimate contact) with BION-1, they are not required for binding of the mAb. Rather, a set of adjacent residues, including Met^{363} or Arg^{364}, Glu^{366} and Arg^{418}, provides the key determinant for binding BION-1 (Figure 4). While the basis for the roles of these residues can be seen clearly from the structure, the absence of productive contributions to binding from other residues, especially Tyr^{365} and His^{367}, suggests that their corresponding contacts in BION-1 may be targets for mutagenesis. This may lead to improved forms of the mAb or derivatives of it, which may be higher affinity antagonists. Because BION-1 has been shown to inhibit the GM-CSF/IL-3/IL-5–induced proliferation of eosinophils in vitro,[10] this highlights the possibility of developing single-molecule antagonists of several cytokines. This approach of targeting a common receptor subunit may also be extended to other receptor chains, such as the common subunit of the IL-4/IL-13 receptors, which mediates allergen-induced asthma induced by IL-4 and IL-13.[36]

Note added in proof: The coordinates have been deposited in the Research Collaboratory for Structural Bioinformatics Protein Data Bank, code 1EGJ.

Acknowledgments

We thank Craig Gaunt, Betty Zacharakis, and Frosa Katsis for technical assistance and Elspeth Garman for advice on flash freezing of crystals. We also thank Harry Tong and other staff at BioCARS for their help with data collection during our visit to Advanced Photon Source.

References

1. Hilton DJ, Watowich SS, Katz L, Lodish HF. Saturation mutagenesis of the WSXWS motif of the erythropoietin receptor. J Biol Chem. 1996;271:4699.
2. Wells JA, De Vos AM. Hematopoietic receptor complexes. Ann Rev Biochem. 1996;65:609.
3. Bagley CJ, Woodcock JM, Stomski FC, Lopez AF. The structural and functional basis of cytokine receptor activation: lessons from the common β subunit of the granulocyte-macrophage colony-stimulating factor, interleukin-3 (IL-3) and IL-5 receptors. Blood. 1997;89:1471.
4. Till S, Li B, Durham S, et al. Secretion of the eosinophil-active cytokines interleukin-5, granulocyte/macrophage colony-stimulating factor and interleukin-3 by bronchoalveolar lavage $CD4^+$ and $CD8^+$ T cell lines in atopic asthmatics, and atopic and non-atopic controls. Eur J Immunol. 1995;25:2727.
5. Lantero S, Sacco O, Scata C, Rossi GA. Stimulation of blood mononuclear cells of atopic children with the relevant allergen induces the release of eosinophil chemotaxins such as IL-3, IL-5 and GM-CSF. J Asthma. 1997;34:141.
6. Shaver JR, Zangrilli JG, Cho S-K, et al. Kinetics of the development and recovery of the lung from IgE-mediated inflammation: dissociation of pulmonary eosinophilia, lung injury, and eosinophil-active cytokines. Am J Crit Care Med. 1997;155:442.
7. Lock P, Metcalf D, Nicola NA. Histidine-367 of the human common beta chain of the receptor is critical for high-affinity binding of human granulocyte-macrophage colony-stimulating factor. Proc Natl Acad Sci U S A. 1994;91:252.
8. Woodcock JM, Zacharakis B, Plaetinck G, et al. Three residues in the common β chain of the human GM-CSF, IL-3 and IL-5 receptors are essential for GM-CSF and IL-5 but not IL-3 high affinity binding and interact with Glu^{21} of GM-CSF. EMBO J. 1994;13:5176.
9. Woodcock JM, Bagley CJ, Zacharakis B, Lopez AF. A single tyrosine residue in the membrane-proximal domain of the GM-CSF, IL-3 and IL-5 receptor common β chain is necessary and sufficient for high affinity binding and signalling by all three ligands. J Biol Chem. 1996;271:25,999.
10. Sun Q, Jones K, McClure B, et al. Simultaneous

antagonism of interleukin-5, granulocyte-macrophage colony-stimulating factor, and interleukin-3 stimulation of human eosinophils by targeting the common cytokine binding site of their receptors. Blood. 1999;94:1943.

11. Otwinowski Z, Minor W. Processing of X-ray diffraction data collected in oscillation mode. Methods Enzymol. 1997;276:307.
12. Collaborative Computational Project Number 4. The CCP4 suite: programs for protein crystallography. Acta Crystallogr D Biol Crystallogr. 1994; 50:760.
13. Laskowski RA, MacArthur MW, Moss DS, Thornton JM. PROCHECK: a program to check the stereochemical quality of protein structures. J Appl Cryst. 1993;26:283.
14. Navaza J. AMoRe: an automated package for molecular replacement. Acta Crystallogr. 1994; A50:157.
15. Charbonnier JB, Golinelli-Pimpaneau B, Gigant B, et al. Structural convergence in the active sites of a family of catalytic antibodies. Science. 1997; 275:1140.
16. Jones TA, Zou J-Y, Cowan SW, Kjeldgaard M. Improved methods for building protein models in electron density maps and the location of error in these models. Acta Crystallogr. 1991;A47:110.
17. Brünger AT, Adams PD, Clore GM, et al. Crystallography & NMR system: a new software suite for macromolecular structure determination. Acta Crystallogr. 1998;D54:905.
18. Lüthy R, Bowie JU, Eisenberg D. Assessment of protein models with 3-dimensional profiles. Nature. 1992;356:83.
19. Stomski FC, Sun Q, Bagley CJ, et al. Human interleukin-3 (IL-3) induces disulphide-linked receptor α and β chain heterodimerization which is required for receptor activation but not high affinity binding. Mol Cell Biol. 1996;16:3035.
20. Kraulis P. MOLSCRIPT: A program to produce both detailed and schematic plots of protein structures. J Appl Cryst. 1991;24:946.
21. Merritt EA, Murphy MEP. Raster3D Version 2.0, a program for photorealistic molecular graphics. Acta Crystallogr D Biol Crystallogr 1994;509:869.
22. Nicholls A, Sharp KA, Honig B. Protein folding and association: insights from the interfacial and thermodynamic properties of hydrocarbons. Prot Struct Funct Genet. 1991;11:218.
23. Woodcock JM, McClure B, Stomski FC, Elliott MJ, Bagley CJ, Lopez AF. The human granulocyte-macrophage colony-stimulating factor (GM-CSF) receptor exists as a preformed receptor complex that can be activated by GM-CSF interleukin-3, or interleukin-5. Blood. 1997;90:3005.
24. Davies DR, Cohen GH. Interactions of protein antigens with antibodies. Proc Natl Acad Sci U S A. 1996;93:7.
25. Kabsch WS, Sander C. Dictionary of protein secondary structure: pattern recognition of hydrogen-bonded and geometrical features. Biopolymers. 1983;22:2577.
26. De Vos AM, Ultsch M, Kossiakoff AA. Human growth hormone and extracellular domain of its receptor: crystal structure of the complex. Science. 1992;255:306.
27. Somers W, Ultsch M, De Vos AM, Kossiakoff AA. The X-ray structure of a growth hormone-prolactin receptor complex. Nature. 1994;372:478.
28. Livnah O, Stura EA, Johnson DL, et al. Functional mimicry of a protein hormone by a peptide agonist: the EPO receptor complex an 2.8Å. Science. 1996;273:464.
29. Yamasaki K, Naito S, Anaguchi H, Ohkubo T, Ota Y. Solution structure of an extracellular domain containing the WSxWS motif of the granulocyte colony-stimulating factor receptor and its interaction with ligand. Nat Struct Biol. 1997;4:498.
30. Bravo J, Staunton D, Heath JK, Jones EY. Crystal structure of a cytokine-binding region of gp130. EMBO J. 1998;17:1665.
31. Hage T, Sebald W, Reinemer P. Crystal structure of the interleukin-4/receptor α chain complex reveals a mosaic binding interface. Cell. 1999;97: 271.
32. Jenkins BJ, Bagley CJ, Woodcock J, Lopez AF, Gonda TJ. Interacting residues in the extracellular region of the common β subunit of the human GM-CSF, IL-3 and IL-5 receptors involved in constitutive activation. J Biol Chem. 1996;271:29,707.
33. Hercus TR, Bagley CJ, Cambareri B, et al. Specific human granulocyte-macrophage colony-stimulating factor antagonists. Proc Natl Acad Sci U S A. 1994;91:5838.
34. Tavernier J, Tuypens T, Verhee A, et al. Identification of receptor-binding domains on human interleukin 5 and design of an interleukin 5-derived receptor antagonist. Proc Natl Acad Sci U S A. 1995;92:5194.
35. Barry SC, Bagley CJ, Phillips J, et al. Two contiguous residues in human interleukin-3, Asp^{21} and Glu^{22}, selectively interact with the α- and β-chains of its receptor and participate in function. J Biol Chem. 1994;269:8488.
36. Vogel G. Interleukin-13's key role in asthma shown. Science. 1998;282:2168.

Proc. Natl. Acad. Sci. USA
Vol. 91, pp. 5592–5596, June 1994
Medical Sciences

Granulocyte/macrophage colony-stimulating factor-deficient mice show no major perturbation of hematopoiesis but develop a characteristic pulmonary pathology

(hematopoietic growth factors/gene targeting/homologous recombination/pulmonary diseases)

EDOUARD STANLEY*†, GRAHAM J. LIESCHKE*, DIANNE GRAIL*, DONALD METCALF‡, GEORGE HODGSON*, JOHN A. M. GALL§, DARRYL W. MAHER*, JONATHAN CEBON*, VINCENT SINICKAS¶, AND ASHLEY R. DUNN*‖

*Ludwig Institute for Cancer Research, Melbourne Tumour Biology Branch, ‡Cancer Research Unit, Walter and Eliza Hall Institute of Medical Research, §Department of Anatomical Pathology, and ¶Department of Microbiology, Post Office, The Royal Melbourne Hospital, Victoria, 3050, Australia

Contributed by Donald Metcalf, February 14, 1994

ABSTRACT **Mice homozygous for a disrupted granulocyte/macrophage colony-stimulating factor (GM-CSF) gene develop normally and show no major perturbation of hematopoiesis up to 12 weeks of age. While most GM-CSF-deficient mice are superficially healthy and fertile, all develop abnormal lungs. There is extensive peribronchovascular infiltration with lymphocytes, predominantly B cells. Alveoli contain granular eosinophilic material and lamellar bodies, indicative of surfactant accumulation. There are numerous large intraalveolar phagocytic macrophages. Some mice have subclinical lung infections involving bacterial or fungal organisms, occasionally with focal areas of acute purulent inflammation or lobar pneumonia. Some features of this pathology resemble the human disorder alveolar proteinosis. These observations indicate that GM-CSF is not essential for the maintenance of normal levels of the major types of mature hematopoietic cells and their precursors in blood, marrow, and spleen. However, they implicate GM-CSF as essential for normal pulmonary physiology and resistance to local infection.**

Granulocyte/macrophage colony-stimulating factor (GM-CSF) is a hematopoietic growth factor that *in vitro* stimulates the survival, proliferation, differentiation, and function of myeloid cells and their precursors, particularly neutrophil and eosinophil granulocytes and monocyte/macrophages (for a review, see ref. 1). The *in vivo* effects of GM-CSF have been studied in murine models by injecting pharmacological doses of GM-CSF (2), by generating GM-CSF transgenic mice (3), and by reconstituting mice with marrow cells overproducing GM-CSF (4). These studies confirm the hematopoietic activity of GM-CSF *in vivo* and suggest that excess levels may be implicated in some disease processes. However, the usual physiological role of GM-CSF is not well defined (1, 5). We sought to define the physiological role of GM-CSF by generating GM-CSF-deficient mice through targeted disruption of the GM-CSF gene in embryonic stem cells. While GM-CSF-deficient mice have no major perturbation of hematopoiesis, they do have abnormal lungs, implicating GM-CSF as essential for normal pulmonary physiology.

MATERIALS AND METHODS

GM-CSF Targeting Vector and Isolation of Targeted Embryonal Stem (ES) Cell Clones. The GM-CSF targeting vector (Fig. 1) contained, from 5′ to 3′ in pIC20H, 900 bp of the GM-CSF gene promoter (*Rsa* I–*Sca* I) (6, 7), the *Escherichia coli lacZ* gene, a 700-bp fragment of the human β-globin gene 3′ untranslated region and a poly(A) addition motif (*Eco*RI–*Acc* I; gift of F. Grosveld, National Institute for Medical Research, London), the PGK-neo selectable marker (8), and approximately 10 kb of GM-CSF genomic sequence (7). The targeting vector was constructed to delete GM-CSF exons 1 and 2 and intron 1 between *Sca* I and *Sma* I sites. The linearized vector was electroporated into 129/OLA-derived E14 ES cells (9). Individual G418-resistant colonies were cloned and screened by PCR. The PCR primers were as follows (Fig. 1): **a**, 5′-CCAGCCTCAGAGACCCAGGTATCC-3′; **b**, 5′-GTTAGAGACGACTTCTACCTCTTC-3′; and **c**, a M13 (−47) 24-mer sequencing primer (New England Biolabs; no. 1224). In PCRs, primers **a** and **b** generate a 1.2-kb product from wild-type DNA, and **a** and **c** generate a 1.0-kb product from DNA containing a correctly integrated targeted construct. The reactant mixture for PCR (20 μl) contained approximately 250 ng of DNA, 67 mM Tris·HCl (pH 8.8), 16.6 mM $(NH_4)_2SO_4$, 0.45% Triton X-100, 200 μg of gelatin per ml, 1.5 mM $MgCl_2$, 250 μM of each dNTP, 12.5 ng of each primer, and 1.5 units of *Taq* polymerase. After initial denaturation (95°C for 150 s), 40 amplification cycles were performed (95°C for 50 s, 60°C for 50 s, and 72°C for 60 s). For Southern blot analysis, *Bgl* II-digested tail DNA was probed with a radiolabeled DNA fragment corresponding to GM-CSF genomic sequences deleted from the targeting construct (probe A) and was reprobed with probe B (Fig. 1) corresponding to sequences lying outside the targeting construct.

Mice. Chimeras from two independent ES cell clones with a disrupted GM-CSF gene transmitted the mutation in matings with C57BL/6 females. GM-CSF genotypic status was assessed by PCR analysis of tail DNA and is designated as follows: wild-type, GM+/+; heterozygous, GM+/−; and homozygous null, GM−/−. GM−/− mice were subsequently bred from GM−/− × GM−/− matings; similarly, outbred 129/OLA × C57BL/6 GM+/+ control mice were bred from first- and second-generation GM+/+ littermates. Mice were kept in a conventional animal house.

Spleen-Conditioned Media (SCM) and GM-CSF Assays. SCM were prepared (10) from splenocytes stimulated with concanavalin A (5 μg/ml; Boehringer Mannheim) and interleukin 2 (IL-2; 100 units/ml; Amgen Biologicals). To assay immunoreactive GM-CSF, an ELISA was used with the anti-GM-CSF antibody MP1-22E9 and biotinylated MP1-

The publication costs of this article were defrayed in part by page charge payment. This article must therefore be hereby marked "*advertisement*" in accordance with 18 U.S.C. §1734 solely to indicate this fact.

Abbreviations: G-CSF, M-CSF, and GM-CSF, granulocyte, macrophage, and granulocyte/macrophage colony-stimulating factors; SCM, spleen-conditioned media/medium; PAS, periodic acid/Schiff reagent (stain); IL-2, IL-3, and IL-6, interleukins 2, 3, and 6; SCF, stem cell factor; H&E, hematoxylin/eosin; ES cells, embryonal stem cells.

†Present address: National Institute for Medical Research, The Ridgeway, Mill Hill, London, NW7 1AA, United Kingdom.
‖To whom reprint requests should be addressed.

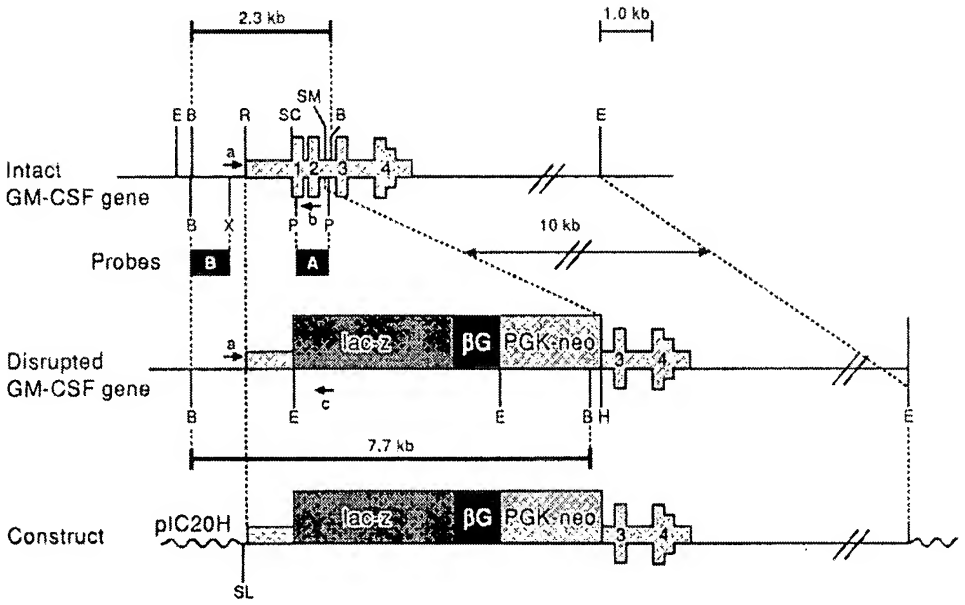

FIG. 1. Generation of GM-CSF deficient mice. Strategy for disruption of GM-CSF gene, showing intact and disrupted GM-CSF gene (exons labeled 1, 2, 3, and 4) and targeting construct, locations of restriction enzyme sites (E = *Eco*RI, B = *Bgl* II, SC = *Sca* I, SM = *Sma* I, X = *Xmn* I, P = *Pst* I, H = *Hin*dIII, SL = *Sal* I), probe A (corresponding to deleted sequences), probe B (external to construct, diagnostic for targeted disruption), and sites of PCR primer hybridization (a, b, and c; see text). In the disrupted allele, exons 1 and 2 and intron 1 are deleted, replaced by the *E. coli lacZ* gene, human β-globin gene 3′ untranslated and poly(A) addition sequences (βG), and PGK-neo (see text).

31G6 (PharMingen) with an avidin–biotinylated horseradish peroxidase (Dako) detection system (sensitivity, 50 pg/ml). To assay bioactive GM-CSF, the FDC-P1 proliferative response ([^{3}H]thymidine incorporation) was used with adjustment for interleukin 3 (IL-3) bioactivity on 32-D cells (11). The MP1-22E9 antibody was used to confirm specificity of putative GM-CSF bioactivity. Standards were recombinant murine GM-CSF (Schering–Plough) and IL-3 (10^7 units/mg; Boehringer Mannheim).

Immunohistochemistry and Electron Microscopy. Immunoperoxidase staining of lung tissue was performed on 4-μm frozen sections with the following antibodies (and specificity): RA3-6B2 (B220) (12), 187.1 (κ light chain) (13), GK1.5 (CD4) (14), 53.6-7 (CD8) (15), and 53-7.8 (CD5) (PharMingen). For electron microscopy, samples of fresh lung tissue were processed by standard techniques into Araldite–Epon resin, and thin sections were stained with alkaline lead citrate and uranyl acetate.

Hematological Analysis. Hemoglobin, total leukocyte, and platelet estimates were performed on 1:4 dilutions of eye-bleed samples with a Sysmex-K1000 automated counter; manual 100-cell leukocyte differential counts were performed on May–Grunwald/Giemsa-stained smears. Semisolid agar cultures of bone marrow, spleen, or peritoneal cells were prepared and scored as described (10, 16). Colony formation was stimulated by the following recombinant growth factors (at the specified final concentrations): human granulocyte colony-stimulating factor (G-CSF; 10 ng/ml), murine GM-CSF (10 ng/ml), murine IL-3 (10 ng/ml), murine macrophage colony-stimulating factor [M-CSF (CSF-1); 10 ng/ml], rat stem cell factor (SCF; 100 ng/ml), murine interleukin 6 (IL-6; 500 ng/ml), and SCM (10%).

Statistics. Data are given as means ± SD. To test for statistically significant differences, the unpaired Student *t* and χ^2 tests were used.

RESULTS

Verification of GM-CSF Gene Disruption. Southern blotting analysis of *Bgl* II-digested tail DNA confirmed the structure of the targeted allele in GM−/− mice: the 2.3-kb species hybridizing with the GM-CSF probe containing exons 1–2 was absent from GM−/− DNA, but GM−/− DNA contained the predicted 7.7-kb species hybridizing with the GM-CSF promoter probe external to the targeting vector (Fig. 2 *A*). GM−/− SCM contained no detectable immuno- or bioactive GM-CSF (Fig. 2 *A* and *B*), confirming the inability of GM−/− tissues to make GM-CSF. All GM−/− SCM were potent, containing bioactive IL-3, although GM−/− SCM contained less IL-3 than in GM+/+ SCM (GM−/− SCM, 16 ± 2 units/ml, $n = 4$; GM+/+ SCM, 49 ± 20 units/ml, $n = 4$; $P < 0.01$).

Viability and Fertility. From initial matings of GM+/− mice, litters of 10 ± 3 pups ($n = 8$) resulted with the genotypes GM+/+, GM+/−, and GM−/− represented in approximately Mendelian ratios, indicating no selective fetal or neonatal loss of GM−/− pups. Survival of GM−/− mice was normal [GM−/−, >91%, $n = 35$; GM+/+, >88%, $n = 17$) with the following median follow-up time: (range): GM−/−, 220 (0–334) days; GM+/+, 209 (0–313) days]. The two dead GM−/− mice in this cohort had lymphoid leukemia (died day 153) and the other had hepatitis (died day 167). From initial matings of male and female GM−/− mice, litters of 9 ± 1 pups ($n = 5$) resulted, indicating that GM-CSF deficiency did not grossly impair fertility or fecundity.

Hematological Analysis of GM-CSF-Deficient Mice. The peripheral blood of 6- to 7-wk GM−/− mice showed no significant difference from GM+/+ littermates. Respective values for GM+/+ ($n = 10$) and GM−/− ($n = 10$) mice were as follows: hemoglobin, 162 ± 7 and 163 ± 5 g/liter; platelets, 838 ± 105 × 10^9 and 822 ± 109 × 10^9 per liter; total leukocytes, 5.9 ± 1.0 × 10^9 and 7.4 ± 2.4 × 10^9 per liter; neutrophils, 1.1 ± 0.3 × 10^9 and 1.2 ± 0.6 × 10^9 per liter; lymphocytes, 4.7 ± 1.1 × 10^9 and 6.0 ± 2.0 × 10^9 per liter; monocytes, 0.12 ± 0.10 × 10^9 and 0.13 ± 0.13 × 10^9 per liter; and eosinophils, 0.09 ± 0.06 × 10^9 and 0.13 ± 0.13 × 10^9 per liter. GM−/− mice tended to have greater variation in their granulocyte levels [e.g., granulocyte levels of 5- to 7-wk mice were as follows: GM−/−, 1.7 ± 1.5 × 10^9 per liter ($n = 33$; range, 0.2–6.6); and GM+/+, 1.3 ± 0.7 × 10^9 per liter ($n = 15$; range, 0.29–3.1)]. Spleens of GM−/− mice showed increased variability in mass [e.g., spleen mass (range) of 6-wk mice, $n = 6$ per group, were as follows: GM+/+, 106 ± 9 (94–120) mg; and GM−/−, 114 ± 42 (64–191) mg]. Femoral cellularity was equivalent (GM+/+, 34.0 ± 5.3 × 10^6; and GM−/−, 27.4 ± 7.0 × 10^6 cells per femur, $n = 3$), and the myeloid:erythroid ratios were equivalent (20 ± 2% and 17 ± 6% erythroid cells, respectively). There was no major difference in marrow total progenitor cell frequency (Table 1), and colony typing indicated no differences in frequencies of granulocyte, granulocyte-macrophage, macrophage, eosinophil, megakaryocyte, erythroid, and blast marrow progenitor cells. In crowded unstimulated cultures of up to 2 × 10^5 GM−/− marrow cells per ml, colony formation

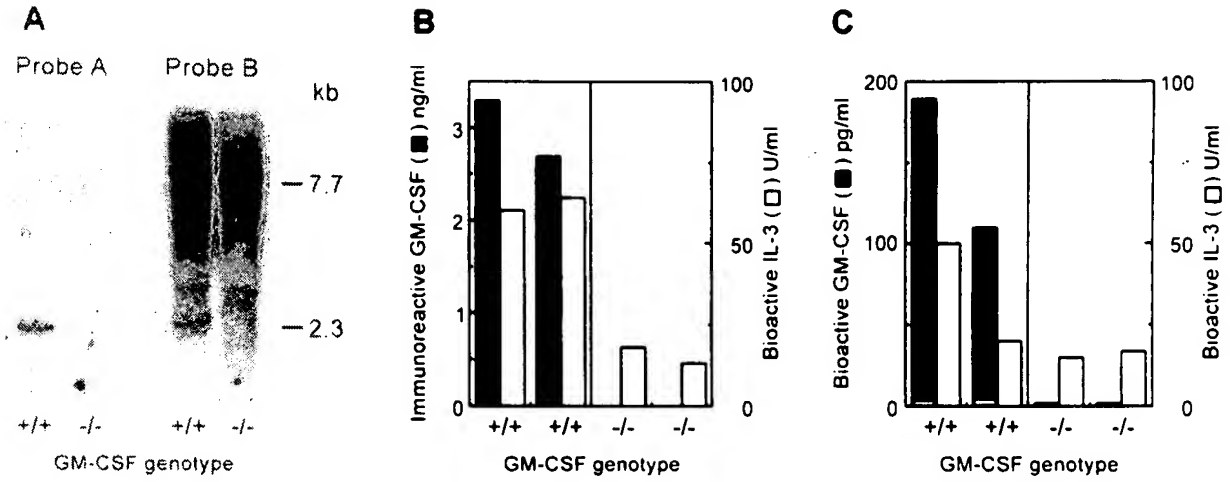

FIG. 2. Deletion of GM-CSF exons 1–2 results in lack of GM-CSF immunoreactivity and bioactivity in SCM. (*A*) Southern blot is shown of *Bgl* II-digested tail DNA from PCR-genotyped GM+/+ and GM−/− mice probed first with probe A (see Fig. 1), confirming that GM-CSF exons 1 and 2 are present in wild-type DNA but deleted from GM−/− DNA, and then reprobed with probe B, confirming that the GM−/− mouse is homozygous for the disrupted GM-CSF allele. (*B* and *C*) Levels of immunoreactive (*B*) and bioactive (*C*) GM-CSF (solid columns) and bioactive IL-3 (open columns) in media conditioned by concanavalin A- and IL-2-stimulated splenocytes are shown for individual GM+/+ and GM−/− mice. In *C*, the open portion of the solid column shows GM-CSF bioactivity after neutralization with an anti-GM-CSF antibody.

was only somewhat reduced, indicating that "spontaneous" colony formation *in vitro* is not solely dependent on GM-CSF production. There was a 3- to 6-fold increase in frequency of splenic progenitor cells in GM−/− mice and an absolute increase in splenic progenitor cell number (Table 1). Peritoneal washings recovered $6.0 \pm 1.4 \times 10^6$ and $5.1 \pm 1.4 \times 10^6$ cells from GM+/+ and GM−/− mice (65% and 63% macrophages, respectively).

Histological Characterization of Pulmonary Disease in GM-CSF-Deficient Mice. Although at birth the lungs of GM−/− and GM+/+ animals were indistinguishable, by 3 weeks of age striking abnormalities were evident. Individual GM−/− lungs consistently showed focal peribronchovascular aggregates of lymphoid cells but little infiltration of alveolar septa (Fig. 3 *A–C*). Immunostaining of 12- to 16-wk GM−/− lungs showed these cells to be predominantly B lymphocytes and about 20% T cells, predominantly $CD4^+$ (Fig. 3 *E–H*). The lymphoid infiltrate was particularly marked around hilar vessels, occasionally assuming a follicular organization, but the cells exhibited little mitotic activity. Characteristically, the perivascular infiltrate extended peripherally with a predilection for the perivascular area (Fig. 3*B*). Focal consolidation was prevalent, consisting of an eosinophilic alveolar exudate containing numerous mature and fragmented neutrophils and macrophages (Fig. 3*D*), occurring most commonly in the tips of lobes, but frequently was more extensive. In older 6- to 12-wk lungs, the lymphoid hyperplasia predominated, alveoli contained large foamy macrophages and granular debris, and focal acute inflammation sometimes occurred (Fig. 3*D*). One 6-wk GM−/− mouse had a chronic pulmonary abscess with an organized wall lined by foamy macrophages. Granular, eosinophilic, periodic acid/Schiff reagent (PAS)-positive, diastase-resistant material within alveoli was present in all lungs examined (3-wk- to 10-month-old mice) (e.g., Fig. 3 *D, K, O,* and *P*), apparently accumulating and becoming confluent in some alveoli. In some areas of GM−/− lungs, the appearances of contiguous alveoli containing this material resembled those of *alveolar proteinosis* (Fig. 3 *O* and *P*). Surfactant-producing type-II alveolar cells were readily identified by their cytoplasmic lamellar bodies (Fig. 4*A*); the alveolar debris included numerous type-C lamellar bodies (Fig. 4*B*), and these were seen within phagosomes of alveolar macrophages (Fig. 4*C*). Some alveolar spaces in older lungs were large, suggesting an emphysematous process (Fig. 3*Q*). One 4-wk-old GM−/− mouse died with lobar pneumonia (Fig. 3*N*) from which *Pasteurella pneumotropica* was isolated. Grocott and PAS stains identified foci of 5- to 10-μm-diameter fungal elements in 3 of 15 GM−/− lungs but in none of 7 GM+/+ lungs (e.g., Fig. 3 *I–K*). Gram-positive coccobacilli were present in one pneumonic area (Fig. 3 *L* and *M*). No mycobacterial infections were evident with Ziehl–Neelson and Wade–Fite stains.

Table 1. Hematopoietic progenitor cells in GM-CSF-deficient mice

Cells cultured, no.	*n*	Stimulus	Total colonies, mean ± SD GM+/+	GM−/−
Bone marrow				
25,000	5	GM-CSF	59 ± 12	51 ± 19
		G-CSF	19 ± 3	15 ± 7
		M-CSF	64 ± 16	59 ± 25
		IL-3	68 ± 12	68 ± 19
		SCF	29 ± 3	22 ± 13
		IL-6	18 ± 8	18 ± 10
		SCF + GM-CSF	66 ± 12	63 ± 26
200,000	5	Saline	79 ± 62	39 ± 44
Spleen				
100,000	3	GM-CSF	3 ± 4	8 ± 2
		SCF	0	4 ± 2*
		SCF + GM-CSF	3 ± 1	20 ± 2*
		SCM	4 ± 3	18 ± 2*

Genotype is indicated as wild-type (GM+/+) or GM-CSF-deficient (GM−/−). The spleen masses were 64 ± 8 mg for GM+/+ mice and 114 ± 22 mg for GM−/− mice ($P < 0.05$). *n* is the number of mice studied.
*$P < 0.05$.

DISCUSSION

Since the actions of hematopoietic regulators appear to overlap, it is possible that individual regulators might be wholly or partially redundant (5). This proposition is most directly assessed by analysis of mice deficient in individual or multiple regulators. Our analysis of GM−/− mice (up to 12 wk of age) indicates no perturbation of major hematopoietic populations in marrow or blood. There are two obvious interpretations: either GM-CSF may not be an important regulator of normal hematopoiesis, or alternatively, GM-CSF may contribute to the maintenance of steady-state he-

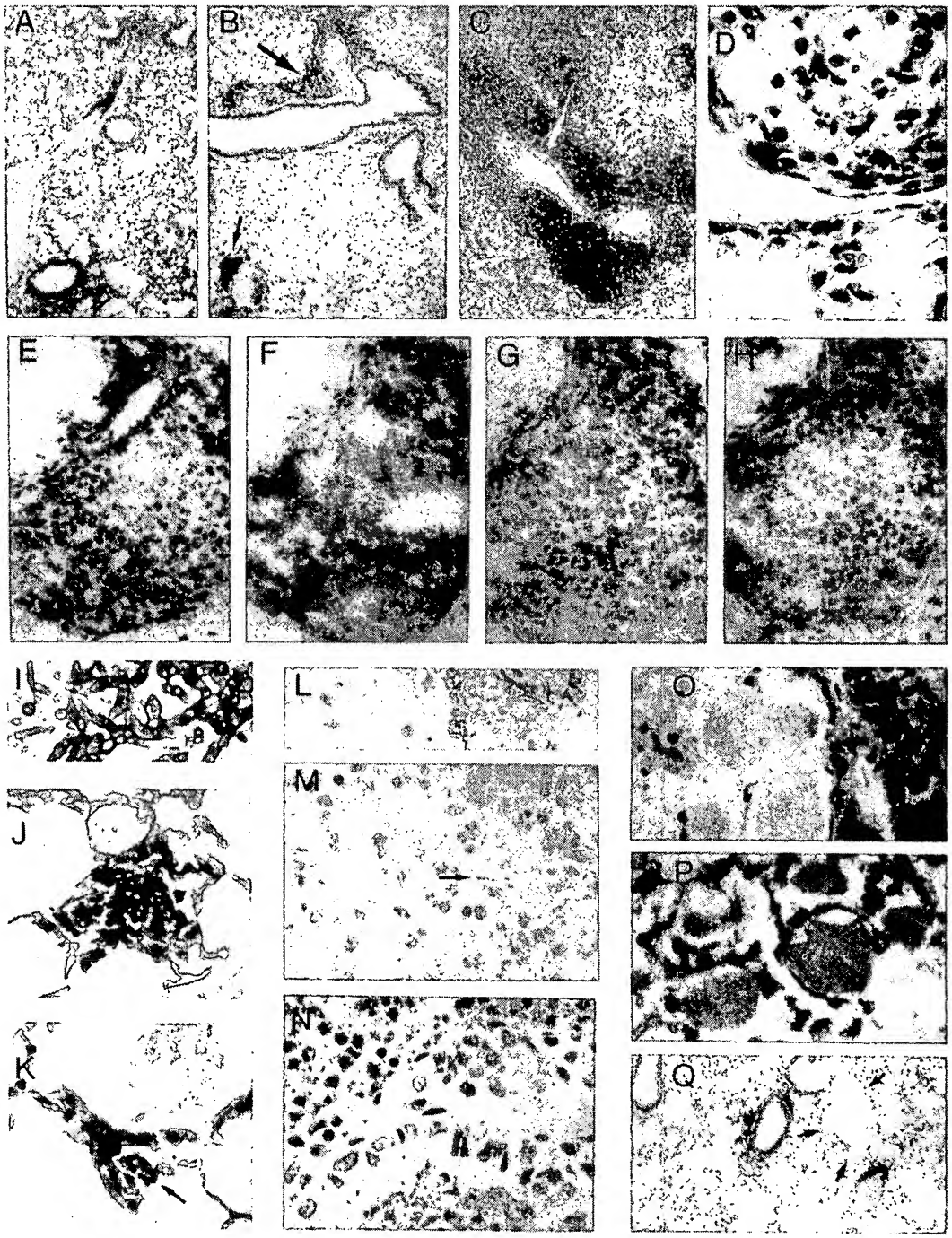

FIG. 3. Lung histopathology of GM-CSF-deficient mice. (*A*) Normal C57BL/6 lung (13 wk), central region. [Hematoxylin/eosin (H&E); ×20.] (*B* and *C*) GM−/− lung (11 wk) with moderate (*B*) and extensive (*C*) lymphoid hyperplasia around central and peripheral vessels. (H&E; ×20.) (*D*) Detail of alveoli in GM−/− lung (7 wk) with large foamy macrophages, neutrophils, and eosinophilic alveolar debris. (H&E; ×200.) (*E–H*) Immunoperoxidase staining of perivascular mononuclear cells in GM−/− mouse lung (16 wk) ×100 with the following primary antibodies (and specificity): none (phosphate-buffered saline; negative control) (*E*); RA3-6B2 (B220) (*F*); GK1.5 [CD4] (*G*); and 53.6-7 [CD8] (*H*). The same nodule is in each panel. (*E–H*, ×100.) (*I–K*) Focus of infection with fungal element in GM−/− lung (16 wk). (*I*) Positive control for Grocott stain. (*J*) Grocott-positive fungal particles of 5–10 μm. (*K*) PAS-positive fungal particles in same location of the contiguous section. (*I–K*, ×200.) (*L–N*) Bacterial infections in GM−/− lungs. (*L*) Gram stain control with Gram-positive and Gram-negative bacilli. (*M*) Gram-positive coccobacilli in 7-wk pneumonic consolidated area. (*N*) Purulent acute *Pasteurella pneumotropica* lobar pneumonia in mouse dying at 4 wk. (*N*, H&E; *L–N*, ×200.) (*O–Q*) Features of 24-wk GM−/− lung. (*O* and *P*) Granular refractile PAS-positive homogenous eosinophilic material in contiguous alveoli. (*Q*) Emphysematous area (e.g., arrow) with persistent peribronchovascular lymphoid hyperplasia. (H&E in *O* and *Q*, PAS in *P*; *O–Q*, ×200.)

matopoiesis, but in its absence other regulators are able to replace its usual role. Splenic progenitor cell levels were increased in GM−/− mice, but this may reflect subclinical pulmonary infection.

The possibility that GM-CSF is wholly redundant can be discounted because all GM−/− mice develop abnormal lungs. Our initial studies have not identified the nature of the intrinsic pulmonary defect that characterizes GM-CSF deficiency. The alveolar material that accumulates may be a local product, such as surfactant phospholipid and protein, either produced in excess or cleared too slowly possibly because of a functional defect of macrophages. The presence of numer-

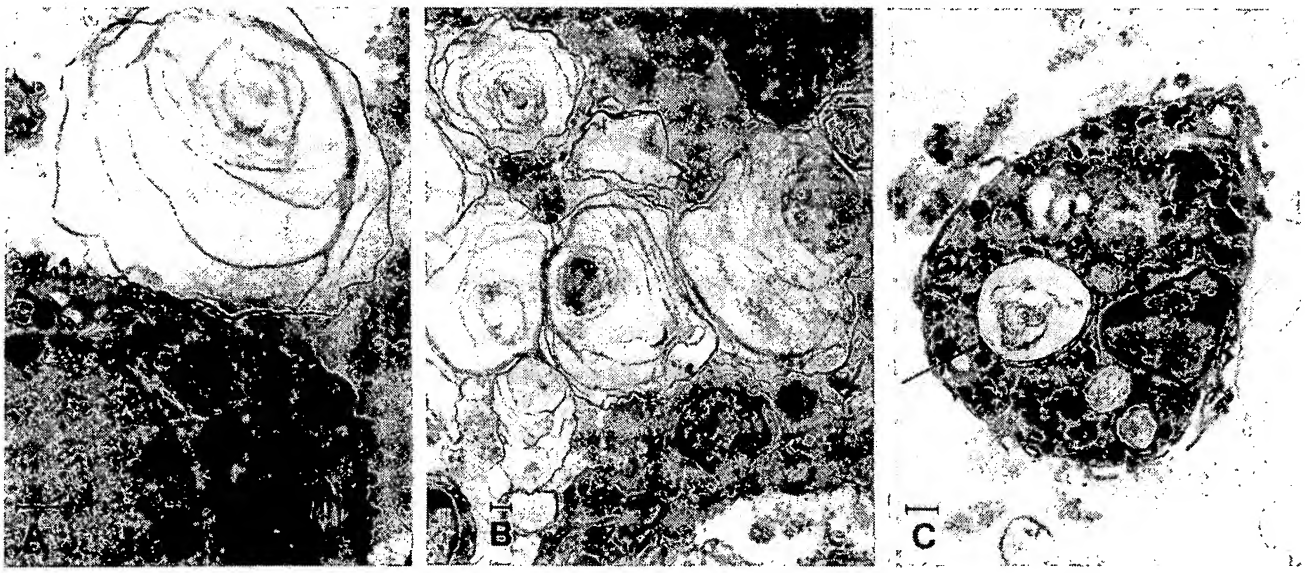

FIG. 4. Ultrastructure of lungs from GM-CSF-deficient mice. Electron microscopic sections of 24-wk GM−/− lung (same mouse lung as in Fig. 3 *O–Q*). (*A*) Type II surfactant-producing alveolar cell with characteristic intracytoplasmic lamellar bodies. Adjacent alveolus contains type-C lamellar body. (*B*) Numerous intraalveolar type-C lamellar bodies with characteristic "onion" appearance. (*C*) Intraalveolar macrophage with phagosomes containing "onion" structures resembling type-C lamellar bodies. (Bars = 1 μm.)

ous type-C lamellar bodies within alveoli and macrophages is consistent with the accumulation of surfactant components (17). In some areas, the histological appearance of lungs from GM−/− mice resembles that of some forms of alveolar proteinosis, a heterogeneous group of congenital and acquired lung disorders characterized by accumulation of surfactant protein within alveoli and often complicated by infection (17–19). The role of GM-CSF in the production and clearance of surfactant has not been studied.

A prominent feature of the lung pathology of GM−/− mice is infection with a range of opportunistic bacterial and fungal organisms. The lymphoid hyperplasia may be part of the general pulmonary response to infection; these appearances resemble those of *Pneumocystis carinii* infection in immunocompromised mice (20). When infection occurs, the response of GM−/− mice is usually adequate to prevent death, but the ongoing pathology in mice of all ages indicates that the host response to infection is defective. In the absence of GM-CSF, inflammatory cells can still be localized in tissues such as the lung, although their functional competence may be impaired. Alveolar macrophages are particularly responsive to GM-CSF, and many cell types present in the lung are capable of GM-CSF synthesis (21, 22). A significant component of the intrinsic pulmonary defect may therefore be the absence of local GM-CSF-dependent activation of macrophages involved in either surfactant clearance or infection control. It will be interesting to gauge the influence of environmental factors on both the hematologic and pulmonary manifestations of GM-CSF deficiency by comparing GM−/− mice raised in conventional and gnotobiotic animal facilities.

The pulmonary pathology accompanying absolute GM-CSF deficiency suggests therapeutic potential for GM-CSF in lung disorders characterized by infection or by the accumulation of alveolar material such as occurs in alveolar proteinosis. Acquired forms of alveolar proteinosis may reflect a local relative deficiency of GM-CSF. Among congenital forms of alveolar proteinosis, there may be a human counterpart to murine GM-CSF deficiency, for which GM-CSF replacement therapy would be appropriate.

We thank R. Williams, G. Mann, A. Gabriel, K. Fowler, J. Boyd, N. Kountouri, J. Layton, A. Burgess, and D. Henderson for assistance and comments on the manuscript. The Anti-Cancer Council of Victoria supported E.S. and G.J.L. (John Maynard Hedstrom Research Scholarship) and D.M. (Carden Fellowship Fund).

1. Gasson, J. C. (1991) *Blood* **77**, 1131–1145.
2. Metcalf, D., Begley, C. G., Williamson, D. J., Nice, E. C., De Larmarter, J. D., Mermod, J.-J., Thatcher, D. & Schmidt, A. (1987) *Exp. Hematol.* **15**, 1–9.
3. Lang, R. A., Metcalf, D., Cuthbertson, R. A., Lyons, I., Stanley, E., Kelso, A., Kannourakis, G., Williamson, D. J., Klintworth, G. K., Gonda, T. J. & Dunn, A. R. (1987) *Cell* **51**, 675–686.
4. Johnson, G. R., Gonda, T. J., Metcalf, D., Hariharan, I. K. & Cory, S. A. (1989) *EMBO J.* **8**, 441–448.
5. Metcalf, D. (1993) *Blood* **82**, 3515–3523.
6. Miyatake, S., Otsuka, T., Yokota, T., Lee, F. & Arai, K. (1985) *EMBO J.* **4**, 2561–2568.
7. Stanley, E., Metcalf, D., Sobieszczuk, P., Gough, N. M. & Dunn, A. R. (1985) *EMBO J.* **4**, 2569–2573.
8. Tybulewicz, V. L. J., Crawford, C. E., Jackson, P. K., Bronson, R. T. & Mulligan, R. C. (1991) *Cell* **65**, 1153–1163.
9. Handyside, A. H., O'Neil, G. T., Jones, M. & Hooper, M. L. (1989) *Roux's Arch. Dev. Biol.* **198**, 8–55.
10. Metcalf, D. (1984) *The Hemopoietic Growth Factors* (Elsevier, Amsterdam).
11. Kelso, A. & Gough, N. M. (1989) *Growth Factors* **1**, 165–177.
12. Morse, H. C., Davidson, W. F., Yetter, R. A. & Coffman, R. L. (1982) *Cell Immunol.* **70**, 311–320.
13. Yelton, D. E., Desaymard, C. & Scharff, M. (1981) *Hybridoma* **1**, 5–11.
14. Dialynas, D. P., Quan, Z. S., Wall, K. A., Pierres, A., Quintans, J., Loken, M. R., Pierres, M. & Fitch, F. W. (1983) *J. Immunol.* **131**, 2445–2451.
15. Ledbetter, J. A. & Herzenberg, L. A. (1989) *Immunol. Rev.* **49**, 63–90.
16. Metcalf, D. (1991) *Proc. Natl. Acad. Sci. USA* **88**, 11310–11314.
17. Shelburne, J. D., Wisseman, C. L., Broda, K. R., Roggli, V. L. & Ingram, P. (1983) in *Diagnostic Electron Microscopy*, eds. Trump, B. F. & Jones, R. T. (Wiley, New York), Vol. 4, pp. 475–532.
18. Rosen, S. H., Castleman, B. & Liebow, A. A. (1958) *N. Engl. J. Med.* **258**, 1123–1142.
19. Nogee, L. M., De Mello, D. E., Dehner, L. P. & Colten, H. R. (1993) *N. Engl. J. Med.* **328**, 406–410.
20. Beck, J. M., Warnock, M. L., Curtis, J. L., Sniezek, M. J., Arraj-Peffer, S. M., Kaltreider, H. B. & Shellito, J. E. (1991) *Am. J. Respir. Cell Mol. Biol.* **5**, 186–197.
21. Bilyk, N. & Holt, P. G. (1993) *J. Exp. Med.* **177**, 1773–1777.
22. Smith, S. M., Lee, D. K. P., Lacy, J. & Coleman, D. L. (1990) *Am. J. Respir. Cell Mol. Biol.* **2**, 59–68.